Università degli Studi di Trieste

Graduate School in MOLECULAR BIOMEDICINE

PhD Thesis

HMGA1 PROTEINS REGULATE GENE EXPRESSION BY MODULATING HISTONE H3 PHOSPHORYLATION

Laura Arnoldo

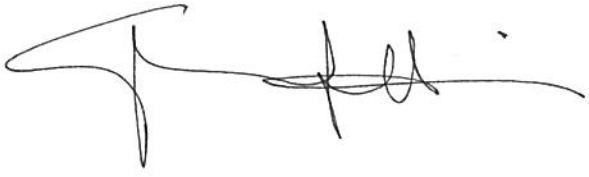

XXV ciclo – Anno Accademico 2012-2013

UNIVERSITÀ DEGLI STUDI DI TRIESTE

XXV CICLO DEL DOTTORATO DI RICERCA IN BIOMEDICINA MOLECOLARE

HMGA1 PROTEINS REGULATE GENE EXPRESSION BY MODULATING HISTONE H3 PHOSPHORYLATION

Settore scientifico-disciplinare: **BIO/10**

DOTTORANDA
LAURA ARNOLDO

COORDINATORE
PROF. GUIDALBERTO MANFIOLETTI

SUPERVISORE DI TESI
PROF. GUIDALBERTO MANFIOLETTI

CO-SUPERVISORE DI TESI
RICCARDO SGARRA, PhD

ANNO ACCADEMICO 2012 / 2013

ABSTRACT

HMGA1 is an oncogene encoding for an architectural transcription factor that affects fundamental cell processes, leading to neoplastic transformation.

The two main mechanisms by which HMGA1 protein is known to be involved in cancer concern the regulation of gene expression by altering DNA structure and interacting with a conspicuous number of transcription factors. Here we provide evidence of an additional level of gene expression regulation exploited by HMGA1 to exert its oncogenic activity. Starting from protein-protein interaction data showing that HMGA1 interacts with histones, we show that HMGA1 regulates gene expression by affecting the epigenetic status of cancer cells. In particular, it modulates the signalling cascade mediated by the RAS/RAF/MEKK/ERK/RSK2 pathway regulating the levels of histone H3 phosphorylation at Serine 10 and Serine 28. We demonstrate that the down-regulation of these two H3 post-translational modifications by HMGA1 silencing and by inhibitors of the RAS/RAF/MEKK/ERK pathway is linked to cell migration decrease and morphological changes resembling the mesenchymal to epithelial transition.

TABLE OF CONTENTS

1. INTRODUCTION

1.1 Transduction pathways

In pluricellular organisms, cells communicate with each other in order to maintain individual homeostasis and survival. They accomplish this function by means of signalling molecules, such as cytokines and growth factors, which are secreted and directed to target cells, delivering specific messages that induce alterations in the biological activity of the targeted cells. This objective is achieved by forwarding the signal from the extracellular environment to the cell nucleus, where transcriptional machinery responds by increasing or decreasing the expression levels of biological effectors (Karin, 1992).

Signalling molecules are recognized by specific receptors exposed on the cell surface. In general, they are proteins exhibiting an extracellular domain for ligand binding, a transmembrane domain, and an intracellular domain, making contact with specific cytoplasmic factors responsible for signal transduction. This domain can be associated with proteins showing enzymatic activity or can possess it *per se*. In any case, ligand binding to the receptor induces a chemical reaction activating intracellular downstream effectors responsible for spreading the signal towards the nucleus. In most situations, downstream effectors are kinases inducing a phosphorylation cascade (Karin, 1992), which finally leads both to the activity modulation of nuclear factors controlling gene expression (Hill and Treisman, 1995) and to the alteration of the epigenetic status of the cell, i.e. all those chromatin/DNA modifications which constitute the DNA sequence-independent genetic information. The existence of different types of signals, receptors and effectors leads to the establishment of a plethora of interconnected pathways that are responsible for regulating fundamental biological processes, such as proliferation, differentiation and apoptosis. Mutations affecting signal transduction factors cause misregulation of these pathways and often lead to neoplastic transformation (Karin, 1992).

1.2 Chromatin structure

In eukaryotic cells, DNA is packaged into the nucleus to form chromatin. Its fundamental elements are repeating subunits called nucleosomes, which are composed of approximately 146 base pairs of DNA, wrapped around a histone octamer containing two copies each of histone H2A, H2B, H3 and H4, also termed *core* histones. They are small basic proteins

exhibiting a globular C-terminal domain making contact with DNA to form the nucleosome core and an N-terminal flexible tail, which protrudes from this complex in the nuclear environment making contact with adjacent nucleosomes and other chromatin factors (Luger et al., 1997). This structure can be stabilised by histone H1, which associates with the DNA entry/exit site of the nucleosome (Zhou et al., 2013) leading to the formation of the so-called "beads-on-a-string" fibre. "Beads" are specifically spaced on the genome but their occupancy can change depending on biological requirements, e.g. they can be repositioned or removed when DNA is transcribed and needs to be freely accessible to allow transcription factors and RNA polymerase landing (Iyer, 2012).

H1 differs from core histones for dimension and structure. It is much larger than the core counterpart and even though it shows a globular domain as well, it exhibits two unstructured tails, among which the C-terminal one is very basic and seems to be essential for the formation of higher order chromatin structures (Caterino and Hayes, 2011). Indeed, histone H1 is able to bind *linker* DNA, i.e. the DNA region included between two nucleosomal subunits (Zhou et al., 2013). Thanks to this capability, it allows chromatin condensation and the consequent formation of nucleosomes arrays around a 30-nm fibre. Moreover, it sterically impedes the DNA binding of other proteins, such as transcriptional factors, thus playing a repressive role in transcription (Bustin et al., 2005).

Chromatin is not always tightly packaged. Its macroscopic organisation depends primarily on the cell cycle phase: during interphase the overall structure is quite loose to allow replication and transcription, while it becomes much more compacted when chromosome condensation takes place during mitosis. At local level chromatin can be distinguished in two different areas according to gene expression. When genes are actively transcribed, chromatin is structurally open to allow transcriptional machinery access and is termed *euchromatin*. Conversely, chromatin regions consisting of inactive genes remain condensed even during interphase and constitute the *heterochromatin*. It is in turn distinguished in constitutive and facultative heterochromatin: the former comprises those genes that are constitutively inactive, e.g. centromeric chromatin; the latter can be converted to euchromatin depending both on the cell type and on the signalling pathways activation.

The fact that chromatin structure can be assembled or disassembled according to cell requirements implies an intrinsic dynamicity. This is a fundamental feature which allows a differential access to DNA in order to respond to multiple stimuli. Indeed, chromatin does not

constitute a static storage of genetic information but rather represents a platform where biological signals integrate and molecular responses take place.

1.3 Histone post-translational modifications

Processes such as DNA replication, DNA damage repair, and gene transcription rely on the ability of chromatin factors to timely access DNA at specific sequences. DNA accessibility is controlled by chromatin state, which in turn depends both on the presence of specific proteins (histones and non-histone chromatin factors) and histone post-translational modifications (PTMs).

Histone PTMs are one of the fundamental mechanisms that cells exploit to modulate chromatin organisation. Along with DNA methylation, they constitute the DNA-sequence independent heritable chromatin information, commonly referred to as *epigenetics*.

More than 100 different PTMs can be added to the core histones, including acetylation, phosphorylation, and methylation (Bernstein et al., 2007). The majority of them localise on the "exposed" N-terminal flexible tails, which protrude from the nucleosome structure (fig. 1.1), but also the globular domains of histones can be post-translationally modified (Bannister and Kouzarides, 2011). The specific PTM status of a histone tail is generally due to the opposite activity of enzymes which add and remove the specific post-translational modification, usually referred to as *writer* or *eraser* enzymes.

Histone PTMs mainly act through two mechanisms that however are not mutually exclusive: (i) they can directly influence the overall structure of chromatin by modifying histones/DNA binding properties or (ii) they can positively/negatively regulate the binding of effector molecules (Bannister and Kouzarides, 2011), which in turn will affect chromatin organisation and function. Among these factors, chromatin remodelling complexes are particularly relevant, because they are enzymes utilising the energy derived from ATP hydrolysis for nucleosome reposition or sliding, fundamental processes to allow DNA accessibility (Iyer, 2012).

Molecules able to land onto nucleosomes and to bind to histones are frequently characterised by the presence of domains that recognise specific histone PTMs (e.g. bromodomain: acetylated lysine (Wilkinson and Gozani, 2014); chromodomain: methylated lysine (Wilkinson and Gozani, 2014); 14-3-3 proteins: phosphorylated serine/threonine (Macdonald et al., 2005).

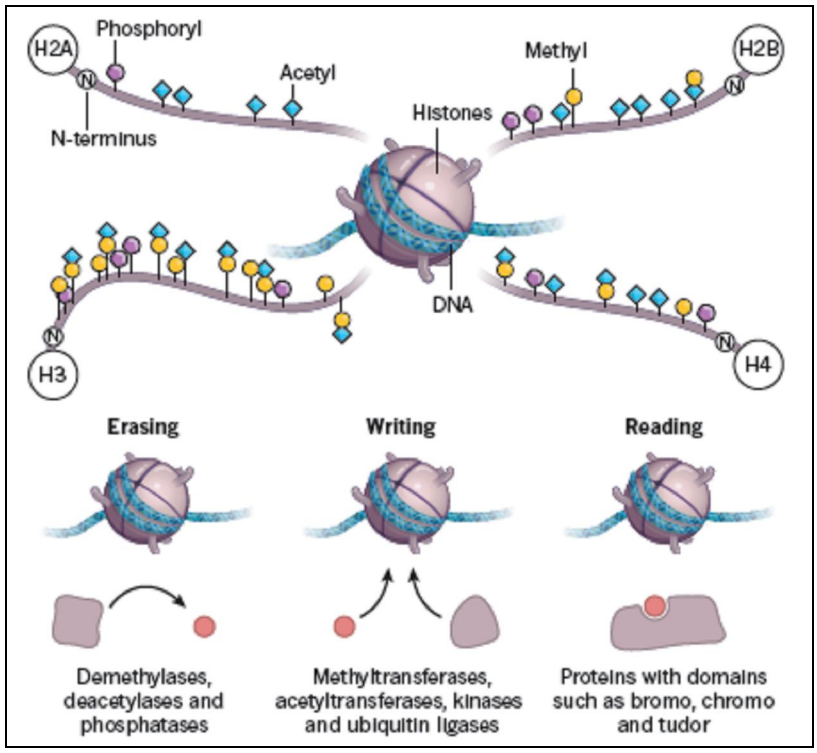

Figure 1.1: Histone post-translational modifications. DNA is wrapped around histones (H2A, H2B, H3, and H4) to form nucleosomes. The N-terminal tails of histones protrude from nucleosome core and are modified by *writer* and *eraser* enzymes and are *read* by proteins with specific binding domains (Helin and Dhanak, 2013).

Acetylation

Acetylation occurs on lysine residues by the action of histone-acetyltransferases and is removed by histone-deacetylases. The addition of an acetyl group to the lysine side chain has the peculiar property of neutralizing the positive charge of this aminoacid residue, weakening the interactions between histones and the negatively charged DNA (Bannister and Kouzarides, 2011). Several histone acetylations, such as that on H3K14 (H3K14ac), have been found at the level of enhancers and promoters of actively transcribed genes, suggesting that this modification can facilitate transcription factors accessibility favouring chromatin structure decondensation (Wang et al., 2008). This hypothesis is supported by the finding that H4K16 acetylation inhibits *in vitro* the formation of the 30-nm fibre (Shogren-Knaak et al., 2006). As mentioned before, a direct structural role does not exclude a role in mediating the binding of effector molecules and indeed, acetylated lysines are specifically bound by bromodomain-containing proteins within nucleosome remodelling complexes. For instance, Brg1 (Brahma-related gene 1) protein belonging to the SWI/SNF (SWItch/Sucrose NonFermentable)

chromatin remodeling complex contains a bromodomain by which it binds to H3K14ac (Shen et al., 2007).

Phosphorylation

Phosphorylation is controlled both by kinases, which add phosphate groups on serines, threonines, and tyrosines and by phosphatases, responsible for their removal. This modification adds net negative charge to the target histone. Therefore, it is supposed to profoundly alter chromatin compaction, even more than histone acetylation. However, it has been mainly described as a modification involved in creating or disrupting nucleosome docking sites. For instance, a genome-wide H3S10 phosphorylation (H3S10ph) taking place during mitosis is associated with chromosome condensation (Wei et al., 1998). In this specific case, it allows the displacement of heterochromatin protein 1 (HP1), a heterochromatin organising factor that is bound to H3K9 tri-methylated (H3K9me3) and whose presence is not compatible with the formation of mitotic chromosomes (Hirota et al., 2005). Conversely, it has been demonstrated that H3S10ph acts as a docking site for 14-3-3 adaptor protein during Immediate-Early genes transcriptional activation. By specifically recognising this modification, 14-3-3 allows SWI/SNF chromatin remodelling complex recruitment at regulatory sequences in order to facilitate nucleosome sliding and hence transcription initiation (Drobic et al., 2010).

Methylation

Histone methylation occurs on lysines and arginines by histone methyl-transferases and is removed by histone demethylases. This modification differs from the previous ones because it does not alter the charge of the histone proteins. Moreover, the resulting output is much more complex since up to three methyl groups can be added to lysines (mono-, di- and tri-methylated) while arginines can be mono- or di-methylated in a symmetrical or asymmetrical way (Bannister and Kouzarides, 2011). This allows the establishment of different docking sites on the same aminoacidic residue. Methylation can have different functions according to which residue is modified. For example, tri-methylation of H3K36 (H3K36me3) is associated with transcribed chromatin (Bernstein et al., 2007) whereas the same modification on H3K9 and H3K27 (H3K27me3), which are bound by the repressive factors HP1 and Polycomb Repressive Complex family members (PRC1 and PRC2), respectively, correlate with transcriptional repression (Hirota et al., 2005; Margueron and Reinberg, 2011).

An additional level of complexity is achieved by the combination of adjacent modifications. They can act synergistically giving rise to a specific docking site, different from those constituted by the single modifications or, vice versa, the addition of the second modification can "counteract" the function of the first one.

Indeed, it has emerged the concept that the various PTM combinations on core histones constitute a complex histone code, which is interpreted and translated in specific biological outcomes (Chi et al., 2010). Moreover, often the output of several histone PTMs is context-dependent. As regards these considerations, two set of modifications can be considered as prototype of multivalent PTMs: H3K9me3/H3S10ph and H3K27me3/H3S28ph, in which the repressive role of lysine methylation is counteracted by phosphorylation of the adjacent serine residue (fig. 1.2).

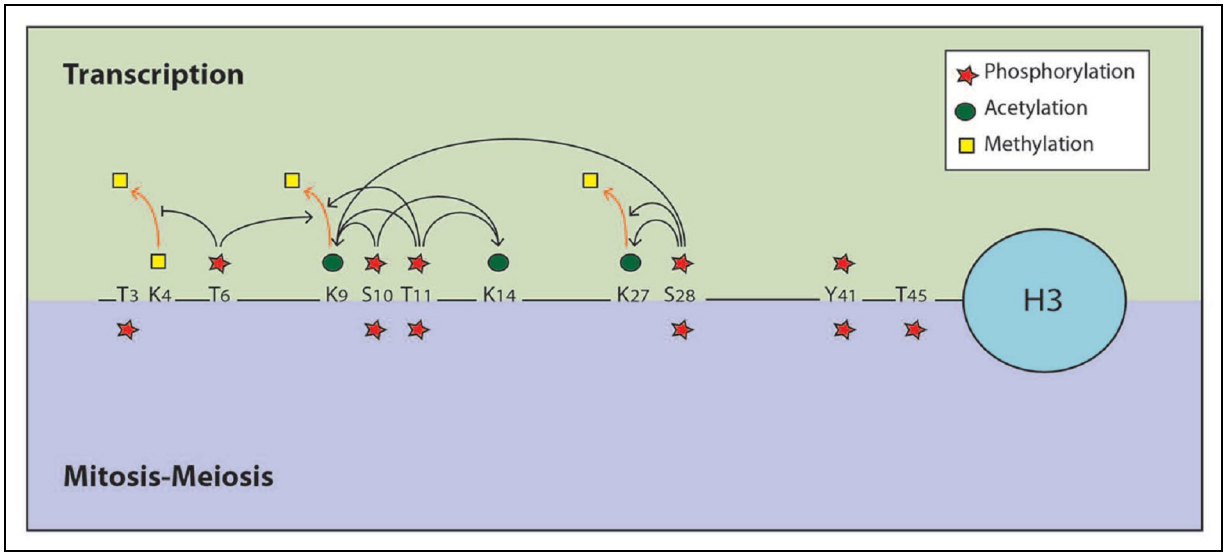

Figure 1.2: Crosstalk between phosphorylation and other histone post-translational modifications. Adjacent modifications can cooperate or counteract with each other (Rossetto et al., 2012).

1.4 H3S10/S28 phosphorylation: the prototype of cell context-dependent histone PTMs

Histone H3 phosphorylation at Serine 10 and Serine 28 can be considered prototype of PTMs with opposite roles depending on the specific context. On the one hand, they are considered hallmarks of mitosis (Goto et al, 1999). On the other hand they have specific transcriptional activating roles. Indeed, they are associated with chromosome condensation and segregation during cell division and show a similar expression pattern, even though with slightly difference with regard to the timing. Indeed, H3S10ph initiates in heterochromatin in late G2

(Hendzel et al., 1997) and continues until telophase (Goto et al, 2002) whereas H3S28ph starts in condensing chromosomes at prophase (Goto et al, 1999) and terminates at anaphase (Goto et al, 2002). It is still unclear whether these modifications share a redundant role. As regards H3S10ph, it has been proposed that this phosphorylation may act as a phospho/methyl switch able to displace HP1 from heterochromatin, which is highly enriched in H3K9me3. The reason why HP1 has to be removed is not clear, but it seems that this removal could facilitate mitotic chromatin condensation. Similarly, the phospho/methyl switch model has been extended to H3S28ph. Indeed, it has been suggested that this modification could displace Polycomb repressive complexes PRC1 and PRC2 from their binding sites on H3K27me3 in mitosis (Wang and Higgins, 2013). However, only recently a direct mechanistic evidence of the role of H3 phosphorylation in chromosome condensation has been found out. It has been demonstrated that H3S10ph recruits the histone deacetylase Hst2p (Sir2p homolog) to nucleosomes, where it subsequently removes an acetyl group from H4K16. As a consequence, H4 N-terminal positive tail is free to interact with the negatively charged acidic patch formed by the H2A-H2B dimer interface on the surface of a neighbouring nucleosome, therefore promoting chromatin condensation (Wilkins et al., 2014).

In the mitotic context, phosphorylation of both H3S10 and H3S28 is performed by Aurora B kinase, which is a key component of the Chromosomal Passenger Complex (CPC) along with Inner CEntromere Protein (INCENP), Survivin and Borealin/Dasra (Wang and Higgins, 2013).

In addition to mitosis, histone H3 phosphorylation at S10 and S28 can be detected also in interphasic cells. Indeed, not only is this modification involved in mitotic chromosome condensation but it also correlates with transcriptional activation during different biological processes, such as cell proliferation and apoptosis (Park et al., 2006; Mishra et al., 2006). In particular, its association with Immediate Early Genes (IEGs) induction has been studied in depth.

IEGs are a class of genes encoding different cellular factors, such as enzymes (e.g. cyclooxygenase-2, COX-2, Rahman et al., 2002) and transcription factors (e.g. jun and fos families, Thomson et al., 1999). They are so called because of their rapidly and transient induction following extracellular signalling and because they do not require the synthesis of any other protein to be transcribed (Healy et al., 2013).

IEGs can be activated by different stimuli, such as growth factors (e.g. epidermal growth factor, EGF or platelet-derived growth factor, PDGF), mitogens and phorbol esters (e.g. 12-O-

tetradecanoylphorbol-13-acetate, TPA), developmental, immunological and neurological signals, and stress (e.g. UV, toxins) (Healy et al., 2013).

As mentioned previously, extracellular signals induce the activation of a plethora of transduction pathways resulting in a transcriptional output. IEGs expression is mainly induced by two mitogen-activated protein kinase (MAPK) effector cascades: the RAS/RAF/MEKK/ERK pathway, activated by growth factors and mitogens and resulting in the activation of extracellular signal-related kinase isoforms 1 and 2 (ERK1/2) and the p38-MAPK pathway, which is activated by UV or stress (Thomson et al., 1999; McKay and Morrison, 2007). These two cascades cause many downstream events, among which the activation of effector kinases that phosphorylate histone H3 at S10 and S28. During this process, HMGN1 protein, which is a chromatin architectural factor tightly associated with nucleosomes, is phosphorylated as well. For this reason, this induction mechanism is named "nucleosomal response" (Thomson et al., 1999).

Mainly two kinases are responsible for histone H3S10/28 phosphorylation downstream ERK1/2 and p38-MAPK activation: MSK1/2 (Mitogen and Stress Activated Kinase isoforms 1 and 2) (Deak et al., 1998) and RSK2 (Ribosomal S6 Kinase 2 or p90-RSK) (Sassone-Corsi et al., 1999). They are serine/threonine kinases belonging to the MKs family (MAPK-activated protein kinase, Roux and Blenis, 2004) and exhibit a very similar structure: they possess two functionally different kinase domains within the same polypeptide (N-terminal kinase domain – NTKD and C-terminal kinase domain - CTKD) (Roux and Blenis, 2004). NTKD belongs to the AGC kinase family, which include kinases such as Protein Kinase A, C and B (PKA, PKC and PKB) whereas CTKD belong to the Calcium and Calmodulin-dependent kinase (CaMK) family (Roux and Blenis, 2004).

MSK1/2

MSK1/2 can be activated in the nucleus both by ERK1/2 and by p38-MAPK (Deak M et al., 1998). Therefore, it is involved in the transduction of both growth/mitogenic signals and stress stimuli. Once activated, it phosphorylates several nuclear proteins, such as the transcription factor CREB, which in turn regulates IEGs expression.

Recently, it has been demonstrated in mouse fibroblasts 10T1/2 that following ERK1/2 activation by TPA stimulation, MSK1/2 was recruited to IEGs regulatory regions (both distal and proximal to the gene), somehow "primed" for activated MSK1/2 binding. At the chromatin level, MSK1/2 phosphorylates histone H3 at S10 or S28. H3S10ph and H3S28ph

are specifically recognised by 14-3-3 adaptor proteins, which in turn have been found in complex with BRG1, the ATPasic subunit of the chromatin remodeler complex SWI/SNF, along with MSK1/2 itself. Thus, after H3 phosphorylation by MSK1/2, 14-3-3 binding to this modification allows BRG1 to contact gene promoters leading to nucleosome remodelling and gene transcription activation (fig. 1.3) (Drobic et al., 2010).

In another work, it has been demonstrated that histone phosphorylation by MSK1/2 at H3S28 can cause Polycomb Group Protein (that are bound via H3K27me3) displacement (fig. 1.3) from IEGs promoters and gene activation in response to mitogenic signalling, stress stimulus and retinoic acid-induced neuronal differentiation (Gehani et al, 2010). Similarly, others demonstrated that H3S28 phosphorylation displaces Polycomb from H3K27me3 at α-globin and fos promoters and moreover disrupts this methylation causing an acetylation/methylation switch (Lau and Cheung, 2011).

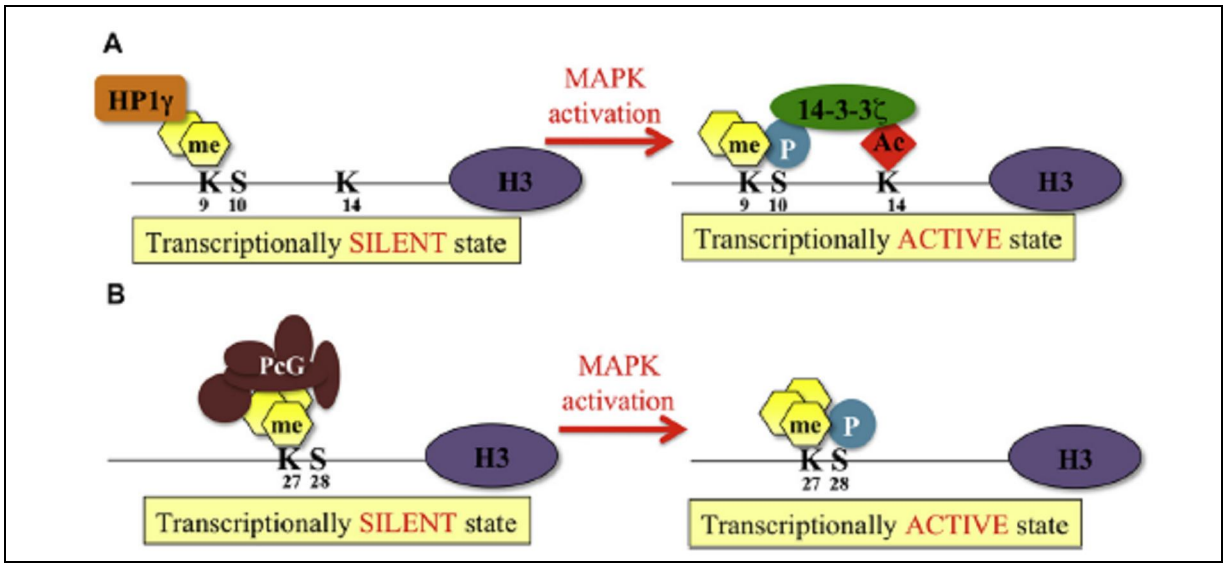

Figure 1.3: Phospho/methyl switch. Phosphorylation of histone H3 at Serine 10 and Serine 28 can displace repressive complexes switching chromatin from a transcriptional silent state towards an active one (Sawicka and Seiser, 2012).

RSK2

RSK2, differently from MSK1/2, is activated solely by ERK1/2 in the cytoplasm and afterwards it translocates to the nucleus (Carriere et al., 1998) where it phosphorylates several substrates, some of which shared with MSK1/2 (e.g. CREB) (Deak et al., 1998). Like MSK1/2, it is involved in the nucleosomal response. Indeed, it has been demonstrated in fibroblasts from Coffin Lowry Sindrome patients, showing mutated and inactive forms of

RSK2, that H3S10 phosphorylation upon EGF stimulation was compromised. Moreover, when these fibroblasts were transfected with RSK2 coding DNA, these cells showed H3S10 phosphorylation, therefore demonstrating that RSK2 was the enzyme responsible for that modification (Sassone-Corsi et al., 1999).

Furthermore, it has been proposed that in quiescent cells RSK2 is in complex with CBP acetyltransferase and that this association is inhibitory both for RSK2 and CBP activity. Upon EGF stimulation and RSK2 phosphorylation, this kinase disrupts this complex and both enzymes can perform their activity. RSK2 phosphorylates H3 at S10 and CREB, which associates with CBP increasing its activity. This enzyme in turn acetylates H3 at K14 (Merienne et al., 2001). These two modifications are known to act synergistically in activating transcription (Cheung et al., 2000). However, the molecular mechanism by which RSK2-mediated H3 phosphorylation activates transcription in this context is still unclear.

From the above mentioned literature, it is evident that MSK1/2 and RSK2 have overlapping roles and that they act by activating very similar molecular mechanisms. Despite the fact that MSK1/2 and RSK2 are the most known and studied among the kinases responsible for H3 phosphorylation in interphasic cells, they are not the only ones. Indeed, it has been demonstrated that H3S10 is phosphorylated also by IkK-α kinase at the level of IkBα promoter in response to inflammatory cytokines (Yamamoto et al., 2003). Furthermore, PIM1 kinase is recruited by MYC on genes involved in cell cycle, growth and differentiation, where it phosphorylates H3 at the level of E-box DNA sequences (Zippo et al., 2007). Moreover, during apoptosis, H3S10 is phosphorylated by Transglutaminase-2 in specific regions of the genome (Mishra et al., 2006) and by PDZ binding kinase (PBK) during cell cycle progression of breast cancer cells (Park et al., 2006).

A few months ago, it has been surprisingly shown that Aurora B kinase, which is largely known for its role in chromosome condensation as described above, can phosphorylate H3 with transcriptional-related outcomes. Indeed, it has been demonstrated that Aurora B kinase is associated with promoters of active genes in quiescent resting B cells from mice spleen and that it phosphorylates histone H3 at S28 but not at S10 in these regions. Experiments performed in resting B cells from wild-type and AURKB KO mice revealed a significant decrease in primary transcript levels and the data were confirmed by the treatment of resting B cells with the Aurora B inhibitor AZD1152. Furthermore, a genome-wide comparison of Aurora B binding and the expression levels measured by RNA-seq revealed that its association with promoters strongly correlates with transcriptional activity. As a matter of fact, they also

showed that Aurora B was bound to the promoters as part of the CPC complex (described above) (Frangini et al., 2013). However, it still remains unclear the role of H3S28 phosphorylation in the activation of these promoters.

1.5 H3 phosphorylation and neoplastic transformation

Since histone H3 phosphorylation is required for the activation of genes upon mitogenic stimulation, it is not surprising that it has been found to be involved in cancer. Indeed, it has been demonstrated by colony formation assays that both MSK1/2 inhibition by H89 inhibitor and MSK1 down-regulation by means of MSK1 dominant-negative mutants suppresses EGF- and TPA-induced transformation of JB6Cl41 cells. Similar experiments performed in cells transfected with histone H3 point mutants (H3S10A and H3S28A) or histone H3 WT confirmed that H3 phosphorylation itself is responsible for cell transformation. Moreover, MSK1/2 downregulation by siRNA suppresses cell proliferation in this system while its overexpression increases the proliferation rate (Kim et al., 2008).

Subsequently, Perez-Cadahia and collaborators determined the role of MSK1 in the malignant phenotype of Ciras-3 cells, HRas1-transformed 10T1/2 mouse fibroblasts. These cells have a constitutively active RAS-MAPK pathway and show elevated levels of phosphorylated ERK1/2, accompanied by an increased MSK1 activity and elevated steady-state levels of H3S10 and S28 phosphorylation, with respect to the parental 10T1/2 counterpart. They demonstrated how increased MSK1 activity leads to the establishment of high steady-state levels of IEGs products and this augmented expression is responsible for conferring malignant properties to these cells. In fact, they demonstrated that MSK1 knockdown, which in turn causes IEGs encoded proteins decrease, reduces anchorage-independent growth of these cells. Similar experiments performed with H89 MSK1/2 inhibitor confirmed these data (Perez-Cadahia et al., 2011).

In support of this study, up-regulated expression levels of IEGs have been found in many types of tumours and correlate with cancer progression (Healy et al., 2013). This is probably due to the fact that 30% of all cancers exhibit RAS mutations, which continuously provide growing stimuli, making cells independent on external signalling (Bos, 1988; Dunn et al., 2005).

H3 phosphorylation by RSK2 kinase has been correlated to neoplastic transformation as well. In fact, it has been demonstrated that it is involved in tumour induction in a similar way of MSK1/2 (Cho et al., 2007). Indeed, RSK2-overexpressing JB6Cl41 cells showed an increased

anchorage-independent colony formation with respect to the mock cells with or without EGF or TPA stimulation. Moreover, the transfection of siRNA against RSK2 in Ras^{G12V} transformed NIH3T3 cells blocked foci formation. The treatment of JB6Cl41 cells with kaempferol, an RSK2 specific inhibitor, suppressed cell proliferation and EGF-induced transformation. These events were accompanied by a reduction of H3S10 phosphorylation, indicating that RSK2 kinase activity is fundamental for cell transformation (Cho et al., 2007).
As a matter of fact, MSK1/2 and RSK2 seem to have overlapping roles (i.e. IEGs induction and modulation of invasive properties of cancer cells) and targets (i.e. H3S10/28 and CREB) and are also modulated by the same upstream activating pathways (i.e. ERK1/2); this highlights the existence of additional regulatory mechanisms to selectively switch on/off one, the other, or both.

1.6 Histone modifications and cancer

The previously described data regarding H3 phosphorylation and neoplastic transformation highlight the role of epigenetic changes in both initiation and progression of cancer. Indeed, it has increasingly appeared evident that the misregulation of histone PTMs is linked to cancer, since it can alter gene expression profiles and affect genome integrity (Bannister and Kouzarides, 2011). Notably, several works reported a link between global histone modification pattern alterations, tumour phenotype, and prognostic information in human cancer samples (Seligson et al., 2005; Elsheikh et al., 2009).
This histone PTMs imbalance is thought to arise from mutations in the regulators of the PTMs (Waldmann and Schneider, 2013). For instance, "gain-of-function" mutations in *writers* or *erasers* would result in PTM up-regulation and down-regulation, respectively, while "loss-of-function" mutations would cause the opposite effect. In some cases, the formation of fusion products can lead to aberrant modification patterns as well. A striking example is represented by the MOZ-TIF2 fusion, which is associated with acute myeloid leukaemia (AML). MOZ is a histone acetyltransferase (HAT) whereas TIF2 is a nuclear receptor coactivator that binds to another HAT, CBP. This fusion product cause neoplastic transformation through the establishment of an altered histone acetylation profile given by the aberrant recruitment of CBP to MOZ nucleosome-binding sites (Bannister and Kouzarides, 2011).
In addition, altered expression levels of PTM enzymes are often related to their misregulated activity. For instance, the histone methyltransferase EZH2 (Enhancer of Zeste Homolog 2), which is responsible for H3K27 methylation, is found overexpressed in various tumours and it

has been demonstrated that its overexpression and the consequent augmented H3K27 HMT activity is responsible for conferring invasiveness to fibroblasts and immortalised benign mammary epithelial cells. The oncogenic function of EZH2 has been ascribed to its role in tumour suppressor genes silencing (Chi et al, 2010).
It is therefore evident that histone PTMs regulation can be altered at different levels, including the activity modulation of specific enzymes and the mechanisms by which they can access or be recruited to chromatin.

1.7 HMG protein superfamily

High Mobility Group (HMG) proteins are small nuclear factors involved in chromatin structural organisation and dynamics. They were discovered in mammalian cells more than 30 years ago and named according to their high mobility in acetic acid/urea electrophoresis (Goodwin et al., 1973). This family is the most abundant among non-histone nuclear proteins (Bustin et al., 1990) and comprises three sub-families, called HMGN, HMGB and HMGA.
They all exhibit an acidic C-terminal tail containing negative charged amino acids but differ from each other for the presence of specific DNA binding domains and for the peculiar functions they accomplish in biological processes (Hock et al., 2007).
HMGN show a positive charged binding domain which allows them to contact nucleosomes (*Nucleosomal Binding Domain*) (Reeves and Adair, 2005). Indeed, they are able to interact both with histone H3 and H2B and nucleosomal DNA (Bustin, 2001).
HMGB contain two functional motifs (HMG-*boxes*), each consisting of three alpha-helixes by which they are able to enter the minor groove of DNA (Reeves and Adair, 2005).
Finally, HMGA are characterised by the presence of three DNA binding domains, named *AT-hooks*. These motifs are rich in positively charged amino acids and are so called for their peculiar capacity to bind to the minor groove of AT-rich DNA sequences (Sgarra et al., 2004).

1.8 HMGA and their mechanisms of action

HMGA family mainly consists of three proteins: HMGA1a, HMGA1b and HMGA2. The former are splicing variants of HMGA1 gene localising on 6p21 human locus (Friedmann et al., 1993) and are composed by 106 and 95 amino acids, respectively. The latter is encoded by the homologous gene HMGA2 localizing on 12q14-15 human locus (Chau et al., 1995) and is composed of 107 amino acids (fig. 1.4). Both these genes are highly expressed during embryogenesis, to a lesser extent during organogenesis, and become almost undetectable in

adult tissues (Chiappetta et al, 1996). In particular, HMGA2 expression has been never detected in human and murine adult tissues (Fusco and Fedele, 2007), while HMGA1 is expressed at very low levels in mice and humans (Chiappetta et al, 1996).

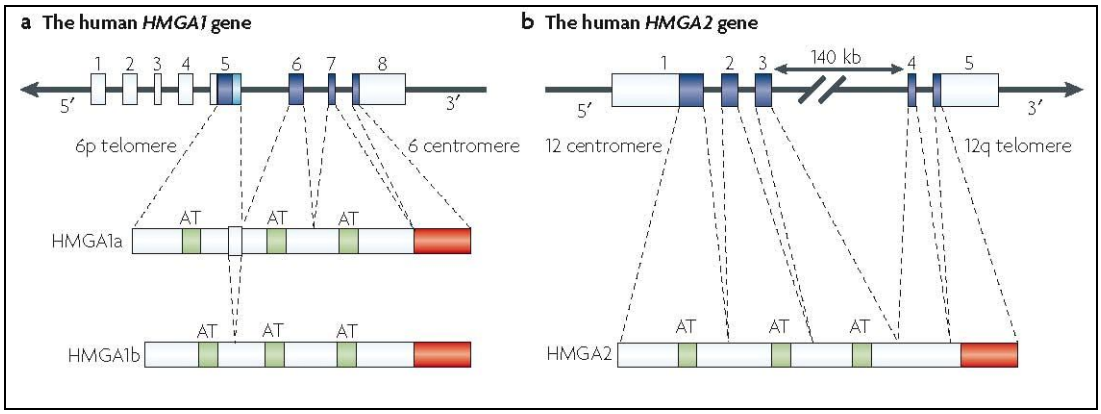

Figure 1.4: HMGA encoding genes. Schematic representation of the two different genes encoding for HMGA1a/b and HMGA2 proteins (Fusco and Fedele, 2007).

In addition to be involved in embryonic development, they play an important role both in physiological and pathological processes, e.g. glucose homeostasis, virus integration, and neoplastic transformation (Sgarra et al, 2004).

Several transduction pathways regulate HMGA expression, including those activated by RAS-MAPK (Cleynen et al., 2007), Wnt/β-catenin (Akaboshi et al., 2009) and Transforming Growth Factor-β (TGF-β-Smad) (Thuault et al., 2006).

RAS-activated MAPK cascade regulates HMGA1 gene expression with a mechanism that has been suggested to require a complex cooperation between SP1 family members and AP1 factors (Cleynen et al., 2007). In gastric cancer cells, Wnt/β-catenin increases HMGA1 levels through c-myc activation (Akaboshi et al., 2009). Finally, TGF-β pathway induces HMGA2 expression through the intracellular transduction factor Smad. In this context, HMGA2 mediates epithelial-to-mesenchymal transition process by regulating the expression of Snail, Snug, Twist, and inhibitor of differentiation 2 genes (Thuault et al., 2006).

HMGA expression is also post-transcriptionally regulated by microRNAs (miRNAs), e.g. miR-26a and let-7 down-regulate HMGA1 and HMGA2 mRNAs, respectively, suppressing their oncogenic roles (Lin et al., 2013; Lee and Dutta, 2007). In addition, HMGA1 mRNA has been demonstrated to be destabilised also by the expression of a pseudogene HMGA1 mRNA (HMGA1-p) (Chiefari et al., 2010).

HMGA proteins do not show secondary and tertiary structures. For this reason, they belong to the intrinsically disordered protein family (IDPs). Indeed, more than 70% of HMGA1 sequence exhibits a random coil conformation (Evans et al., 1995). This status confers them both the ability to contact many partners along with they establish complex molecular networks and to be highly accessible to modifying enzymes (Sgarra et al., 2010). Indeed, HMGA are highly regulated by PTMs (Sgarra et al., 2009).

It is thought that HMGA can be partially structured when bound to other factors. For instance, AT-hook domains assume a convex planar configuration upon binding to the DNA minor groove (Evans et al., 1995; Huth et al., 1997). These peculiar properties are related to their involvement in many aspects of cellular biology.

HMGA are defined as architectural transcription factors. Indeed, they do not possess transcriptional activity per se, but they regulate gene expression by constituting nucleoprotein-DNA transcriptional complexes. They recognize specific structures rather than determinate sequences. In fact, as well as the minor groove of type B DNA, they are able to bind non canonical structures such as supercoiled DNA (Nissen and Reeves, 1995), four-way DNA junctions (Hill and Reeves, 1997) and nucleosomal DNA regions associated with the histone octamer (Reeves and Nissen, 1993).

HMGA perform their regulatory activity also by means of protein-protein interactions with several partners involved in different biological processes. Proteomic screenings (Sgarra et al., 2005-2008; Fusco et al., 2007) shed light on the interaction among HMGA and different classes of interactors, including transcription factors and proteins involved in RNA-splicing, DNA damage repair, and chromatin remodeling.

HMGA regulate gene expression mainly through three different but not mutually exclusive, mechanisms: chromatin/DNA structure alterations, the assembly of multiprotein complexes called enhanceosomes at the level of enhancer and promoters and the interaction with transcriptional factors (fig. 1.5).

Experimental evidence demonstrated that HMGA are able to bind to SAR/MAR regions (Scaffold/Matrix Associated Regions) (Zhao et al., 1993). These sequences are AT-rich DNA regions that associate with nuclear matrix forming chromatin loops (Laemmli et al., 1992). HMGA1 binding to SARs causes histone H1 re-localisation, allowing the local chromatin opening and consequently gene transcription (Zhao et al., 1993).

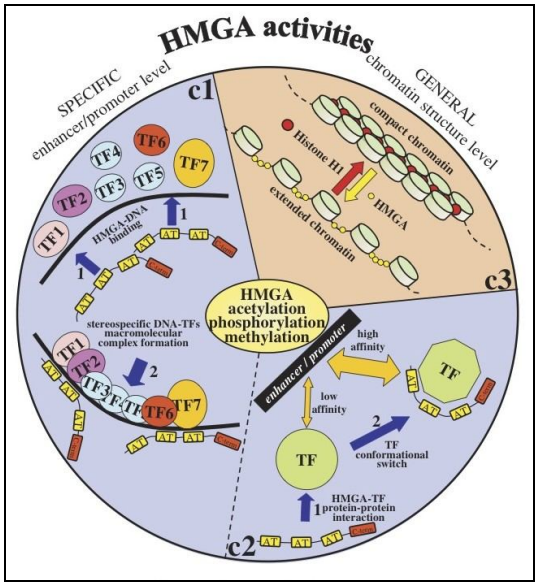

Figure 1.5: HMGA regulatory mechanisms. HMGA can modulate gene expression at the level of specific enhancers and promoters (c1), by binding to transcription factors and modulating their DNA binding affinity (c2), and by altering chromatin accessibility competing with histone H1 (c3) (Sgarra et al., 2004).

In addition, it has been demonstrated that HMGA associate *in vitro* and *in vivo* with nucleosomes at the level of histones H2A, H2B and H3, by interacting both with the histone N-terminal tails and DNA (Reeves and Nissen, 1993). Their binding to nucleosomal DNA causes an alteration in the periodicity of the double helix and its wrapping pattern (Reeves and Wolffe, 1996). As a matter of fact, it has been showed that these architectural factors participate in the nucleosome phasing process at the level of transcription start sites or enhancers (Reeves et al., 2000).

As it is thought that the majority of chromatin remodeling complexes contains proteins exhibiting motifs for the binding of AT-rich sequences (Bourachot et al., 1999), it is presumable that HMGA can recruit this type of complexes at the level of repressed sequences in order to activate transcription or they can help them for nucleosome sliding or DNA rotation during transcriptional activation (Reeves and Beckerbauer, 2001).

The second mechanism that HMGA exploit to regulate gene expression involves the formation of multiprotein complexes, called enhanceosomes, which allow the interaction between distal (enhancers) and proximal (promoters) regulatory elements. In this way, general transcription factors can contact specific activators, co-activators, and chromatin structure modifiers leading to the recruitment of the RNA Pol II complex and transcription initiation. A striking example is represented by interferon-β (IFN- β) gene regulation. In this case, HMGA1a protein

participates in the formation of a multifactor complex, composed of NF-kB (Nuclear factor k-light-chain-enhancer of activated B cells), IRF (INF-regulatory factor 1) and ATF2 (Activating Transcription Factor 2)/cJUN transcription factors, which assemble on the enhancer region of this gene. In this context, HMGA1a plays a dual role: first, it induces an allosteric change in DNA structure, therefore allowing transcription factors access and their right positioning; second, it directly interacts with the transcription factors to complete the assembly of the nucleoprotein complex and promote its stability. This complex comprises also CBP, P/CAF and RNA Pol II holoenzyme. CBP and P/CAF are co-activators that have acetyltransferase activity towards histone tails whose function is to further open the chromatin fiber to allow RNA Pol II to start transcription (fig. 1.6) (Thanos and Maniatis, 1995; Yie et al., 1999). HMGA regulate several other genes in this way, including IR gene (Foti et al., 2003) and interleukin-2 receptor (IL-2Rα) gene in T cells (John et al., 1995).

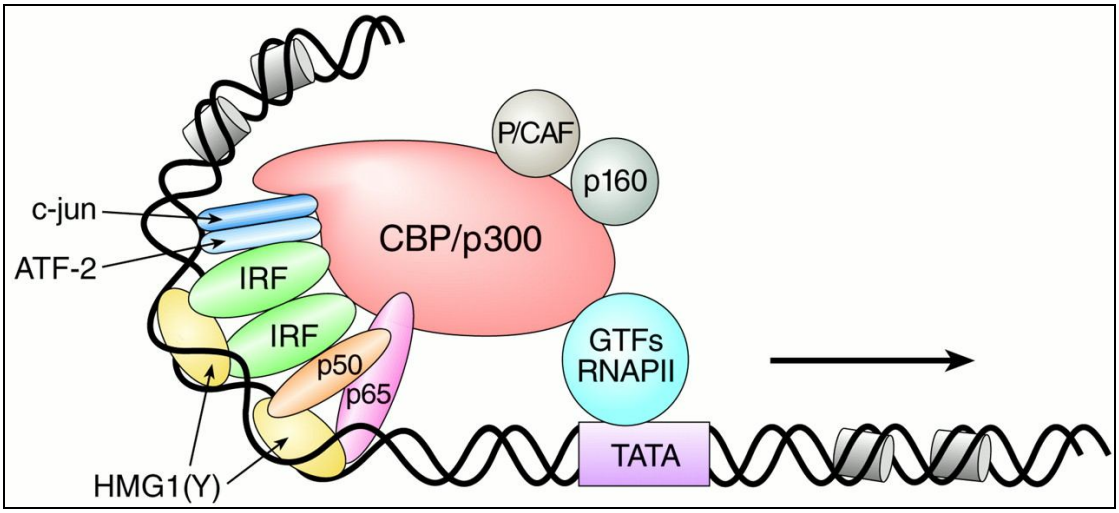

Figure 1.6: Enhanceosome formation on Interferon β gene (IFN β). By binding to IFN β enhancer, HMGA1 coordinates the assembly of a stereospecific macromolecular complex composed by c-jun, ATF-2, IRF, NFkB (p50 and p65), CBP/p300, P/CAF and p160, which in turn recruit to promoters the RNApol II complex, to start transcription (Vo and Goodman, 2001).

HMGA can activate or repress gene expression even just by interacting with transcription factors. Indeed, HMGA can modify their DNA binding affinity by means of direct protein-protein interactions. For instance, HMGA1a binding to PU.1 transcription factor induces a conformational change in this protein causing an affinity increase for its binding site at the level of the immunoglobulin IgM heavy chain gene (Lewis et al., 2001). Conversely, HMGA2 allows Cyclin A gene transcription by binding to the repressor $p120^{E4F}$ (E1A-regulated

transcriptional repressor) and causing its displacement from the CRE (cAMP responsive element) site on DNA. Afterwards, HMGA2 recruits at the same level the ATF/CREB family factors to activate transcription (Tessari et al., 2003).
By this mechanism of action HMGA proteins modulate the activity of a plethora of nuclear factors (Sgarra et al., 2010), among which it is relevant to cite, given their central role in cell proliferation and survival, pRB and p53 (Fedele et al., 2006; Ueda et al., 2007; Frasca et al., 2006).

1.9 HMGA and neoplastic transformation

As previously mentioned, HMGA proteins are almost undetectable in normal adult tissues. On the contrary, they are found to be highly expressed in cancer cells (Bustin and Reeves, 1996). Many works indicate that their increment is not only associated to neoplastic transformation but rather they have a causal role in this process (Fusco and Fedele, 2007). Indeed, when over-expressed in cells they promote cancer progression and metastasis (Reeves et al, 2001), while it has been demonstrated by antisense strategies in thyroid cells that HMGA1 is fundamental for the neoplastic transformation process induced by the MPSV and KiMSV transforming viruses (Berlingieri et al, 2002). In addition, transgenic mice over-expressing HMGA genes develop different types of tumors, further demonstrating HMGA oncogenic properties *in vivo* (Fedele et al., 2002; Fedele et al., 2005).
Immunohistochemical screenings demonstrated that wild-type HMGA1a and HMGA1b proteins are highly expressed in different types of human carcinomas, such as the pancreas, thyroid, colon, mammary gland, and uterine cervix ones (Fusco and Fedele, 2007). In addition, many benign tumors, such as lipomas and leiomyomas, show chromosomal rearrangements leading to the formation of chimeric HMGA proteins. In particular, this has been shown for HMGA2 gene (Hess, 1998).
Most of the known mechanisms by which HMGA induce cell transformation regards their ability to regulate directly or indirectly the expression of genes playing a crucial role in controlling cell proliferation and invasion (Fusco and Fedele, 2007). Indeed, it has been demonstrated by gene array analyses that HMGA proteins are involved in the regulation of hundreds of genes, including cell cycle regulators, signal transduction factors and cell adhesion, motility and invasion genes (Reeves et al., 2001, Pegoraro et al., 2013, Shah et al., 2013).

As previously described, HMGA2 induces E2F1 transcription factor activity. E2F1 allows cell S phase entry by targeting genes involved in cell cycle regulation. In this way, HMGA2 over-expression promotes tumorigenesis. In particular, Cyclin A gene is one of the E2F1 targets. It is required both for the progression in S phase and for the transition G2/M. As well as being activated by HMGA2 through E2F1, this gene is also de-repressed by the association between HMGA2 and $p120^{E4F}$ transcriptional repressor (Tessari et al., 2003).

In addition, HMGA can regulate Cyclin A expression by activating AP1 transcriptional complex (Vallone et al., 1997; Casalino et al., 2007), which is involved in controlling cell proliferation, tumorigenesis and metastasis. Another HMGA-related aspect revealing their oncogenic role is the epithelial-to-mesenchymal transition (EMT) induction, which is a cell process linked to cell invasion and metastasis. In pancreatic cancer cells, RAS oncogenic pathway leads to HMGA2 over-expression by activating a MAPK phosphorylation cascade. Concomitantly, cells partially lose peculiar epithelial properties and acquire a mesenchymal phenotype characterized by an augmented motility (Watanabe et al, 2009). Similarly, expression of antisense or dominant-negative HMGA1 constructs inhibits MCF-7 breast cancer cells anchorage-independent growth (Reeves et al, 2001). Always linked to HMGA role in EMT, it has been recently demonstrated that HMGA1 down-regulation causes a re-localisation of cytoskeletric proteins F-actin and β-catenin, as well as the decrease in vimentin mRNA (mesenchymal marker) and stress fibers (Pegoraro et al, 2013, Shah et al, 2013).

Interestingly, very recently Hmga2 has been demonstrated to promote lung cancer progression acting as a competing endogenous RNA (ceRNA) for the let-7 miRNA family. Indeed, Hmga2 mRNA possesses let-7 binding sites by which it decoys this miRNA family to regulate TGF-β co-receptor (Tgfbr3) expression and enhance TGF-β signaling (Kumar et al, 2014).

As well as being oncogenes, HMGA have been surprisingly demonstrated to act also as oncosuppressors. Indeed, $Hmga1^{-/-}$ and $Hmga1^{+/-}$ mice develop age-dependent splenomegaly associated with lymphoid cell expansions, resembling various human B cells lymphomas (Fedele et al., 2006). In addition, HMGA proteins have been demonstrated to have a role in the formation of senescence-associated heterochromatic foci, which represent structures preventing the expression of proliferation-associated genes and block cell transformation. This unexpected dual role in cell transformation (oncogene vs oncosuppressor) could depend on their peculiar mechanism of action. Indeed, HMGA perform their various functions always in cooperation with other factors/partners and therefore, their functional output is strictly cell context-dependent.

2. AIM OF THE STUDY

Gene expression is widely regulated by histone PTMs, which modulate chromatin structure and the binding of specific proteins responsible for transcription regulation. Given their functional role, histone PTMs alterations have been found to be involved in cancer development and progression.

HMGA are oncoproteins regulating a huge number of genes, which underlie different cellular processes, ranging from signal transduction to cell cycle regulation. Several mechanisms of action have been well characterised for these architectural factors, including enhanceosome formation and DNA bending. Nevertheless, information regarding the functional role of the interaction between HMGA and core histones is still lacking.

We hypothesised that HMGA1 protein can regulate gene expression even by interacting with core histones and consequently by modulating their post-translational modification level.

3. MATERIALS AND METHODS

3.1 Cell lines and culture conditions

MDA-MB-231, MDA-MB-157, MDA-MB-468, and MDA-MB-453 breast cancer cell lines were cultivated in DMEM (*Dulbecco's Modified Essential Medium,* Euroclone, #ECB75011L) supplemented with 10% FBS (*Fetal Bovine Serum,* Euroclone, #ECS0180L), 2 mM L-glutamine (Euroclone, #ECB3000D), 100 U/ml penicillin, and 100 μg/ml streptomycin (EuroClone, #ECB3001D). Cells were grown at 37 °C in humidified 5% CO_2 incubator and expanded every 3-4 days in a sub-cultivation ratio depending on confluence level and ATCC recommendations. Cell monolayers were dissociated by trypsin-EDTA (EuroClone, #ECB3052D) at 37° C. Trypsin was neutralized by adding culture medium. Cells were collected by centrifugation (200 g, RT (Room Temperature), 5 min), resuspended in fresh medium, and seeded. For long term storage cells were resuspended in FBS 10% (v/v) DMSO (AnalaR BDH, #10336N) and conserved in cryovials in liquid nitrogen.

3.2 Cell counting

Cells in suspension were counted by means of Scepter 2.0 (Merck Millipore, #PHCC20060). This instrument takes advantage of the Coulter principle: as cells flow through the aperture in the sensor, resistance increases, and, by Ohm's law, this increase in resistance causes a subsequent increase in voltage. Voltage changes are recorded as spikes with each passing cell. Spikes of the same size are bucketed into a histogram and counted.

3.3 Drug treatments

Cells were seeded at $9{,}2x10^3$ cells/cm^2 density in culture medium. After 72 h, cells were treated with culture medium containing the drug or DMSO, as negative control. The following drugs have been used: H89 (Sigma Aldrich, #B1427), BI-D1870 (Axon MedChem, #1528), SB747651A (Axon MedChem, #1897), BIRB796 (Axon MedChem, #1358), UO126 (Merck Chemicals, #662005), and Emodin (Sigma Aldrich, #E7881). H89, BI-D1870, SB747651A, BIRB796, and UO126 treatments were performed for 24 h, while Emodin treatment was performed for 48 h. After treatments, cells were subjected to other assays or harvested for protein or RNA extraction.

3.4 MTS proliferation assay

The MTS assay (Promega, CellTiter 96® AQ_{ueous} Non-Radioactive Cell Proliferation Assay, #G5421) is a colorimetric method for determining the number of viable cells in proliferation, citotoxycity, and chemosensitivity assays. The CellTiter 96® AQueous Assay is composed of solutions of a tetrazolium compound (MTS - 3-(4,5-dimethylthiazol-2-yl)-5-(3-carboxymethoxyphenyl)-2-(4-sulfophenyl)-2H-tetrazolium, inner salt) and an electron coupling reagent (phenazine methosulfate) PMS. MTS is bioreduced by cells into a formazan product that is soluble in tissue culture medium. The absorbance of the formazan product at 490 nm can be measured directly from 96-well assay plates without additional processing. The conversion of MTS into the aqueous soluble formazan product is accomplished by dehydrogenase enzymes found in metabolically active cells. The quantity of formazan product as measured by the amount of 490 nm absorbance is directly proportional to the number of living cells in culture.

Cells were seeded at 5000 cells/well density in a 96-multiwell plate and grown for 72 h. After drug treatments, cells were subjected to MTS assay every 24 h. Culture medium was removed and replaced with 200 µL of MTS reagent diluted 1:6 in PBS (137 mM NaCl, 27 mM KCl, 4.3 mM Na_2HPO_4, 1.4 mM KH_2PO_4, pH 7.4) 4.5 g/L glucose (Huang et al., 2004). Cells were incubated at 37° C 5% CO_2 for 2 h and 30 min in the dark since MTS is photosensitive and after incubation, absorbance at 490 nm was measured by a TECAN microplate reader. By plotting absorbance values versus time-points we obtained a curve indicating metabolic activity and therefore cell proliferation.

3.5 Short interfering RNA (siRNA) assay

For transfection of siRNAs, cells were seeded at $21x10^3$ cells/cm^2 density in culture medium without antibiotics. After 24 h, cells were transfected by adding siRNAs (see the table for details) and LipofectamineTM RNAiMAX reagent (5 µL for 35-mm plates) according to manufacturer's instructions (Invitrogen, #13778-075) diluted in culture medium without antibiotics and FBS. After 72 h, cells were harvested for protein or RNA extraction.

siRNA	FINAL CONCENTRATION
siCTRL – negative control (Pegoraro et al., 2013)	10 nM
siA1_1 – HMGA1 (Pegoraro et al., 2013)	10 nM

siA1_3 – HMGA1 (Pegoraro et al., 2013)	10 nM
siAURKB – AURKB (Pegoraro et al., 2013)	10 nM
Silencer® Select Negative Control (Life Technologies, #4390846)	5 nM
HMGA1 - Silencer® Select Pre-Designed and Validated siRNA (Life Technologies, #4427037-s6667)	5 nM
MSK1 - Silencer® Select Pre-Designed and Validated siRNA (Life Technologies, #4427038-s1769)	5 nM
MSK2 - Silencer® Select Pre-Designed and Validated siRNA (Life Technologies, #4427038-s17138)	5 nM

3.6 *Wound healing* assay

Wound healing assay is an *in vitro* technique which allows you to evaluate migration of adherent growing cells. Cells were cultivated on 50-mm plates and treated with drugs as described above. Cell number was set so that cells could reach 80-90% confluence after treatment. Cells were *scratched* with a 200-µl tip, and wound closure was followed for 4 and 8 hours. Images of the same area were taken for each plate at any time point with Canon PowerShot A630 camera.

3.7 Sodium Dodecyl Sulphate (SDS) protein extraction

After treatments, cells were washed twice with cold PBS and lysed with a scraper in SDS sample buffer (125 mM Tris/HCl pH 6.8, 4% (w/v) SDS, 20% (v/v) glycerol, 0.2 M dithiothreitol (DTT) for total protein extraction. After collection, cell lysate was further disrupted with an insulin syringe, boiled for 5 min at 95° C, and conserved at -20° C.

3.8 SDS - PolyAcrylamide Gel Electrophoresis (SDS-PAGE)

Total cell lysates were separated by using an SDS-PAGE gel system. *Stacking gel:* polyacrylamide gel (T=5%, C=3.3%) in 1.15 M Tris/HCl pH 8.45, 0.11% (w/v) SDS and 1 mg/mL ammonium persulfate (APS). Polymerization occurred by addition of TEMED (2 µL for 1 mL solution).

Running gel: polyacrylamide gel (T=15%, C=3.3%) in 1.6 M Tris/HCl pH 8.45, 0.16% SDS and 1 mg/mL APS. Polymerization occurred by addition of TEMED (4 µL for 10 mL solution). Gel thickness: 0.75 mm – length of *stacking* gel: 0.5 cm and length of *running* gel: 8 cm – gel width: 8 cm. *Running buffer – Cathode:* 0.1 M Tris, 0.1 M Tricine, 0.1% (w/v) SDS,

pH 8.25. *Running buffer – Anode:* 0.1 M Tris/HCl, pH 8.9. Electrophoretic run consisted of two steps: accumulation (20 mA V for 30 min) and separation (50 mA for about 1 h).

3.9 Blue Coomassie staining

SDS-PAGE separated proteins were fixed and stained by using a methanol/water/acetic acid solution (in a 5/4/1 volume ratio) containing 0.05% (w/v) Coomassie Brilliant Blue R 250. Dye excess was eliminated by 10% (v/v) acetic acid washes.

3.10 Protein quantification and normalization with densitometry

Optical densities of total cell lysates resolved in SDS-PAGE and Coomassie stained were determined by using Image Scanner and Image Master 2D Software (Amersham Pharmacia Biotech). Unknown protein concentrations were calculated on the basis of a reference protein calibration curve.

3.11 Protein quantification with Bicinchoninic acid assay (BCA)

BCA protein assay (BCA protein assay reagent kit, Pierce, #23225) is a detergent-compatible quantification method. It takes advantage from the biuret reaction whereby Cu^{+2} is reduced to Cu^{+1} by protein in an alkaline medium. The chelation of two molecules of BCA with one cuprous ion (Cu^{+1}) forms a purple-colored reaction product, which is water-soluble and exhibits a strong absorbance at 562 nm. The color intensity is related to the number of peptide bonds, to the macromolecular structure of the protein, and to the presence of four particular aminoacids (cysteine, cystine, tryptophan, and tyrosine).

This assay was performed in 96-multiwell plates according to the manufacturer's instructions and absorbance at 562 nm was measured by a TECAN microplate reader. Protein concentrations were determined on the basis of a Bovine Serum Albumine (BSA) calibration curve.

3.12 Western blot

Proteins separated by SDS-PAGE were transferred to nitrocellulose membrane Ø 0.2 μm (GE Healthcare, Whatman™, #10401396) using a wet transfer system (transfer buffer: 20% methanol, 25 mM Tris, 200 mM Glycine) at 4° C for 16 h at limiting current (75 mA). All the following steps were performed at RT. Transferred proteins were visualized by staining the membrane with Red Ponceau solution (0.2% Red Ponceau S; 3% trichloroacetic acid; 3%

sulfosalicylic acid) for 10 min. Nonspecific binding sites were saturated by shaking incubation of the membrane with blocking solution (5% NFDM - nonfat dry milk (w/v) and 0.1% (v/v) Tween 20 in PBS) for 1 h. Afterwards, the membrane was shaking incubated with primary antibody diluted in blocking solution (see the table for details) for 1 h and subsequently washed three times for 5 min with blocking solution. The membrane was then shaking incubated with horseradish peroxidase-conjugated secondary antibodies diluted in blocking solution for 1 h (see the table for details) and washed again for three times with blocking solution and once with PBS. Bands were visualized with ECL kit, (Thermo Scientific, #2106) on autoradiography films (GE Healthcare, #28-9068-48).

PRIMARY ANTIBODY
α-HMGA1 1:500
α-H3 1:4000 (Abcam, #ab1791)
α-H3K9me3 1:1000 (Abcam, #ab8898)
α-H3S10ph 1:1000 (Abcam, #ab5176)
α-H3K14ac 1:2000 (Abcam, #ab52946)
α-H3K27me3 1:1000 (Cell Signaling Technology, #C36B11)
α-H3S28ph 1:500 (Millipore, #07-145)
α-MSK1 1:1000 (Cell Signaling Technology, #C27B2)
α -ERK1/2 1:1000 (Sigma Aldrich, #M5670)
α-pERK1/2 1:1000 (Sigma Aldrich, #M8159)
α-AURKB 1:1000 (Novus Biologicals, # NB100-294)
α-RSK2 1.500 (Millipore, #06-918)
SECONDARY ANTIBODY
α-Rabbit IgG (Whole molecule) Peroxidase conjugate 1:5000 (Sigma-Aldrich, #A0545)

3.13 Co-ImmunoPrecipitation (Co-IP)

*Cell lysi*s: Cells were cultivated on 150-mm plates until reaching 70-80% confluence. They were washed twice with cold PBS and gently collected with scrapers. After centrifugation (4° C, 450 g, 5 min), supernatant was discarded and pellet resuspended in PBS and again centrifuged. Supernatant was eliminated and pellet resuspended in lysis buffer (1 mL for each 150-mm plate) (25 mM Tris/HCl pH 8, 0.5% (v/v), 125 mM NaCl, 10% v/v glycerol) supplemented with PMSF, (*Phenylmetylsulfonyl Fluoride*, satured solution in isopropanol) in a

ratio of 1:1000 (v/v), 1 mM $NaVO_3$, 5 mM NaF, 10 mM Sodium Butyrate and protease inhibitor cocktail (PIC, Protease Inhibitor Cocktail, Sigma Aldrich, #P8340) in a ratio of 1:100 (v/v). Lysate was then incubated for 15 min on ice, sonicated (*Digital Sonifier 250, Branson*) at 30% potency for 60 sec (10 sec ON, 20 sec OFF on ice, for six times) and centrifuged (4° C, 8385 g, 10 min). Supernatant was transferred to a new tube and stored at -80° C.

Co-IP: 30 µL of Protein G Sepharose (Protein G Sepharose™ 4 Fast Flow, Amersham Biosciences, #17-0618-01) for each sample (experiment and negative control) were washed three times with 1 mL of 50 mM Tris/HClpH 7 (centrifugation 4° C, 1027 g, 1 min) in low-binding tubes (Sigma Aldrich, #T3406-250EA). 40 µg of antibody and pre-immune serum (used as negative control) diluted in 500 µL of 50 mM Tris/HCl pH 7 were added to the tubes and shaking incubated for 1h at 4° C. After incubation, samples were washed three times as above and at the end, supernatant was discarded.

Nonspecific binding sites were saturated by shaking incubation of Protein G Sepharose conditioned with antibody/pre-immune serum with 1 mg/mL BSA in lysis buffer for 1 h at 4° C. At the end, samples were washed trhee times with lysis buffer as above and supernatant was discarded. 250 µg of cell lysate (quantified by BCA protein assay, see paragraph 3.2.5) in 1 mL volume were added to each tube and shaking incubated for 3 h at 4° C. After incubation, tubes were centrifuged (4° C, 1027 g, 1 min), supernatant was eliminated and samples were washed three times with lysis buffer as above. At the end, all the supernatant was removed and 40 µL of SDS sample buffer were added to the tubes in order to elute co-immunoprecipitated proteins. Samples were then boiled at 95° C for 5 min and analyzed by Western blot.

3.14 Chromatin Immuno-Precipitation (ChIP)

Chromatin preparation: Cells were cultivated on 100-mm dishes and treated with 10 µM BI-D1870 (24 h) until reaching 80% confluency. Cells were then incubated with 1% formaldehyde medium in agitation for 10 min to crosslink proteins and DNA. Then, they were washed twice with PBS RT and incubated with 125 mM Glycine/PBS (RT) for 5 min. After two washing with cold PBS, cells were gently scraped with cold PBS and pelletted (4° C, 450 g, 10 min). Pellet was then resuspended with 1 mL of cold Lysis Buffer (5 mM PIPES pH 6.8, 85 mM KCl, 0,5% NP40 (v/v)) supplemented with PIC (Protease Inhibitor Cocktail, Sigma Aldrich) and shaking incubated for 10 min at 4° C. Afterwards, solution was centrifuged (4° C, 2100 g, 10 min) and pellet was resuspended with 1 mL of cold RIPA 100 (20 mM Tris-HCl pH 7.5, 100 mM NaCl, 1mM EDTA, 0,5% NP40 (v/v), 0,05% Na-deoxycholate (v/v), 0,1%

SDS (w/v)) supplemented with PIC. Samples were then sonicated (*Digital Sonifier 250, Branson*) at 30% potency for 1 min 20 sec (10 sec ON, 30 sec OFF on ice, for eight times) in order to achieve DNA fragments of 500 bp in average length.

DNA fragment size control: 100 µL of each sample were supplemented with 400 µL H_2O mQ and 20 µL NaCl 5M and shaking incubated at 65° C o/n, to decrosslink DNA/protein complexes. Afterwards, samples were complemented with 20 µL 1 M Tris/HCl pH 6.5, 10 µL 0.5 M EDTA pH 8, 50 µg Proteinase K, and 20 µg RNaseA and shaking incubated at 55° C for 2 h. DNA was then extracted by phenol/chloroform, precipitated o/n, and pellet was resuspended with 20 µL H_2O mQ. DNA was then analysed by 2% agarose gel electrophoresis (2% agarose in Tris Acetate EDTA, 0,5 µg/mL EtBr). Electrophoretic run was executed at 50 V for 40 min and gel visualised with *Gel Doc* (*Biora*d).

DNA quantification: Samples were quantified with Qubit fluorometer (Invitrogen) following Quant-iT ^{TM} dsDNA BR Assay kit (Invitrogen^{TM}|MOLECULAR PROBES, #Q32850).

Blocking and pre-clearing: for each IP, 20 µL of Protein A/G (Protein G Sepharose^{TM} 4 Fast Flow, #17-0618-01; Protein A Sepharose^{TM} 4 Fast Flow #17-0974-01, Amersham Biosciences) were washed (4° C, 1000 g, 2 min) twice with cold RIPA 100 and blocked by shaking incubation with 1 mL RIPA 100 (1 µg/µL Salmon Sperm DNA, 1 µg/µL BSA) for 1 h at 4° C. Equal amounts of cell lysate (corresponding to 20 µg of DNA) for each sample were then precleared by shaking incubation with blocked A/G beads for 1 h at 4° C.

Lysate/antibody incubation: After incubation, samples were centrifuged (4° C, 1000 g, 2 min), beads discarded, and supernatant (precleared lysate) was shaking incubated o/n at 4° C with 1 µg of specific antibody or IgG (Abcam, #ab37415) as negative control. An aliquot from precleared lysate was conserved as input.

Immunoprecipitation (IP): for each IP, 20 µL of A/G beads blocked o/n as described above were washed twice with RIPA 100 and shaking incubated with lysate/antibody solution for 3 h at 4° C. Beads were then washed twice with cold RIPA 100 supplemented with PIC (one quick washing and one 15 min washing), twice quickly with cold RIPA 250 (20 mM Tris-HCl pH 7.5, 250 mM NaCl, 1mM EDTA, 0,5% NP40 (v/v), 0,05% Na-deoxycholate (v/v), 0,1% SDS (w/v)) supplemented with PIC, and once with cold LiCl solution (10 mM Tris/HCl pH8, 1 mM EDTA, 250 mM LiCl, 0,5% Na-deoxycholate (v/v), 0,5% NP40 (v/v)) for 10 min at 4° C.

Decrosslinking: Afterwards, beads were washed with TE (10 mM Tris/HCl pH 8, 1 mM EDTA pH 8) and resuspended with 100 µL TE. IP and input samples were then complemented with 400 µL H_2O mQ and 20 µL NaCl 5 M. All samples were shaking incubated at 65° C o/n,

to decrosslink DNA/protein complexes and then added with 20 µL 1 M Tris/HCl pH 6.5, 10 µL 0.5 M EDTA pH 8, 50 µg Proteinase K, and 20 µg RNaseA (IP were also complemented with 10 µL 10% SDS) and shaking incubated at 55° C for 2 h.
DNA from all samples was then extracted by phenol/chloroform, precipitated o/n, and pellet was resuspended with 20 µL H_2O mQ. DNA was then analysed by qPCR.

3.15 Far-western

1 µg of recombinant H1.0, H2A, H2B, H3.1, H4 (New England Biolabs, #M2501S, #M2502S, #M2505S, #M2503S, and #M2504S, respectively), and Cytochrome C (CytC - Sigma Aldrich) were resolved on SDS-PAGE and transferred to nitrocellulose membrane (see paragraphs 3.2.2 and 3.2.5). Membrane was then treated with decreasing concentrations of guanidium (6 M, 3 M, 1.5 M, 0.75 M, 0.375 M, and 0.187 M) in HBB (10 mM Hepes, 60 mM KCl, 1 mM EDTA, DTT 1 mM, pH 7.5) for 10 min for each guanidium concentration, in order to completely denaturate and subsequently renaturate proteins on the membrane. Afterwards, membrane was washed four times for 5 min with HBB, once for 1 h at 4° C with 5% NFDM, 0.5% NP40, in HBB, once for 30 min at 4° C with 1% NFDM, 0.5% NP40 in HBB, and once for 5 min at 4° C with 1% NFDM, 0.5% NP40 in PIB (15 mM Hepes, 50 mM KCl, 13 mM NaCl, pH 7.5). Membrane was then incubated for 16 h at 4° C with 2 µg/mL recombinant HA-HMGA1a (homemade) in 1% NFDM, 0.5% NP40, in PIB. After incubation, membrane was washed at RT three times for 10 min with 1% NFDM, 0.5% NP40, in PIB, once for 2 min with PIB, and once for 5 min with 5% NFDM, 0.1% Tween20, in PBS. At the end, membrane was subjected to Western blot analysis (see paragraph 3.2.5).

3.16 Immunofluorescence

Cells were grown on glass coverslips. After treatments cells were washed twice with PBS, fixed for 20 min in 4% (v/v) paraformaldehyde in PBS, washed three times with PBS and incubated with 0.1 M Glycine in PBS for 5 min. Cells were then permeabilized with 0.3% (v/v) Triton X-100 in PBS for 5 min, washed three times with PBS and blocked in 0.5% (w/v) BSA in PBS (blocking solution) for 30 min. Cells were incubated with primary antibody diluted in blocking solution (see the table for details) for 90 min in humidified chamber, then washed three times with blocking solution and incubated with secondary antibody diluted in PBS (see the table for details) for 1 h in humidified chamber. After three times washing, cells were stained with 0.2 µg/mL Hoechst (Sigma Aldrich) in PBS for 5 min. Cells were then

washed twice with PBS and once with H_2O mQ. Afterwards, coverslips were mounted on microscope slides with Vectashield (Vector Lab, #H-1000).

PRIMARY ANTIBODY
α-H3S10ph 1:200 (Abcam, #ab5176)
α-H3S28ph 1:100 (Millipore, #07-145)
SECONDARY ANTIBODY
α-Rabbit IgG Alexa Fluor 488 (Invitrogen, #A11008)

Cells were examined with Nikon Eclipse e800 microscope and images were collected with Nikon ACT-1 software.

3.17 RNA extraction

For total RNA extraction cells were cultivated on 35-mm plates. After treatments, cells were washed twice with RT PBS and lysed with 1 mL TRIzol Reagent (Invitrogen, #15596018). Cell lysate was collected and left at RT for 2 min. Afterwards, 200 µL of chloroform were added to the samples and tubes left 2-3 min at RT and then centrifuged at 4° C, 17005 g, 10 min. Aqueous phase was transferred in a new tube and 500 µL of isopropanol were added to the samples. After 10 min RT incubation, samples were centrifuged (4° C, 17005 g, 15 min), supernatant was discarded, and pellet washed with 75% (v/v) ethanol. After centrifugation (4° C, 17005 g, 30 min), supernatant was eliminated and pellet air-dried. Pellet was then resuspended with 30 µL of RNase-free water.

3.18 DNase I digestion

In order to eliminate DNA, RNA samples were subjected to DNase digestion. 1 µL of DNase I (Invitrogen^{TM}, Deoxyribonuclease I, Amplification Grade, #1808-015) and 4µL of 10X DNase I reaction Buffer (200 mM TrisHCl pH 8.4, 20 mM $MgCl_2$, 500 mM KCl) were added to each sample. After 15 min RT incubation, reaction was inactivated by the addition of EDTA to a final concentration of 2 mM and by incubating tubes at 65° C for 10 min.

3.19 RNA cleanup

RNA was column-purified with RNeasy® Mini Kit (*Qiagen,* #74104) according to the manufacturer's protocol. At the end, samples were eluted with 50 µL of RNase-free water and stored at -80° C.

3.20 RNA quantification

RNA was quantified by means of Qubit fluorometer (Invitrogen) following Quant-iT ™ RNA Assay kit (Invitrogen™|MOLECULAR PROBES, #Q328521) datasheet.

3.21 RNA quality control: agarose gel electrophoresis

RNA samples were subjected to agarose gel electrophoresis in order to evaluate its quality and exclude DNA contamination. *Agarose gel*: 1% (w/v) agarose, 6,67% (v/v) formaldehyde, in MOPS buffer (20 mM MOPS, 5 mM sodium acetate, 1 mM EDTA, pH 7). Electrophoresis apparatus was pretreated for 30 min with 0.1 M NaOH to remove contaminant RNases. Before analysis, RNA samples were conditioned with loading buffer (10% (v/v) glycerol, 0,4% (w/v) SDS, 3,34 ng/mL Ethidium Bromide, trace bromophenol blue, in MOPS), denatured at 68° C for 5 min, and left on ice in order to maintain denatured state. Electrophoretic run was executed at 50 V for 40 min and gel visualised with *Gel Doc* (*Biora*d).

3.22 Reverse transcription

For reverse transcription 1 µg of purified RNA was incubated with 150 ng of Random Primers (Invitrogen™*,* #48190-011) and 1 µL of 10mM dNTPs in 12 µL of RNase-free H_2O. After denaturation (65° C, 5 min), samples were maintained on ice and subsequently conditioned with 4 µL of First Strand Buffer 5X (50 mM Tris-HCl pH 8.3, 75 mM KCl, 3 mM $MgCl_2$), 2 µL of DTT 0.1M mM, and 1 µL of RNase OUT 40U (RNase OUT™ Recombinant Ribonuclease Inhibitor, Invitrogen™, #10777-019). After 2 min RT, 200 U SuperScript ™ Reverse Transcriptase (Invitrogen™, #18080-093) were added to the samples and tubes incubated for 5 min RT, 1 h 50° C, and 15 min 70° C. Reverse-transcribed RNA (cDNA) was then stored at -20° C.

3.23 Quantitative Polymerase Chain Reaction (qPCR)

Quantitative PCR was performed by using iQ™ SYBR Green Supermix (*BIO-RAD*, #170-8887), which contains Taq DNA polymerase, dNTPs, $MgCl_2$, SYBR Green I dye, enhancers,

stabilizers, and fluorescein. 1 µL of each sample (cDNAs diluted 1:50 for RT-qPCR or immunoprecipitated DNA for ChIP-qPCR) was mixed in a 96-multiwell plate (*BIO-RAD*, #HSL9605) with gene-specific forward and reverse primers (see the table for sequences) to a final concentration of 150 mM, and 7,5 µL of iQ™ SYBR Green Supermix in 15 µL H_2O mQ. PCR reactions were performed for 40 cycles (denaturation at 95° C, amplification at 60° C) by means of Biorad CFX instrument and data were analyzed with Biorad CFX Manager software. GAPDH and CYC33 mRNA served as endogenous normalization controls (reference genes) for mRNA expression analysis. Relative gene expression was calculated via the Pfaffl method, which takes amplification efficiencies of reference and target genes into consideration, in order to determine expression ratios between samples. Amplification efficiencies were calculated from the slope of standard curves, created for each primer pair.

As regards ChIP-qPCR, signals from immunoprecipitaed DNA were divided by signals obtained from an input sample, which represents the amount of chromatin used in the ChIP.

RT-qPCR:

TARGET GENE	FORWARD PRIMER (5'-3')	REVERSE PRIMER (5'-3')
GAPDH	TCTCTGCTCCTCCTGTTC	GCCCAATACGACCAAATCC
CYC33	CTTCATGCTGCGTTCATTCC	CCTCGGTGCTTTTCTGTTTC
MSK1	TGGAACACATTAGGCAGTCG	ACCTCATGCTCTGTGAAACG
MSK2	CAAGCTCGGCATCATTACC	TCTTTCTCCTCCGTCAGGAAC
HMGA1	ACCAGCGCCAAATGTTCATCCTCA	AGCCCCTCTTCCCCACAAAGAGT
AURKB	TGAGGAGGAAGACAATGTGTGGCA	AGGTCTCGTTGTGTGATGCACTCT
KIF4A	AAGCCAAACGCCATCTGAATGACC	TTGACCACGCACTTCAGTAAGGGA
KIF23	CCTGAGGGCTACAGACTCAACCGA	TCTGGGTGGTGTGAGTGCCAA
HIST1H3B	TGGCTCGTACTAAACAGACAGC	GGTAACGGTGAGGCTTTTTC
CENPF	TCAGGCAAGAGGCAAAGATCCAGT	TGGCTCAAACTCAGTACCTTCCGT
JUN	ATCAAGTGGCATGTGCTGTG	CCACCAATTCCTGCTTTGAG
FOS	GTTGTGAAGACCATGACAGGAG	TCCTTTCCCTTCGGATTCTC
MYC	TTCGGGTAGTGGAAAACCAG	TCGTCGCAGTAGAAATACGG
ATF3	GGTTTGCCATCCAGAACAAG	CGTCGCCTCTTTTTCCTTTC
COX-2	TGAGTGTGGGATTTGACCAG	CTGTGTTTGGAGTGGGTTTC

ChIP-qPCR:

TARGET SEQUENCE	FORWARD PRIMER (5'-3')	REVERSE PRIMER (5'-3')
-800	CAAACAACACGGCAGCTAAC	TCTGACATTCCTGGGAGGAG
TSS	TTGGGTTCCCATGACTTACG	CCCGCAAACAACTGAATCTG
intrag	CCAAACTGCTCAGGCATAAC	ATCAGGCGACAGATTGAAGG

3.24 Statistical analysis

Data were analyzed by a two-tailed Student's t test and results were considered significant at a p-value < 0.05. The results are presented as the mean and standard deviation (±SD).

4. RESULTS

4.1 HMGA proteins interact with histones

Literature data showed that HMGA proteins are able to contact nucleosomes (Reeves and Nissen, 1993). Moreover, blot-overlay experiments performed in our laboratory before this thesis work revealed that HMGA are able to bind directly both to the core histones and to histone H1 (fig. 4.1).

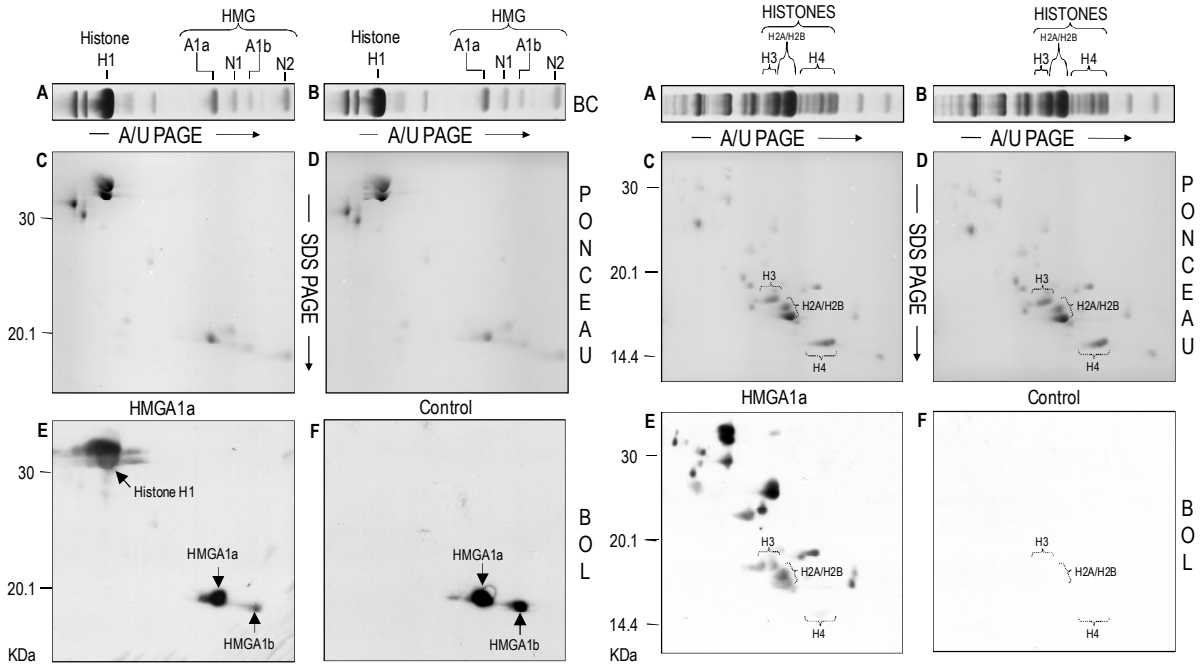

Figure 4.1: HMGA1a interacts with purified histones. Histone H1 (left side) and core histones (right side) were selectively extracted from KG1 cells with PCA 5% and HCl 0.5 M, respectively. Proteins were A/U PAGE (A) and (B) and SDS-PAGE separated, blotted on nitrocellulose membrane, and red ponceau stained (C) and (D). Bands/spots corresponding to histones, HMGA1a, HMGA1b, HMGN1, and HMGN2 are indicated. Membranes were then incubated with recombinant HMGA1a and the interaction detected by western blot using α-HMGA1 antibody (E). As negative control the experiment was performed in the same conditions without HMGA1a (F). Molecular weight markers are indicated on the left (kDa).

To validate blot-overlay results, we performed far western experiments using HA-tagged recombinant HMGA1a and HMGA2 with recombinant histones H1.0, H2A, H2B, H3.1, and H4 (Cytochrome C was used as negative control) (fig. 4.2). This experiment clearly indicates that both HMGA proteins bind *in vitro* to all histones almost equally (lanes 1-5), and that the interaction is specific since HMGA proteins are not able to interact with Cytochrome C (lane 6).

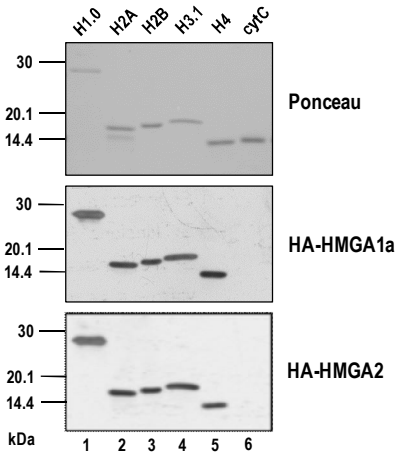

Figure 4.2: HMGA1a and HMGA2 interact with recombinant histones. Equivalent amounts of histones H1.0, H2A, H2B, H3.1, and H4 (lanes 1-5) were SDS-PAGE separated, blotted on nitrocellulose membrane and red ponceau stained. Membranes were then incubated with HA-HMGA1a and HA-HMGA2. Cytochrome C (CytC) was included as negative control (lane 6). Bound proteins were visualised using α-HA antibody. Molecular weight markers are indicated on the left (KDa).

All five histones are subjected to a plethora of post-translational modifications (PTMs). However, at least to our knowledge, histone H3 is the one with the greatest number of modified residues whose function has been assigned. Therefore, we focused our attention on HMGA1/histone H3 interaction (for simplicity, in this thesis work we will refer to both HMGA1a and HMGA1b as a unique protein, i.e. HMGA1). Co-immunoprecipitation was performed in MDA-MB-231 cells, a breast cancer cell line expressing HMGA1 which represents our cellular model, in order to evaluate whether HMGA1 protein can associate with H3 also *in vivo* (fig. 4.3). Total cell lysates were immunoprecipitated with α-HMGA1 antibody (lane 4) or preimmune serum as negative control (lane 2). Western blot analyses clearly demonstrate that HMGA1 was efficiently immunoprecipitated and that histone H3 was specifically co-purified with HMGA1, indicating that these proteins associate also *in vivo*. Since both HMGA1 and H3 are DNA-binding proteins, the same experiment was performed in the presence of ethidium bromide (EtBr) 50 µg/mL (lanes 5 and 3) in order to exclude that this association was DNA-mediated (Lai and Herr, 1992). Results indicate that HMGA1/H3 interaction was still present, thus demonstrating that DNA does not participate in the formation of this complex.

Despite the fact that Co-IP assays cannot distinguish between direct or indirect associations, blot-overlay and far western experiments demonstrated that HMGA make contact directly with histones *in vitro*. Therefore, it is likely that HMGA1 can directly interact with H3 also *in vivo*.

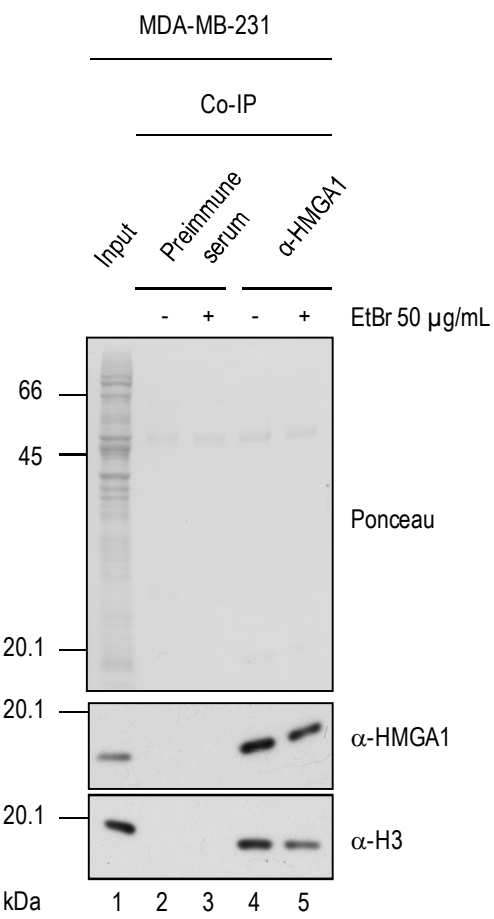

Figure 4.3: HMGA1 interacts with histone H3 *in vivo*. MDA-MB-231 cell lysates were immunoprecipitated with α-HMGA1 antibody and preimmune serum as negative control in the presence (lanes 5 and 3) or absence (lanes 4 and 2) of EtBr and analysed by western blot. 10% and 30% of the input were loaded as control for HMGA1 and H3 expression, respectively (lane 1). A representative red ponceau stained membrane is shown as loading and quantification control. Molecular weight markers (kDa) are indicated on the left.

4.2 H3 post-translational modification level is linked to HMGA1 expression in MDA-MB-231 cells

HMGA proteins are known to regulate chromatin-related processes, both by modulating DNA structure and by interacting with several transcription factors (Sgarra et al., 2004 and 2010). Here we demonstrated that HMGA1 is able to bind *in vivo* to histone H3, which is a fundamental regulator of chromatin functions along with the other histones, thanks to the PTMs it is subjected to. We hypothesised that this interaction could affect H3 PTMs, for instance by sterically impeding or on the contrary promoting enzyme accessibility. To evaluate this possibility, HMGA1 expression was down-regulated by small interfering RNA (siRNA) in MDA-MB-231 cells and samples were analysed by western blot looking at a set of H3 PTMs: Lysine 9 tri-methylation (H3K9me3), Serine 10 phosphorylation (H3S10ph), Lysine 14 acetylation (H3K14ac), Lysine 27 tri-methylation and Serine 28 phosphorylation (H3S28ph) (fig. 4.4). Despite the low efficiency of HMGA1 silencing obtained in this experiment, results indicate that H3S10ph and H3S28ph were significantly down-regulated upon HMGA1 silencing (lanes 2, 4, and 6) with respect to the mock cells (lanes 1, 3, and 5) while H3K14ac

was decreased to a lesser extent. On the contrary, H3K9me3 and H3K27me3 levels were unaffected by HMGA1 presence.

Also total H3 level was slightly reduced upon HMGA1 silencing. Nevertheless, H3S10ph and H3S28ph down-regulation was more substantial, therefore we assume that this decrease could be ascribed to H3 reduction.

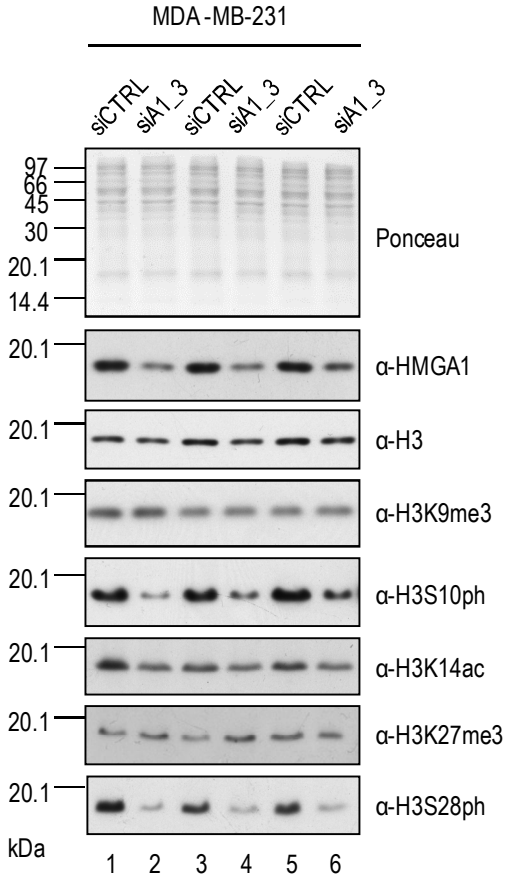

Figure 4.4: HMGA1 affects H3 post-translational modifications in MDA-MB-231 cells. Western blot analysis of MDA-MB-231 cells transfected with control (siCTRL – lanes 1, 3, and 5) and HMGA1 (siA1_3 – lanes 2, 4, and 6) siRNAs and harvested after 72 h. Samples were analysed using antibodies α-HMGA1, α-H3, α-H3K9me3, α-H3S10ph, α-H3K14ac, α-H3K27me3, and α-H3S28ph. The experiment was run and is shown in triplicate. A representative red ponceau stained membrane is shown as loading and quantification control. Molecular weight markers (kDa) are indicated on the left.

Both H3S10ph and H3S28ph are known to be involved in mitotic events and transcriptional activation during interphase (Nowak and Corces, 2004). Data previously obtained in our laboratory by cytofluorimetry demonstrated that HMGA1 silencing does not alter MDA-MB-231 cells distribution among cell cycle phases (G1, G2/S, and M) and that the percentage of cells in M phase was less than 4% (data not shown). Moreover, immunofluorescence analyses show that almost all cells were positive for H3S10ph and H3S28ph staining indicating that these modifications were present in this cell line even during interphase (fig. 4.5). In addition, literature data confirmed that MDA-MB-231 and cancer cells in general exhibit H3S10ph during this cell cycle step (Hsu et al., 2013; Choi et al., 2005). Overall, these data suggest that H3S10ph and H3S28ph affected by HMGA1 expression are modifications carried out during interphase and not linked to mitotic events.

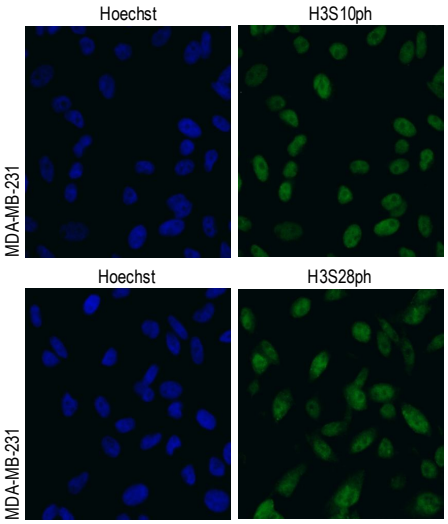

Figure 4.5: H3S10ph and H3S28ph are present in all MDA-MB-231 cells. MDA-MB-231 cells were analysed by immunofluorescence using specific antibodies α-H3S10ph and α-H3S28ph. Hoechst staining indicates nuclei. The experiment was run in triplicate and representative microscopic fields are reported.

The data regarding the modulation of H3 phosphorylation by HMGA1 silencing obtained with siA1_3 (shown in fig. 4.4) were validated by an additional siRNA assay (fig. 4.6), in order to exclude possible *off-target* effects. In particular, MDA-MB-231 cells were transfected with siCTRL (lanes 4, 6, and 8) and siA1_1 (lanes 5, 7, and 9), a siRNA molecule designed like siA1_3 but targeting a different mRNA region (siA1_1: 3' UTR; siA1_3: coding region). Western blot analyses confirmed a substantial H3S10ph down-regulation upon HMGA1 silencing. In fig. 4.6, we can also observe that siCTRL treatment does not alter HMGA1 and H3S10ph levels (lanes 4, 6, 8) with respect to untreated cells (lanes 1-3). This experiment confirms that H3 phosphorylation modulation is specifically dependent on HMGA1 silencing and not due to *off-target* effects.

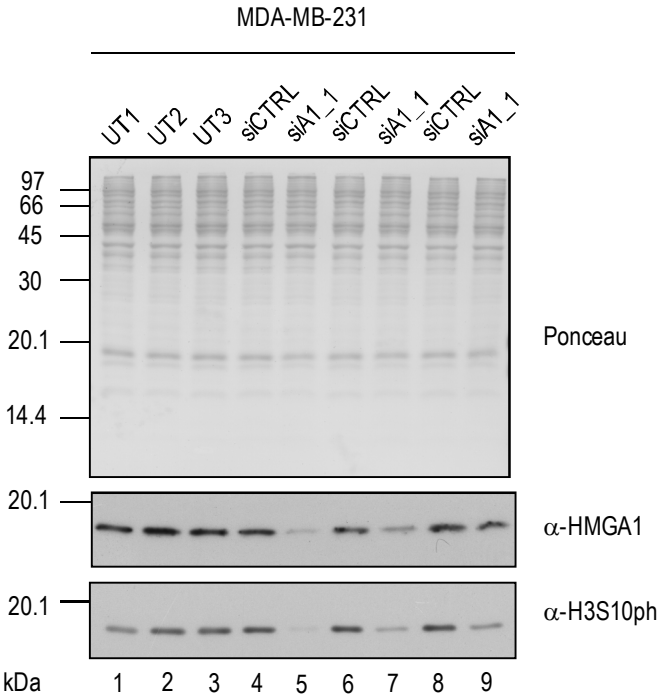

Figure 4.6: H3S10ph modulation is specifically linked to HMGA1 silencing. Western blot analysis of MDA-MB-231 cells transfected with control (siCTRL – lanes 4, 6, and 8) and HMGA1 (siA1_1 – lanes 5, 7, and 9) siRNAs and harvested after 72 h. Lysates from untreated cells were loaded as control for HMGA1 and H3S10ph level (UT1, UT2, and UT3 – lanes 1-3). The experiments were run and are shown in triplicate. A representative red ponceau stained membrane is shown as loading and quantification control. Molecular weight markers (kDa) are indicated on the left.

4.3 HMGA1 silencing modulates H3S10 and H3S28 phosphorylation also in other breast cancer cell lines

In order to test whether HMGA1 regulatory activity towards H3 phosphorylation extended to other cellular contexts, we performed preliminary experiments in MDA-MB-157 and MDA-MB-468, which are triple-negative breast cancer cells, as well as MDA-MB-231. HMGA1 was knocked down by siRNA in these cells and proteins were analysed by western blot (fig. 4.7). Results clearly show that H3S10ph was decreased upon HMGA1 silencing in both cell lines (A and B, lane 2 with respect to lane1). Moreover, also total H3 expression was reduced by HMGA1 down-regulation, as occurred in MDA-MB-231 cells. As discussed for fig. 4.4, also in this case H3S10ph decrease is more evident with respect to H3 down-regulation, therefore again we assume that H3S10ph decrement is attributable solely to H3 reduction.

All these data demonstrate that HMGA1 can regulate H3S10 phosphorylation in different breast cancer cells.

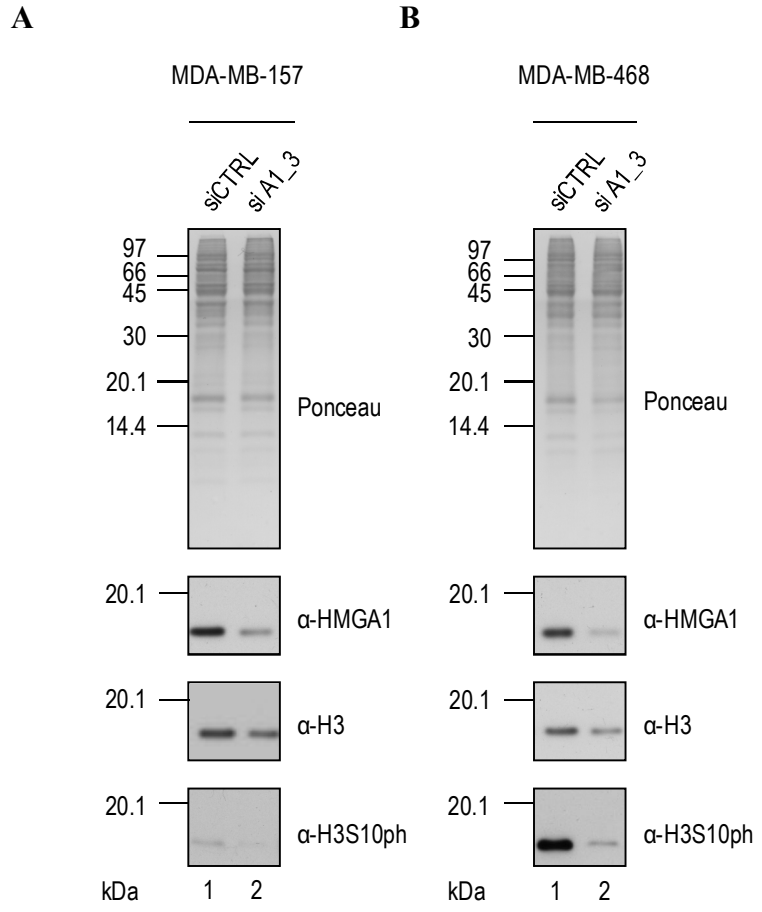

Figure 4.7: HMGA1 affects H3S10ph and H3S28ph also in MDA-MB-157 and MDA-MB-468 cells. (A) Western blot analysis of MDA-MB-157 cells transfected with control (siCTRL – lane1) and HMGA1 (siA1_3 – lanes 2) siRNAs. (B) Western blot analysis of MDA-MB-468 cells transfected with control (siCTRL – lane1) and HMGA1 (siA1_3 – lanes 2) siRNAs. (A) and (B) Cells were harvested after 72 h and samples were analysed using antibodies α-HMGA1, α-H3, and α-H3S10ph. The experiment was run in a single replicate. A representative red ponceau stained membrane is shown as loading and quantification control. Molecular weight markers (kDa) are indicated on the left.

4.4 Interphasic H3S10 and H3S28 phosphorylation is mediated by the RAS/RAF/MEKK/ERK pathway

H3S10 and H3S28 can be phosphorylated by several different kinases depending on cell requirements. The main kinases known to be responsible for these modifications in interphasic cells are RSK2 and MSK1/2. Both can be activated by the RAS/RAF/MEKK/ERK pathway downstream to mitogenic stimuli whereas MSK1/2 is activated also by stress through the p38 MAPK pathway (Sassone-Corsi et al., 1999; Deak et al., 1998). To determine which pathway was responsible for these PTMs in our cellular model, we treated cells with two inhibitors (fig. 4.8), targeting MEK1/2 (UO126 10 μM – fig. 4.8, lanes 2, 5, and 8) and p38 MAPK (BIRB796 10 μM – lanes 3, 6, and 9). Results clearly demonstrate that UO126 treatment significantly inhibited H3S10ph and H3S28ph while these phosphorylations were almost unaffected by BIRB796 with respect to the control cells (lanes 1, 4, and 7), indicating that the pathway leading to H3 phosphorylation that is active in MDA-MB-231 cells is that mediated by RAS/RAF/MEKK/ERK.

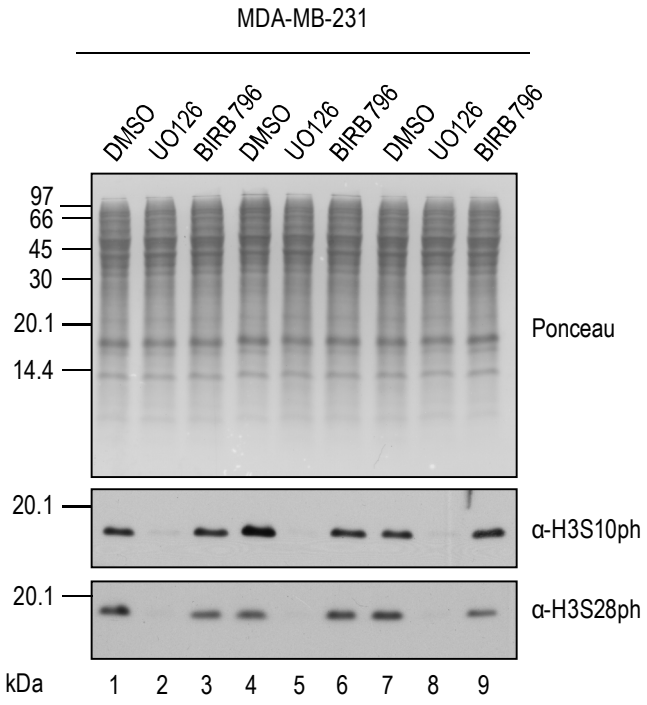

Figure 4.8: H3S10 and H3S28 phosphorylation is mediated by RAS/RAF/MEKK/ERK pathway in MDA-MB-231 cells. Western blot analysis of MDA-MB-231 cells treated with UO126 10 μM (lanes 2, 5, and 8), BIRB796 10 μM (lanes 3, 6, and 9) and DMSO as negative control (lanes 1, 4, and 7). Cells were harvested after 24 h and samples analysed using antibodies α-H3S10ph and α-H3S28ph. The experiment was run and is shown in triplicate. A representative red ponceau stained membrane is shown as loading and quantification control. Molecular weight markers (kDa) are indicated on the left.

4.5 Emodin-mediated phenotype reversion of MDA-MB-453 cells is linked to H3S10ph and H3S28ph down-regulation

We previously demonstrated that HMGA1 knocking down induces the mesenchymal to epithelial transition. In particular, we showed that HMGA1 depletion caused a decrease of migratory and invasive properties of MDA-MB-231, MDA-MB-157, and MDA-MB-468 cell lines (Pegoraro et al., 2013), the same models where we observed H3 phosphorylation down-regulation upon HMGA1 silencing. Therefore, we hypothesised a link between H3S10ph and H3S28ph decrement and the tumour phenotype reversion, both mediated by HMGA1 knocking down.

MDA-MB-453 is a breast cancer cell line over-expressing Her2/neu receptor, which is known to be inhibited by Emodin. When treated with this drug, MDA-MB-453 cells stop proliferating and undergo the tumour phenotype reversion (Zhang et al., 1995). We treated MDA-MB-453 cells with increasing concentrations of Emodin (10, 20, and 40 μM) and observed that, they underwent a morphological change and acquired a more organised distribution similar to that of epithelial cells (fig. 4.9 – A). Importantly, western blot analyses clearly show that the treatment induced a substantial H3S10ph and H3S28ph down-regulation in a dose-dependent manner (fig. 4.9 – B, lanes 2-4, 6-8, and 10- 12), with respect to control cells (lanes 1, 5, and 9). Notably, a reduction in total H3 expression occurred also in this case.

This experiment demonstrates that a morphological change resembling that occurring during mesenchymal to epithelial transition is associated to the decrease of H3S10 and H3S28 phosphorylation.

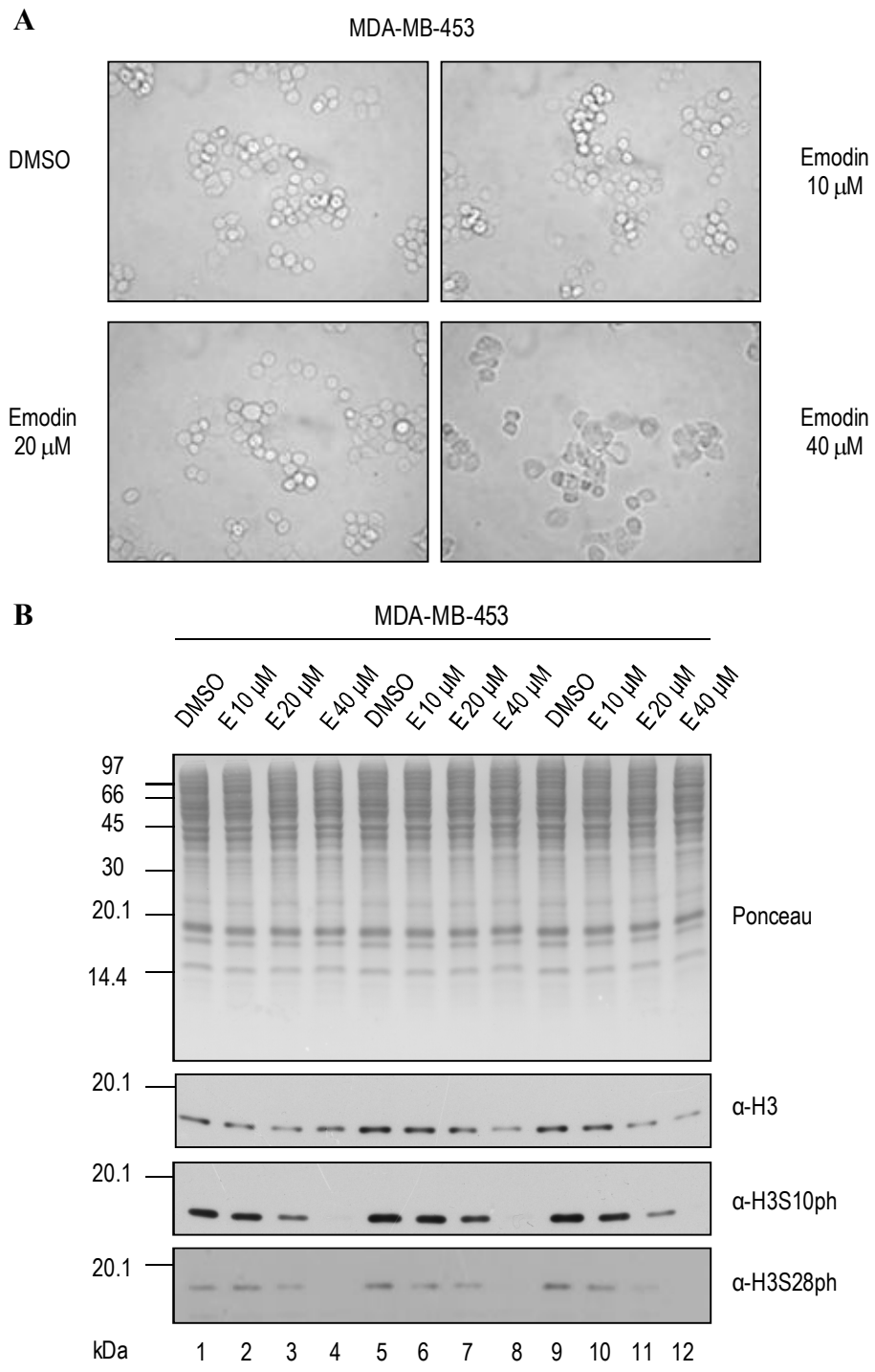

Figure 4.9: Emodin-mediated phenotype reversion is linked to H3S10ph and H3S28ph down-regulation. (A) Microscopic images of MDA-MB-453 cells treated with Emodin 10 μM, 20 μM, and 40 μM and DMSO as negative control. (B) Western blot analysis of MDA-MB-453 cells treated with Emodin 10 μM (lanes 2, 6, and 10), 20 μM (lanes 3, 7, and 11) and 40 μM (lanes 4, 8, and 12), and DMSO as negative control (lanes 1, 5, and 9). Cells were harvested after 48 h and samples analysed using antibodies α-H3, α-H3S10ph, and α-H3S28ph. The experiment was run and is shown in triplicate. A representative red ponceau stained membrane is shown as loading and quantification control. Molecular weight markers (kDa) are indicated on the left.

4.6 HMGA1 depletion does not affect ERK activation

Since interphasic H3S10 and H3S28 phosphorylation is mediated by RAS/RAF/MEKK/ERK pathway in MDA-MB-231 cells (fig. 4.8), we tested whether HMGA1 could affect these modifications by modulating ERK activation. Samples used for fig. 4.4 experiments (MDA-MB-231 cells transfected with siA1_3 and siCTRL) were analysed by western blot using antibodies α-ERK1/2 and phosphorylated ERK1/2 (pERK1/2), which is the activated form of this kinase (fig. 4.10). Results indicate that HMGA1 silencing (lanes 2, 4, and 6) altered neither ERK expression nor ERK phosphorylation with respect to control cells (lanes 1, 3, and 5), suggesting that HMGA1 acts in this context downstream to its activation.

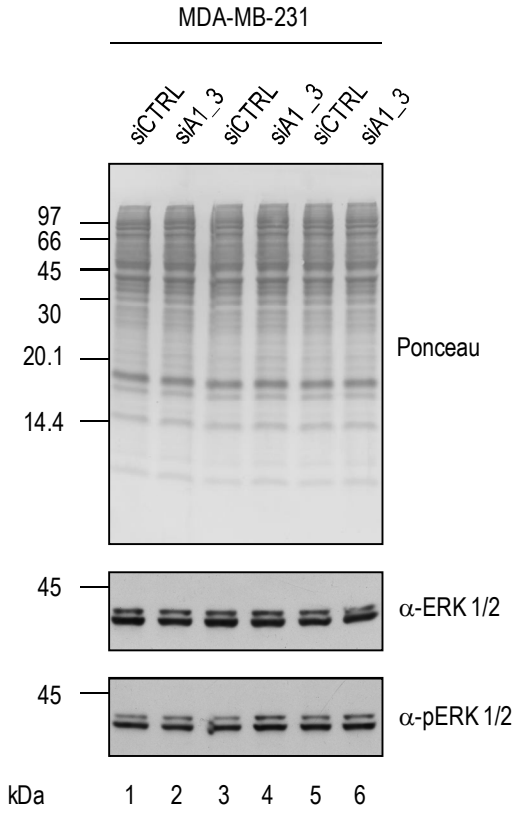

Figure 4.10: ERK activation is not altered by HMGA1 silencing. Western blot analysis of MDA-MB-231 cells transfected with control (siCTRL – lanes 1, 3, and 5) and HMGA1 (siA1_3 – lanes 2, 4, and 6) siRNAs. Cells were harvested after 72 h and samples analysed using antibodies α-ERK1/2 and α-pERK1/2 (phosphorylated ERK1/2). The experiment was run and is shown in triplicate. A representative red ponceau stained membrane is shown as loading and quantification control. Molecular weight markers (kDa) are indicated on the left.

4.7 HMGA1 depletion does not affect MSK1 and RSK2 expression

Our data suggest that HMGA1 did not affect the RAS/RAF/MEKK/ERK pathway upstream to ERK1/2 activation, since its phosphorylation was not altered by HMGA1 silencing. Therefore, we looked into the possibility that HMGA1 could regulate the expression of the main kinases responsible for H3 phosphorylation upon ERK pathway activation, MSK1/2 and RSK2. Samples from MDA-MB-231 cells silenced for HMGA1 expression (fig. 4.4) were analysed

by western blot using α-MSK1 and α-RSK2 antibodies (fig. 4.11). (MSK2 level was not evaluated since a specific antibody for this protein was not available in our laboratory). Results show that HMGA1 silencing (lanes 2, 4, and 6) did not substantially affect the expression of MSK1 and RSK2, with respect to the control cells (lanes 1, 3, and 5).

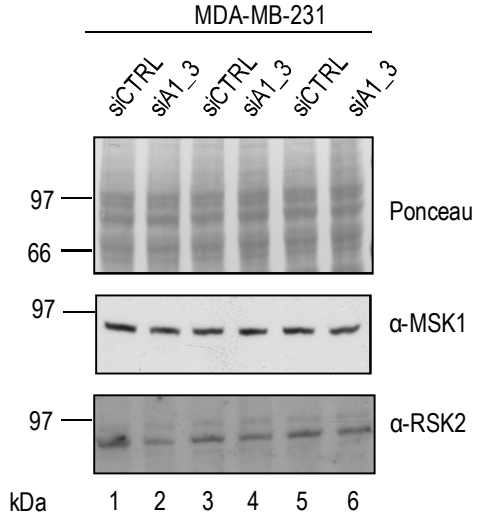

Figure 4.11: HMGA1 does not regulate MSK1 and RSK2 expression. Western blot analysis of MDA-MB-231 cells transfected with control (siCTRL – lanes 1, 3, and 5) and HMGA1 (siA1_3 – lanes 2, 4, and 6) siRNAs. Cells were harvested after 72 h and samples analysed using antibodies α-MSK1and α-RSK2. The experiment was run and is shown in triplicate. A representative red ponceau stained membrane is shown as loading and quantification control. Molecular weight markers (kDa) are indicated on the left.

4.8 H89 kinase inhibitor blocks H3S10 and H3S28 phosphorylation and inhibits cell migration

Since we demonstrated that HMGA1 acts downstream to ERK activation and that it does not regulate the expression of MSK1 and RSK2, we hypothesised that this protein could somehow regulate the activity of these kinases and we focused on searching the kinase responsible for H3S10/H3S28ph.

At first we tested whether MSK1/2 could mediate these PTMs in this context. Therefore, we treated MDA-MB-231 cells with increasing concentrations of the MSK1/2 inhibitor H89 (5, 10, and 20 μM) for 24 h (fig. 4.12). Proteins were analysed by western blot (fig. 4.12 – A) and results show that H3S10ph and H3S28ph were down-regulated in a dose-dependent manner (lanes 2-4, 6-8, and 10-12) with respect to mock cells (lanes 1, 5, and 9). Importantly, H3 expression dropped only with 20 μM H89 (lanes 4, 8, and 12), while its phosphorylation was reduced even at lower concentrations, indicating that it was not attributable to total H3 down-regulation. Moreover, H89 treatment did substantially alter neither MSK1 nor HMGA1 expression levels.

Treated cells were also subjected to the MTS metabolic activity assay, in order to evaluate their proliferation at several time points after drug administration. Cells were analysed at 24, 48, and 72 h (fig. 4.12 – B). At 24 h, treated cells did not exhibit substantial differences in

metabolic activity with respect to control cells, indicating that H3 phosphorylation variations at this time point (fig. 4.12 – A) cannot be ascribed to changes in cell proliferation, being this modification hallmark of mitosis (Goto et al., 1999).

We also observed that H89 treatment led to a morphological change of MDA-MB-231 cells, proportional to drug concentration. In particular, they acquired a more flattened shape, which is typical of epithelial cells (fig. 4.12 – C).

To determine whether tumour phenotype reversion was associated to variations of migratory properties as well, treated cells were analysed by wound healing assay (fig.4.12 – D). Cell dishes were *scratched* after treatment (24 h) and wound closure was measured after 4 and 8 h. Microscopic images and the histogram graphs reporting closure percentages show that H89 significantly inhibited cell migration in a dose-dependent manner, both at 4 and 8 h.

Overall, these data demonstrate that H3S10ph and H3S28ph blockage by MSK1/2 inhibitor is associated with phenotype reversion and partial loss of the migratory capacity of MDA-MB-231 cells.

A

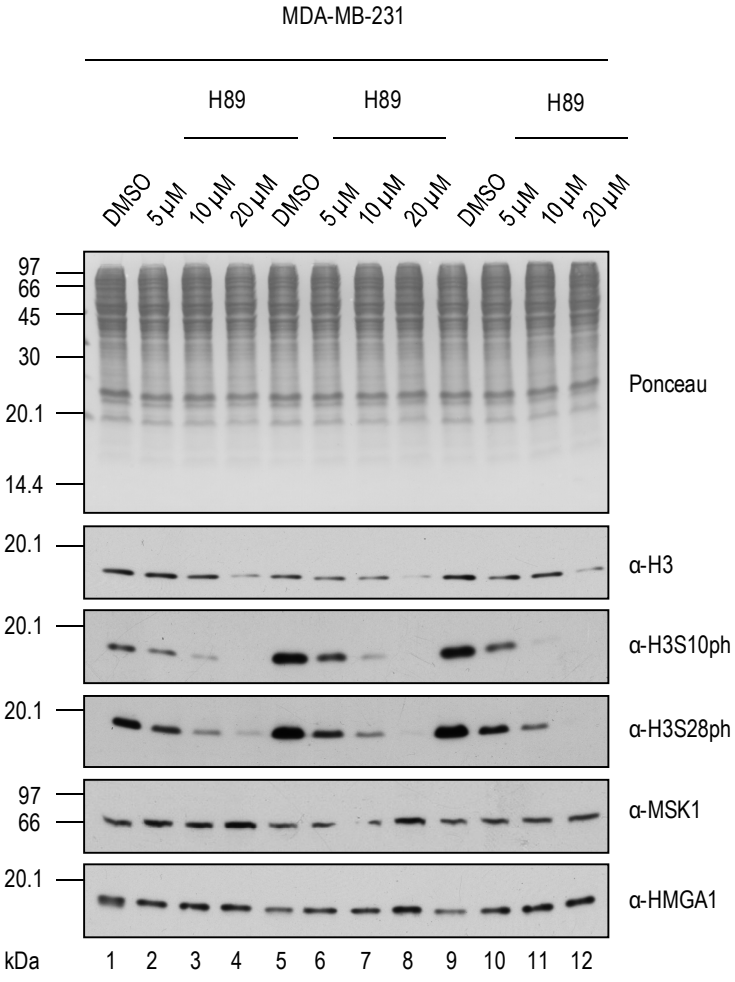

B

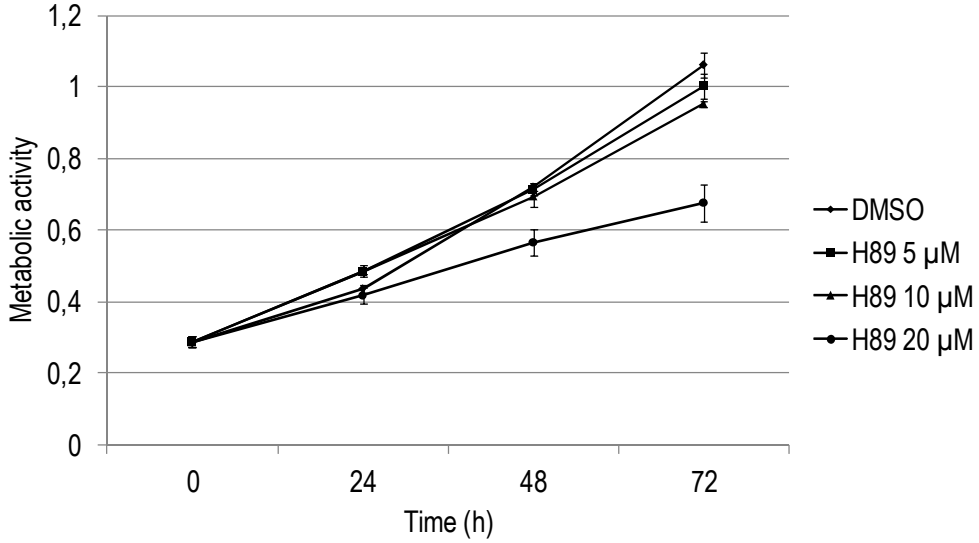
1,2
1
0,8
0,6
0,4
0,2
0
Metabolic activity
0
24
48
72
Time (h)
DMSO
H89 5 µM
H89 10 µM
H89 20 µM

C

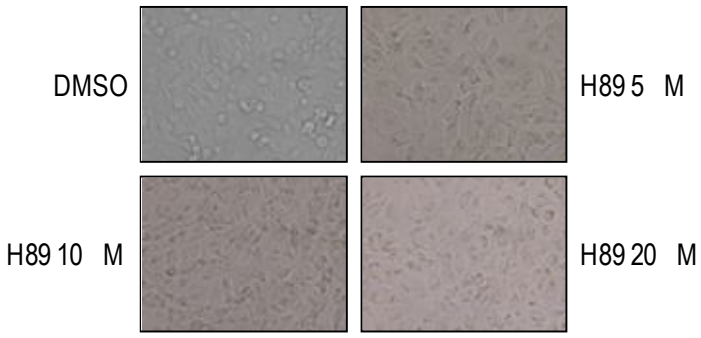
DMSO
H89 5 M
H89 10 M
H89 20 M

D

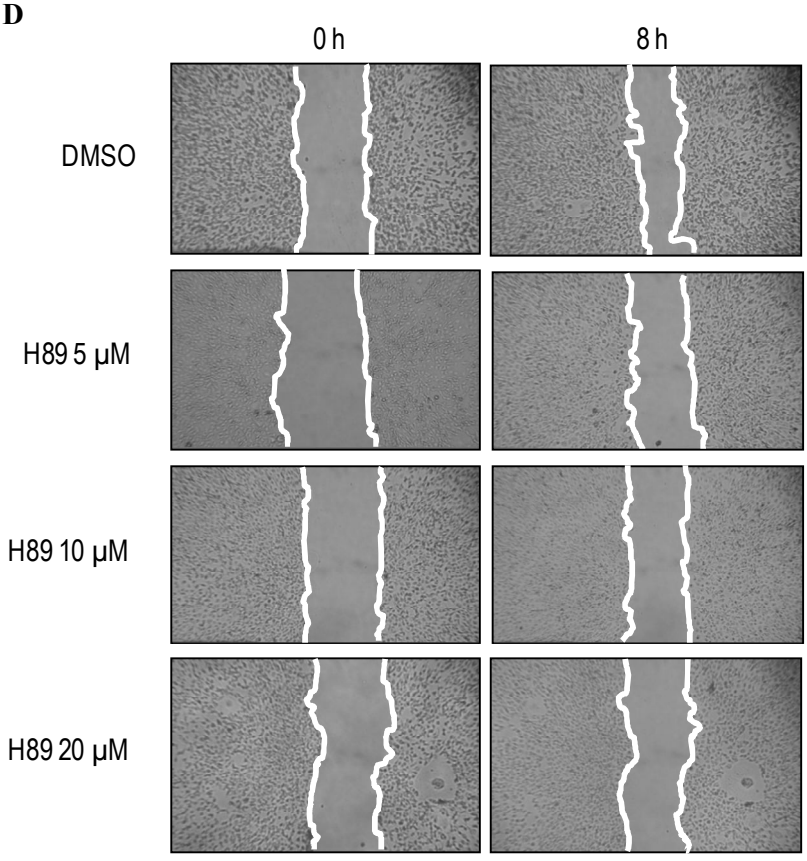
0 h
8 h
DMSO
H89 5 µM
H89 10 µM
H89 20 µM

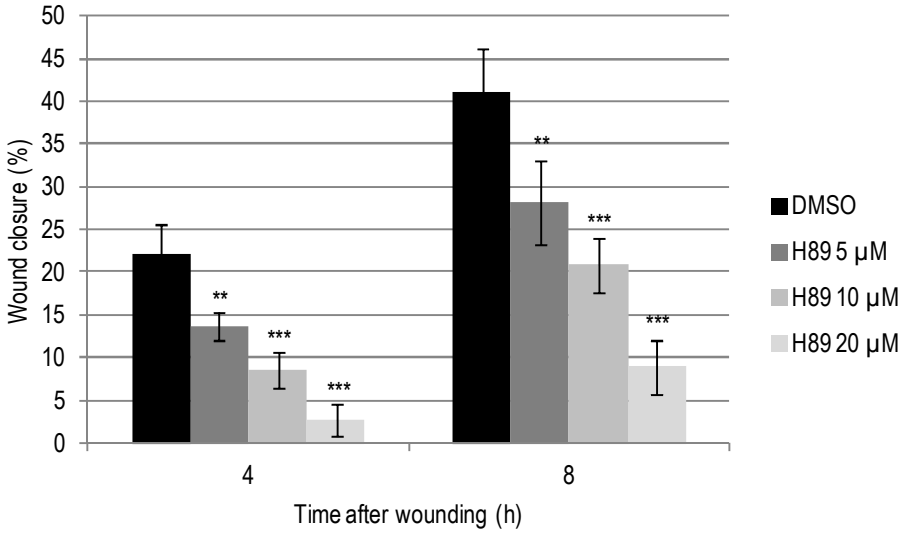

Figure 4.12: H89 inhibits both H3S10/H3S28 phosphorylation and cell migration. (A) Western blot analysis of MDA-MB-231 cells treated with H89 5 µM (lanes 2, 6, and 10), 10 µM (lanes, 3, 7, and 11), and 20 µM (lanes 4, 8, and 12) and DMSO as negative control (lanes 1, 5, and 9). Cells were harvested after 24 h and samples analysed using antibodies α-H3, α-H3S10ph, α-H3S28ph, α-MSK1, and α-HMGA1. The experiment was run and is shown in triplicate. A representative red ponceau stained membrane is shown as loading control. Molecular weight markers (kDa) are indicated on the left. (B) MTS assay of MDA-MB-231 cells treated with H89 5, 10, and 20 µM. The experiment was run in triplicate and standard deviations are reported. (C) Optical microscope images of MDA-MB-231 cells treated with H89 5, 10, and 20 µM. (D) Wound healing assay of MDA-MB-231 cells treated with H89 5, 10, and 20 µM. Representative images of 0 and 8 h time points are reported. The experiment was run in technical duplicate and biological triplicate. The data are represented as the means of the percentage of wound closure relative to time point 0 h. Standard deviations and statistical significance (*t test*) with respect to the controls are indicated (*p-values* *p<0,05; **p<0,01; ***p<0,001).

4.9 Steady-state levels of Immediate-Early Genes are not altered by H3S10/H3S28ph down-regulation

As previously described (see chapter 1), H3S10/H3S28 phosphorylation induction has always been associated to Immediate-Early Genes (IEGs) activation caused by mitogenic stimuli in serum starvation conditions (Thomson et al., 1999; Drobic et al., 2010). These genes have been found to be up-regulated in several types of tumours and their expression correlates with cancer progression (Healy et al., 2013). Notably, it has been demonstrated that HMGA1 binds directly to COX-2 promoter and up-regulates its expression (Tesfaye et al., 2007). These data led us to hypothesise that HMGA1 could regulate IEGs expression by modulating H3 phosphorylation. Therefore, we knocked down HMGA1 expression in MDA-MB-231 cells by siRNA and analysed the expression of several IEGs, including ATF3, FOS, MYC, JUN, and COX-2 genes, by RT-qPCR (fig. 4.13). Results show that HMGA1 depletion did not substantially decrease the expression of any gene. On the contrary, some of them were significantly up-regulated with respect to control cells, such as ATF3 and MYC.

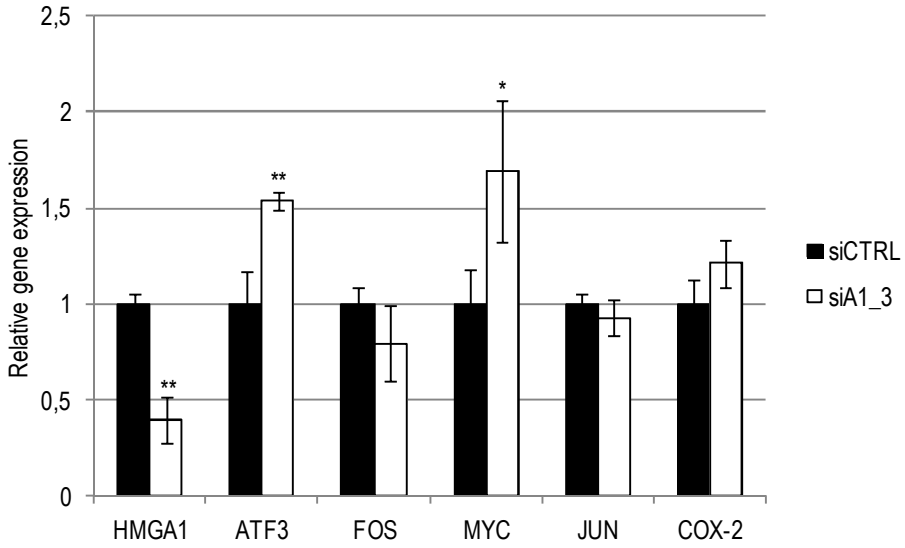

Figure 4.13: Steady-state levels of IEGs are not down-regulated by HMGA1-depletion. RT-qPCR analysis of MDA-MB-231 cells transfected with control (siCTRL) and HMGA1 (siA1_3) siRNAs and harvested after 72 h. mRNA expression of HMGA1, ATF3, FOS, MYC, JUN, and COX-2 genes was analysed using GAPDH as internal control. The experiment was run in triplicate. The data are represented as the means relative to control. Standard deviations and statistical significance (*t test*) are indicated (*p-values* *p<0,05; **p<0,01).

In addition, RT-qPCR preliminary experiments of MDA-MB-231 cells treated with H89 (5, 10, and 20 μM – fig. S1) demonstrated that drug-mediated phosphorylation inhibition did not reduce MYC and JUN expression, as well.

Together, these findings suggest that in MDA-MB-231 cells, H3S10/H3S28 phosphorylation modulation (caused both by HMGA1 silencing and direct enzymatic inhibition) is not related to the transcriptional up-regulation of IEGs.

4.10 HMGA1-regulated genes are affected by H3S10/H3S28 phosphorylation

Data described until now demonstrated that HMGA1-mediated H3 phosphorylation could not have a role in regulating those genes known to be activated by these modifications, i.e. IEGs. Being HMGA1 a transcription factor regulating a huge number of genes belonging to various functional classes (Reeves et al., 2001, Pegoraro et al., 2013, Shah et al., 2013), we decided to investigate whether H3 phosphorylation could be involved in the activation of HMGA1-regulated genes. In particular, we focused on some genes that we recently demonstrated to be down-regulated by HMGA1 silencing in our own model, i.e. MDA-MB-231 cells (Pegoraro et al., 2013). We took into consideration AURKB (encoding Aurora B kinase), KIF23 (kinesin-like protein 23), KIF4A (kinesin family member 4A), and CENPF (centromer protein F)

genes. In addition, we decided to analyse HIST1H3B (Histone cluster 1, H3b: encoding H3.1 variant of H3) levels, since our experiments have revealed that H3 protein expression is linked to H3 phosphorylation.

At first, we analysed by RT-qPCR the expression of these genes in cells treated with siA1_3 (fig.4.15 – A) and siA1_1 (fig.4.15 – B), in order to confirm their down-regulation in our models. The histogram graphs show that all HMGA1-target genes were down-regulated with respect to control cells, even though KIF4A and CENPF reduction was not statistically significant in siA1_1 experiment. It is noteworthy that also HIST1H3B mRNA was dramatically down-regulated in both experiments.

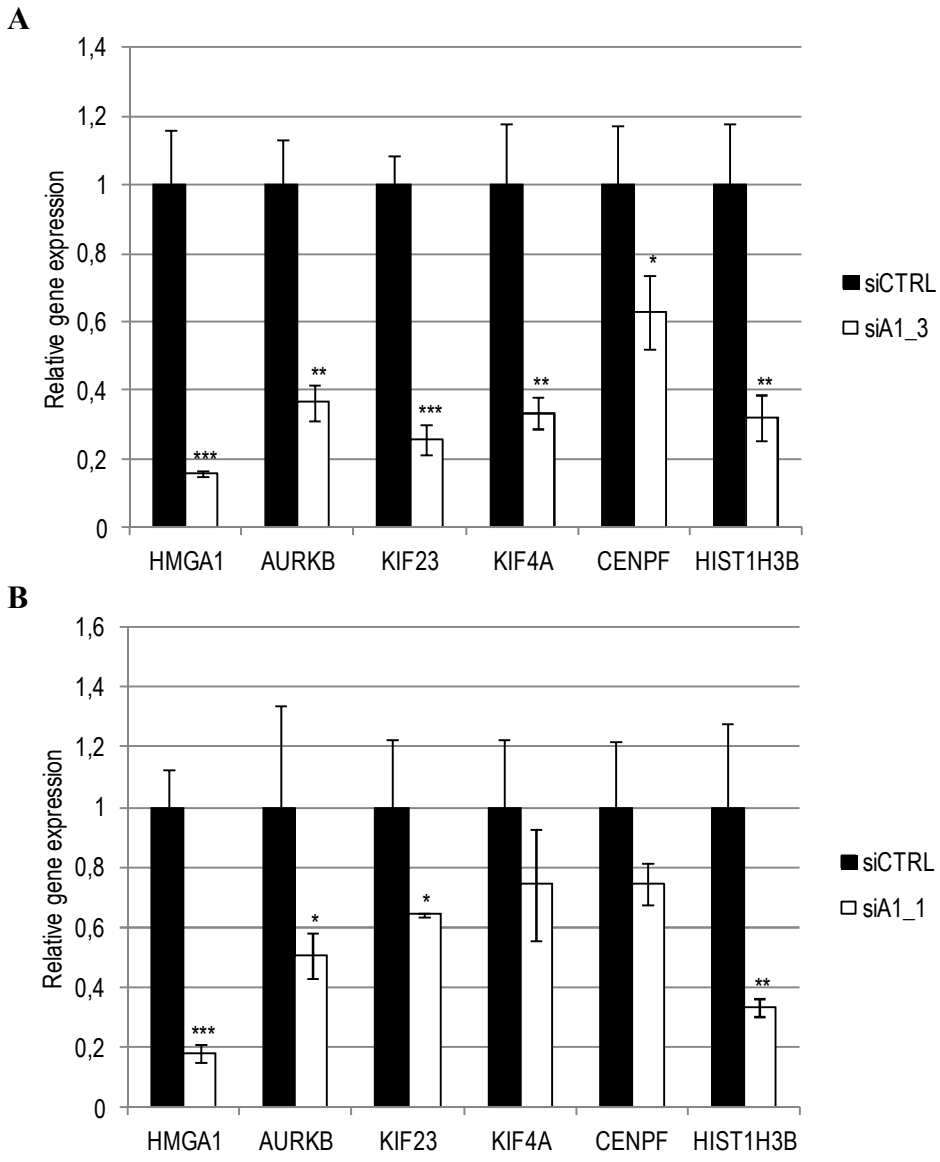

Figure 4.14: HMGA1 regulates AURKB, KIF23, KIF4A, CENPF, and HIST1H3B genes in MDA-MB-231 cells. RT-qPCR analysis of MDA-MB-231 cells transfected with control (siCTRL) and HMGA1 (siA1_3) or (siA1_1) siRNAs (A and B, respectively) and harvested after 72 h. mRNA expression of HMGA1, AURKB, KIF23, KIF4A, CENPF, and HIST1H3B genes was analysed using GAPDH as internal control. The experiment was run in triplicate. The data are represented as the means relative to siCTRL samples. Standard deviations and statistical significance (*t test*) are indicated (*p-values* *p<0,05; **p<0,01; ***p<0,001).

Afterwards, we analysed by RT-qPCR the expression of the same genes in cells treated with H89 5, 10, and 20 μM (fig. 4.15), in order to evaluate the association between H3 phosphorylation and their regulation. Results demonstrate that H89 significantly inhibited the expression of AURKB, KIF23, KIF4A, CENPF, and HIST1H3B with respect to mock cells, in a dose-dependent manner. Moreover, we analysed MSK1, MSK2, and HMGA1 levels to determine whether H89 had altered their expression as well. As we can observe in the histogram, H89 did not affect MSK1 expression while MSK2 was slightly down-regulated at 20 μM concentration. However, the other genes were down-regulated even at lower drug concentrations, therefore we exclude that their decrease could be caused by MSK2 reduction. Conversely, HMGA1 expression seemed to be up-regulated by H89 treatment, albeit not significantly.

Considering that the data obtained by HMGA1 silencing are consistent with those resulting by H89 treatment, we can assume that there is a link among HMGA1, H3S10/H3S28 phosphorylation, and AURKB, KIF23, KIF4A, CENPF, and HIST1H3B expression.

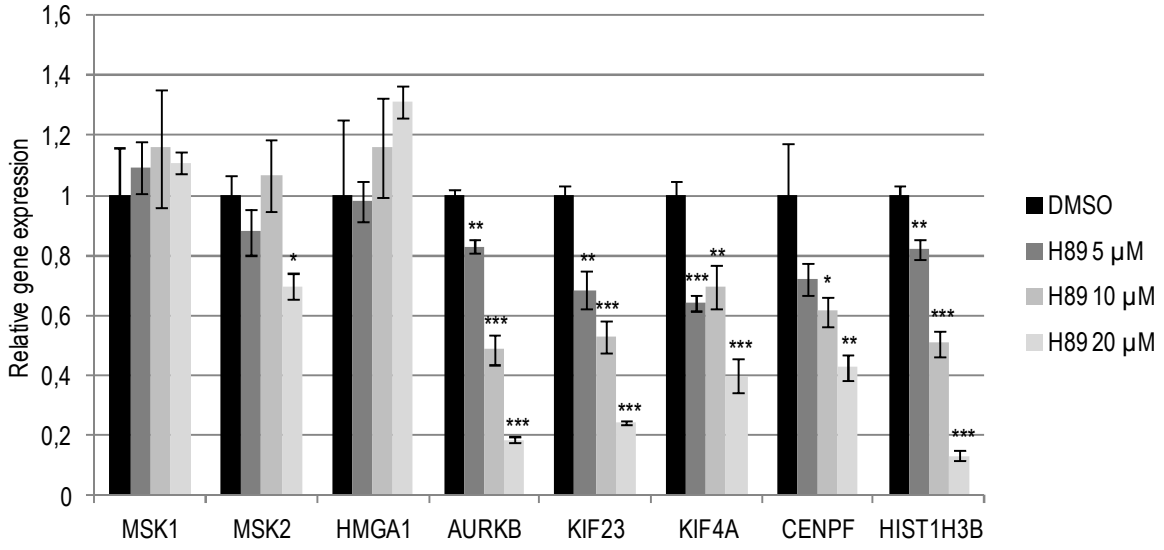

Figure 4.15: H89 inhibits the expression of HMGA1-regulated genes. RT-qPCR analysis of MDA-MB-231 cells treated with H89 5, 10, and 20 μM and harvested after 72 h. mRNA expression of MSK1, MSK2, HMGA1, AURKB, KIF23, KIF4A, CENPF, and HIST1H3B genes was analysed using CYC33 as internal control. The experiment was run in triplicate. The data are represented as the means relative to DMSO-treated control samples. Standard deviations and statistical significance (*t test*) are indicated (*p-values* *p<0,05; **p<0,01; ***p<0,001).

4.11 MSK1/2 silencing does not alter HMGA1-regulated gene expression

Since H89 is an inhibitor used for blocking MSK1/2 kinase activity, we decided to perform knock down experiments using specific siRNAs against MSK1 and MSK2, in order to confirm that these kinases were responsible for H3 phosphorylation in this context. Initially, MDA-MB-231 cells were transfected with siMSK1 or siMSK2 and siCTRL and analysed by western blot (fig. 4.16 – A). MSK1 silencing was verified using a specific antibody α-MSK1, while MSK2 knocking down was not controlled in this experiment since a specific antibody for this variant was not available in our laboratory. Nevertheless, both MSK1 and MSK2 silencing has been controlled in subsequent experiments by RT-qPCR (fig. 4.16 – B, C, and D). Results show that neither MSK1 (lanes 2, 5, and 8) nor MSK2 (lanes 3, 6, and 9) depletion did alter H3S10ph and H3S28ph levels with respect to control cells (lanes 1, 4, and 7), indicating that these kinases do not phosphorylate H3 in these conditions.

However, MSK1/2 is known to phosphorylate many substrates involved in transcription (Deak et al., 1998). Therefore, it is likely that its inhibition by H89 could regulate gene expression through other mechanisms and that H3 phosphorylation decrement was just a concomitant event.

To explore this possibility, cells were treated with siMSK1 and siCTRL (fig. 4.16 – B) and the expression of AURKB, KIF23, KIF4A, CENPF, and HIST1H3B genes was analysed by RT-qPCR. Results indicate that solely AURKB and HIST1H3B were slightly down-regulated with respect to control cells, while the other genes were not affected by MSK1 silencing. In addition, also HMGA1 expression was measured, to evaluate its possible variations upon MSK1 depletion. We can observe that its expression was slightly reduced by MSK1 silencing. Moreover, MSK2 expression analysis was included to verify siRNA specificity.

The same experiment was performed knocking down MSK2 (fig. 4.16 – C). In this case, AURKB was chosen as representative gene and its expression was evaluated. Results show that MSK2 silencing did not alter AURKB levels with respect to control cells. MSK1 expression analysis was included for siRNA specificity control.

Furthermore, we carried out a double silencing experiment using siMSK1 and siMSK2 concomitantly (fig. 4.16 – D). We can observe that none of the analysed genes (HMGA1, AURKB, KIF23, KIF4A, CENPF, and HIST1H3B) was down-regulated with respect to control cells. On the contrary, KIF23 seemed to be up-regulated by MSK1/MSK2 silencing.

Together, these results indicate that MSK1/2 does not substantially modulate the expression of the HMGA1-regulated genes analysed here, neither by phosphorylating H3 nor through other

mechanisms.

A

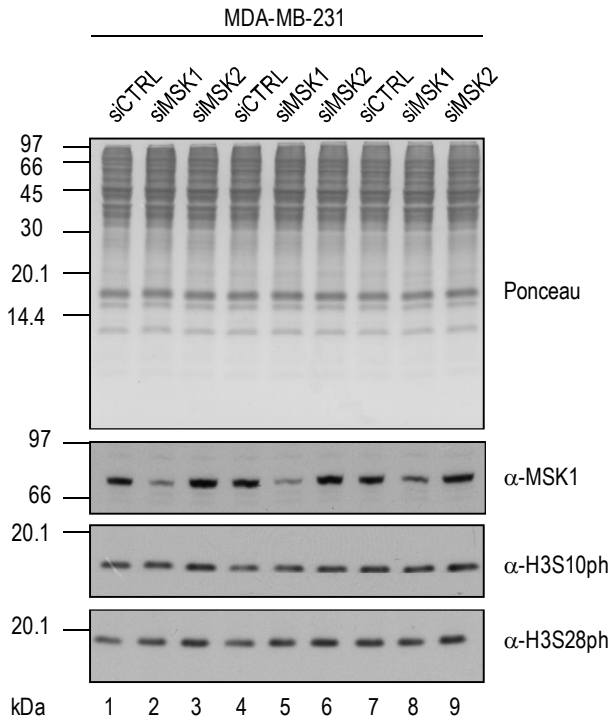

B

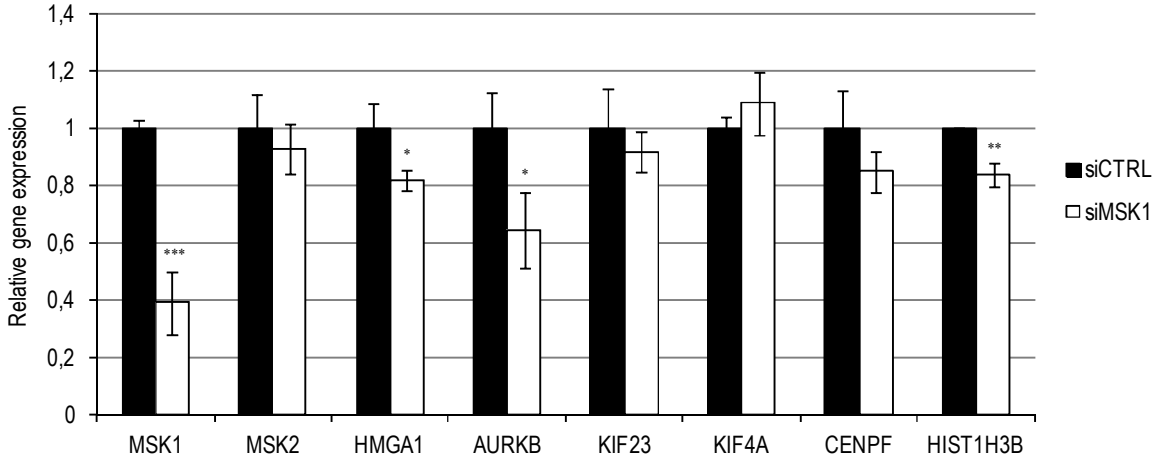

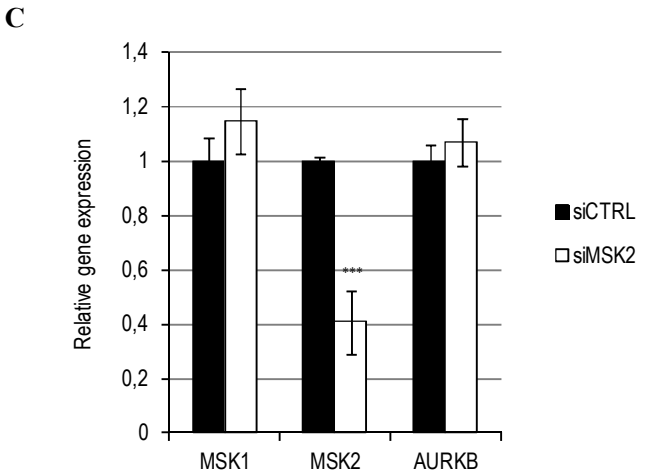

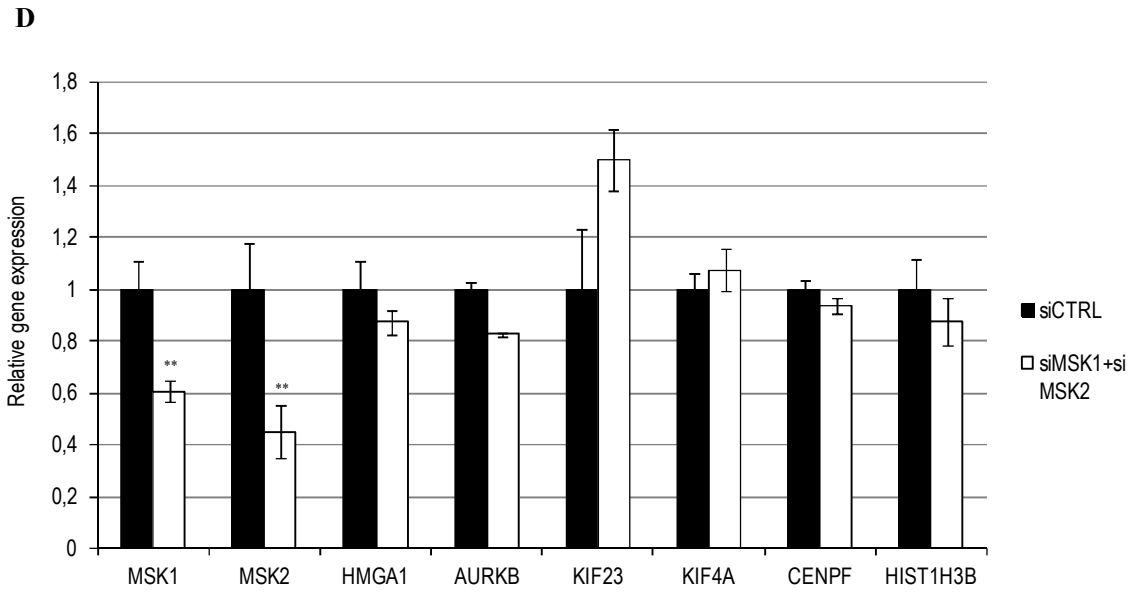

Figure 4.16: MSK1/2 is not responsible for H3S10/H3S28 phosphorylation during interphase in MDA-MB-231 cells. (A) Western blot analysis of MDA-MB-231 cells transfected with control (lanes 1, 4, and 7), MSK1 (lanes 2, 5, and 8) and MSK2 (lanes 3, 6, and 9) siRNAs. Cells were harvested after 24 h and samples analysed using antibodies α-MSK1, α-H3S10ph, and α-H3S28ph. The experiment was run and is shown in triplicate. A representative red ponceau stained membrane is shown as loading control. Molecular weight markers (kDa) are indicated on the left. (B) RT-qPCR analysis of MDA-MB-231 cells transfected with control and MSK1 siRNAs and harvested after 72 h. mRNA expression of MSK1, MSK2, HMGA1, AURKB, KIF23, KIF4A, CENPF, and HIST1H3B genes was analysed using CYC33 as internal control. (C) RT-qPCR analysis of MDA-MB-231 cells transfected with control and MSK2 siRNAs and harvested after 72 h. mRNA expression of MSK1, MSK2, and AURKB genes was analysed using CYC33 as internal control. (D) RT-qPCR analysis of MDA-MB-231 cells transfected with control, MSK1, and MSK2 siRNAs and harvested after 72 h. mRNA expression of MSK1, MSK2, HMGA1, AURKB, KIF23, KIF4A, CENPF, and HIST1H3B genes was analysed using CYC33 as internal control. (B), (C), and (D) The experiment was run in triplicate. The data are represented as the means relative to siCTRL samples. Standard deviations and statistical significance (*t test*) are indicated (*p-values* *p<0,05; **p<0,01; ***p<0,001).

4.12 RSK2 inhibitor BI-D1870 reflects HMGA1-silencing data

The data achieved with MSK1/2 silencing are not consistent with the results obtained with H89. Even though this inhibitor is one of the most used for studying the role of MSK1/2, it has been demonstrated to inhibit eight different protein kinases, four of them with high efficiency: MSK1, PKA, S6K, and Rock II (Davies et al., 2000). Notably, among the kinases inhibited by H89 there is PKA, whose activity can affect the activation of the ERK1/2 pathway in MDA-MB-231 cells (Stork and Schmitt, 2002). Therefore, we decided to adopt another MSK1/2 inhibitor, in order to verify whether H89 acts through MSK1/2 or via other kinases. At the same time, we also tested an inhibitor of RSK2 (BI-D1870), which is the other kinase mainly responsible for interphasic H3 phosphorylation along with MSK1/2, as previously described.
MDA-MB-231 cells were treated with SB747651A, which is a MSK1/2 inhibitor reported to be more specific with respect to H89 (Naqvi et al., 2012). After 24 h treatment, samples were analysed by western blot to detect H3S10ph and H3S28ph levels (fig. 4.17). Results show that this inhibitor did not alter H3S10/H3S28 phosphorylation (lanes 2, 4, and 6) with respect to control cells (lanes 1, 3, and 5), supporting the data obtained with MSK1/2 siRNAs.

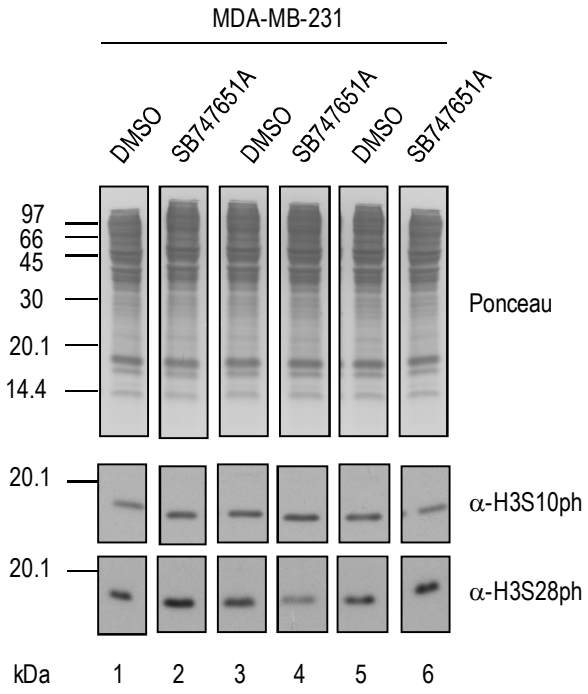

Figure 4.17: The MSK1/2 inhibitor SB747651A does not inhibit H3S10/H3S10 phosphorylation. Western blot analysis of MDA-MB-231 cells treated with SB747651A 10 μM (lanes 2, 4, and 6) and DMSO as negative control (lanes 1, 3, and 5). Cells were harvested after 24 h and samples analysed using antibodies α-H3S10ph and α-H3S28ph. The experiment was run and is shown in triplicate. A representative red ponceau stained membrane is shown as loading control. Molecular weight markers (kDa) are indicated on the left.

Afterwards, cells were treated with increasing concentrations of RSK2 inhibitor (BI-D1870 0,1 μM, 1 μM, and 10 μM) and samples were analysed by western blot to investigate whether RSK2 inhibition affected H3S10/H3S28 phosphorylation (fig. 4.18 – A). Results demonstrate that this drug dramatically inhibited H3S10ph and H3S28ph at 10 μM concentration (lanes 4, 8, and 12) with respect to the control (lanes 1, 5, and 9).

Hence, we investigated whether BI-D1870-dependent H3 phosphorylation decrease was associated with the down-regulation of AURKB, KIF23, KIF4A, CENPF, and HIST1H3B genes. Cells were treated with 10 μM BI-D1870, the drug concentration exhibiting the highest inhibitory activity in fig. 4.18 – A. Samples were harvested after 24 h and analysed by RT-qPCR (fig. 4.18 – B). All the listed genes were significantly down-regulated upon BI-D1870 treatment with respect to the mock cells. Conversely, RSK2 and HMGA1 (included as controls) were up-regulated.

We looked into the possibility that these events were accompanied by changes in tumour properties. Cells were treated as described above for fig. 4.18 – A, and visualised with optical microscope (fig. 4.18 – C). Representative images show that BI-D1870 treatment induced a morphological change with respect to the control, particularly evident at 10 μM concentration. Cells were characterised by a more flattened and organised aspect, which resembled the epithelial ones, indicating a sort of tumour phenotype reversion similar to that obtained with HMGA1 depletion (Pegoraro et al., 2013) and with Emodin and H89 treatment (fig. 4.9 – A and 4.12 – C).

In addition, treated cells were subjected to wound healing assay to evaluate their migratory capabilities with respect to the mock cells (fig. 4.18 – D). Cell dishes were *scratched* after 24 h treatment and wound closure was measured at 4 and 8 h. Microscopic images and the histogram graph reporting closure percentages show that BI-D1870 treatment significantly reduced cell migration in a dose-dependent manner, both at 4 and 8 h.

Overall, these data overlap with those achieved by HMGA1 silencing and H89 treatment, further highlighting the association between H3 phosphorylation at S10 and S28, the expression of the genes taken into consideration, and MDA-MB-231 cell migration.

A

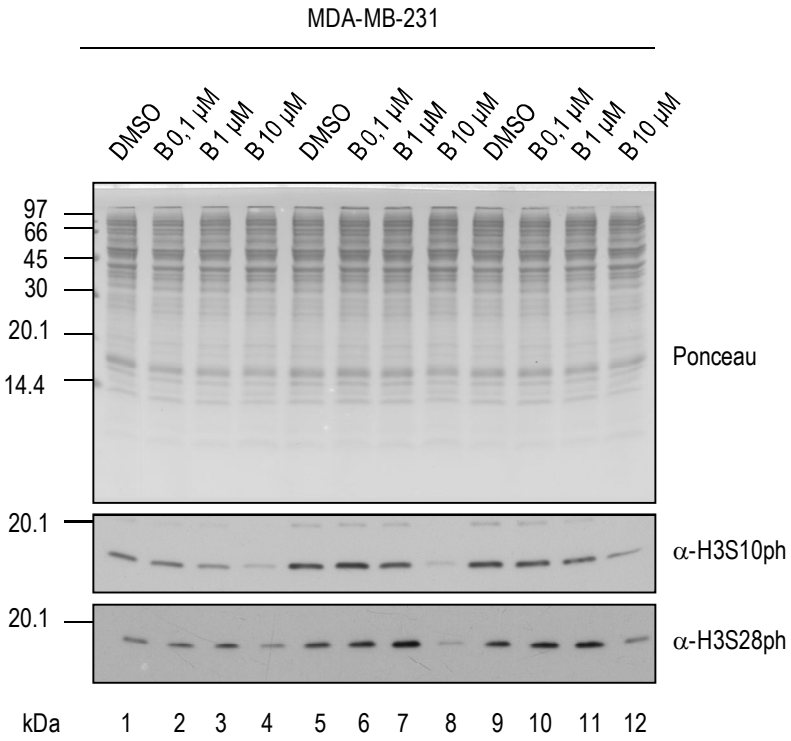
MDA-MB-231
DMSO
B 0,1 µM
B 1 µM
B 10 µM
DMSO
B 0,1 µM
B 1 µM
B 10 µM
DMSO
B 0,1 µM
B 1 µM
B 10 µM
97
66
45
30
20.1
14.4
Ponceau
20.1
α-H3S10ph
20.1
α-H3S28ph
kDa
1 2 3 4 5 6 7 8 9 10 11 12

B

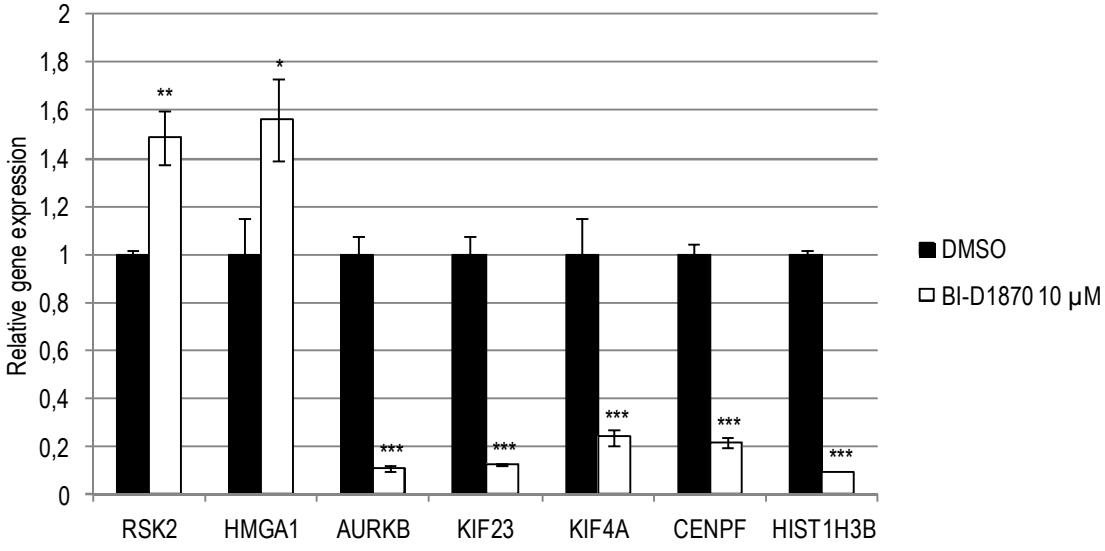
Relative gene expression
2
1,8
1,6
1,4
1,2
1
0,8
0,6
0,4
0,2
0
**
*
***
***
***
***
***
RSK2
HMGA1
AURKB
KIF23
KIF4A
CENPF
HIST1H3B
DMSO
BI-D1870 10 µM

C

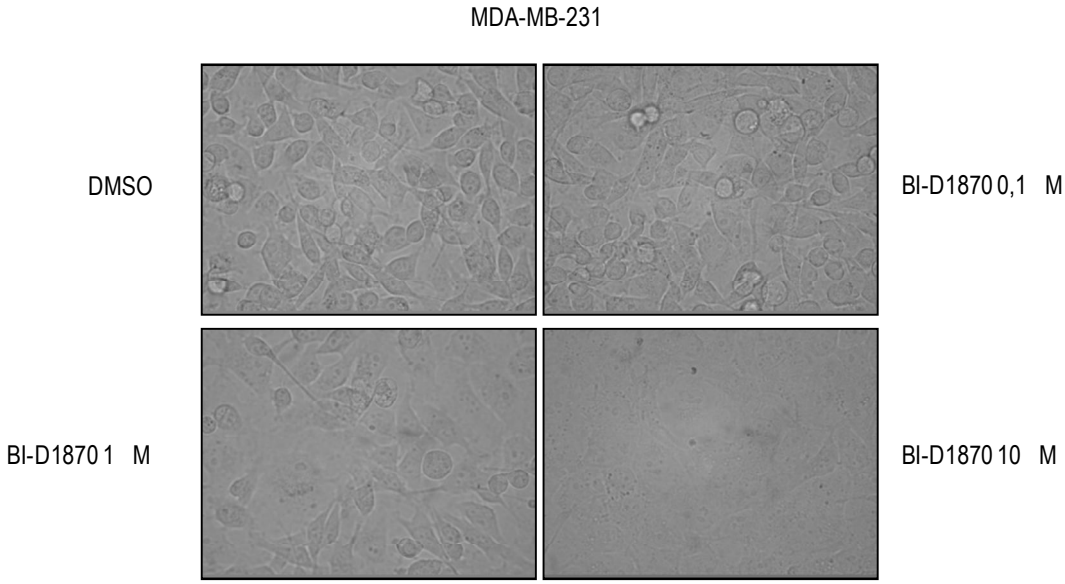
MDA-MB-231
DMSO
BI-D1870 0,1 M
BI-D1870 1 M
BI-D1870 10 M

D

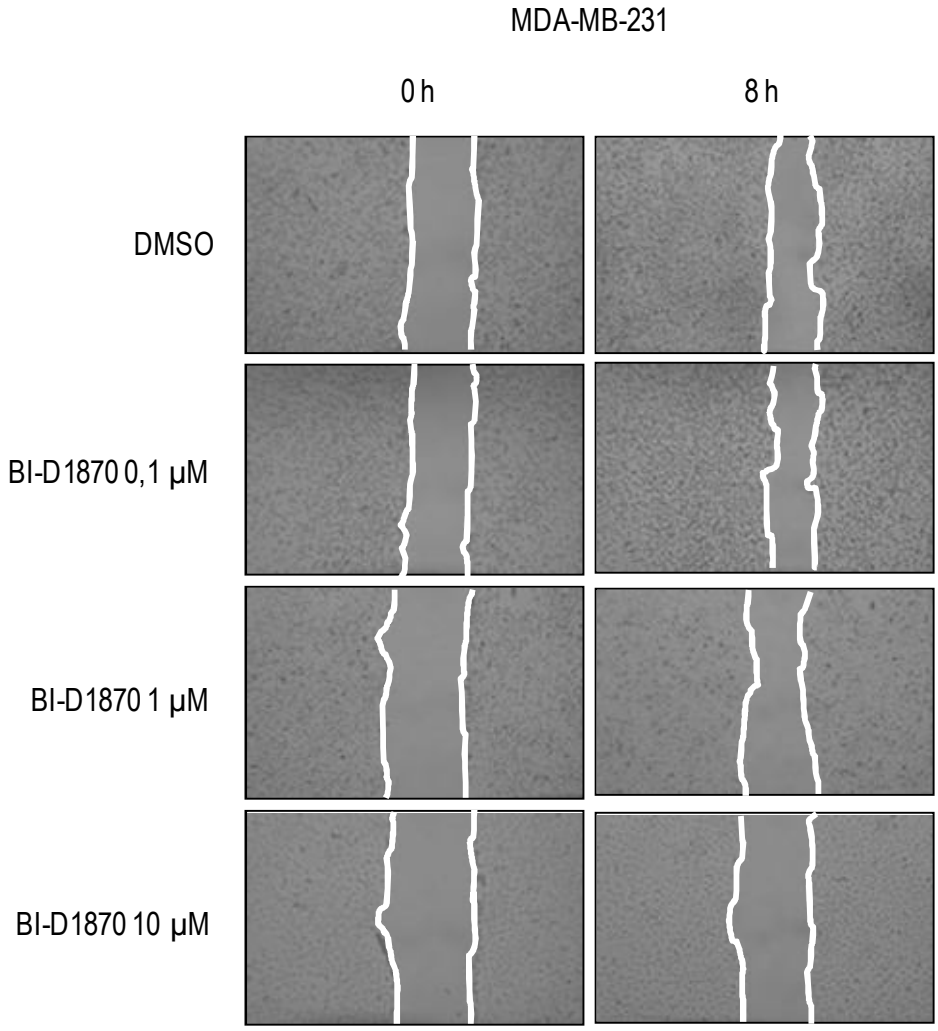
MDA-MB-231
0 h
8 h
DMSO
BI-D1870 0,1 µM
BI-D1870 1 µM
BI-D1870 10 µM

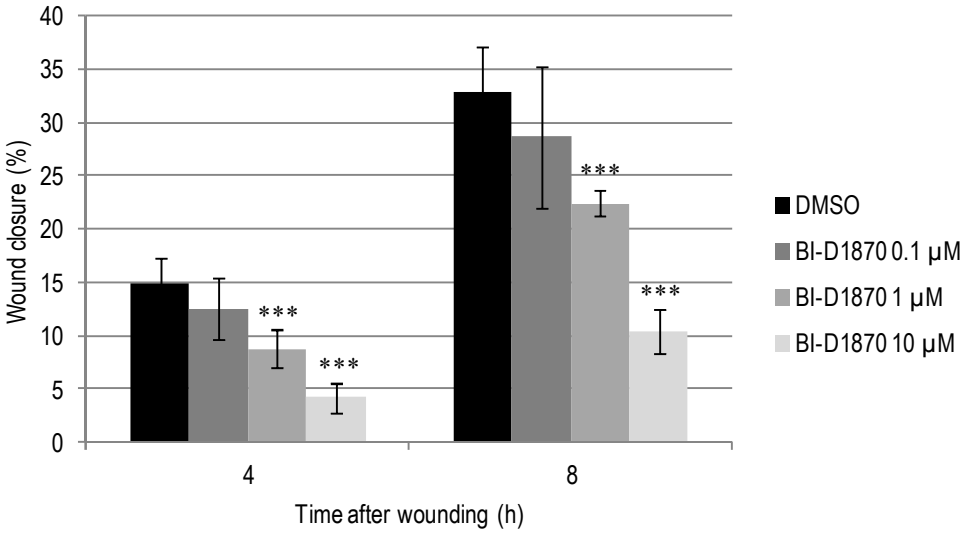

Figure 4.18: BI-D1870 inhibits H3 phosphorylation, gene expression, and cell migration. (A) Western blot analysis of MDA-MB-231 cells treated with BI-D1870 0,1 µM (lanes 2, 6, and 10), 1 µM (lanes, 3, 7, and 11), and 10 µM (lanes 4, 8, and 12) and DMSO as negative control (lanes 1, 5, and 9). Cells were harvested after 24 h and samples analysed using antibodies α-H3S10ph and α-H3S28ph. The experiment was run and is shown in triplicate. A representative red ponceau stained membrane is shown as loading control. Molecular weight markers (kDa) are indicated on the left. (B) RT-qPCR analysis of MDA-MB-231 cells treated with BI-D1870 10 µM. mRNA expression of RSK2, HMGA1, AURKB, KIF23, KIF4A, CENPF, and HIST1H3B genes was analysed using CYC33 as internal control. The experiment was run in triplicate. The data are represented as the means relative to control. Standard deviations and statistical significance (*t test*) are indicated (*p-values* *p<0,05; **p<0,01; ***p<0,001). (C) Optical microscope images of MDA-MB-231 cells treated with BI-D1870 0,1, 1, and 10 µM. (D) Wound healing assay of MDA-MB-231 cells treated with BI-D1870 0,1, 1, and 10 µM.. Representative images of 0 and 8 h time points are reported. The experiment was run in technical duplicate and biological triplicate. The data are represented as the means of the percentage of wound closure relative to time point 0 h. Standard deviations and statistical significance (*t test*) are indicated (*p-values* ***p<0,001).

4.13 Aurora B kinase expression depends on HMGA1 and H3S10/H3S28ph levels

Results described in the previous paragraphs indicated that the expression of some genes is associated both with HMGA1 and H3 phosphorylation levels. We therefore examined whether protein expression levels of these genes could change as well. We focused our attention on AURKB gene, since it was highly down-regulated in our experiments with respect to the controls and it is well-known to be involved in cancer (Vader and Lens, 2008). Moreover, data obtained in our laboratory evidenced that AURKB silencing affects cell motility (Pegoraro et al., 2013).

Thus, we analysed by western blot samples from MDA-MB-231 cells transfected with siA1_3 or siA1_1 and siCTRL (fig. 4.19 – A), using α-AURKB antibody. Results show that Aurora B kinase was down-regulated (lanes 2, 4, and 6) with respect to control cells (lanes1, 3, and 5) in

both experiments. (All ponceau stained membranes used as loading and quantification controls relative to the experiments described in this paragraph are reported in supplementary figures).
Moreover, Aurora B was down-regulated both in MDA-MB-231 cells treated with the MEK1/2 inhibitor UO126 (fig. 4.19 – B, lanes 2, 5, and 8) and in MDA-MB-453 cells treated with 40 μM Emodin (lanes 4, 8, and 12). On the contrary, its expression was not altered by the p38 MAPK inhibitor BIRB796 (lanes 3, 6, and 9). These data support the hypothesis that RAS/RAF/MEKK/ERK pathway and not p38 MAPK pathway is involved in the regulation of Aurora B kinase expression in our model.
In fig. 4.19 – C western blot analyses relative to MDA-MB-231 cells treated with increasing concentrations of H89 are reported. Aurora B levels were down-regulated in a dose-dependent manner (lanes 2-4, 6-8, and 10-12), with respect to control cells (lanes 1, 5, and 9). Conversely, neither MSK1 (lanes 2, 5, and 8) nor MSK2 (lane 3, 6, and 9) silencing by siRNA did alter Aurora B expression with respect to the control (lanes 1, 4, and 7). (RT-qPCR experiments are reported as control for MSK1 and MSK2 silencing – fig. S3).
Finally, experiments performed with MSK1/2 and RSK2 specific inhibitors (SB747651A and BI-D1870, respectively; fig. 4.19 – D) demonstrated that Aurora B levels were unaffected by MSK1/2 inhibition (lanes 2, 4, and 6) with respect to control cells (lanes 1, 3, and 5) while they were substantially down-regulated by RSK2 inhibition with 10 μM BI-D1870 (lanes 4, 8, and 12) with respect to the control (lanes 1, 5, and 9).
Overall, these results demonstrate that Aurora B protein expression was down-regulated by HMGA1 silencing, which concomitantly induced H3S10/H3S28 phosphorylation decrement (fig. 4.4). Consistently, the expression of this kinase was down-regulated upon all those treatments inducing H3 phosphorylation decrease, such as UO126 (fig. 4.8), Emodin (fig 4.9), H89 (fig. 4.12), and BI-D1870 (fig. 4.18) treatment. On the contrary, Aurora B expression was not down-regulated by the treatments that did not alter H3S10/H3S28ph levels, such as BIRB 796 and SB747651A treatments (fig. 4.8 and fig. 4.17, respectively) and siMSK1/siMSK2 transfection (fig. 4.16).

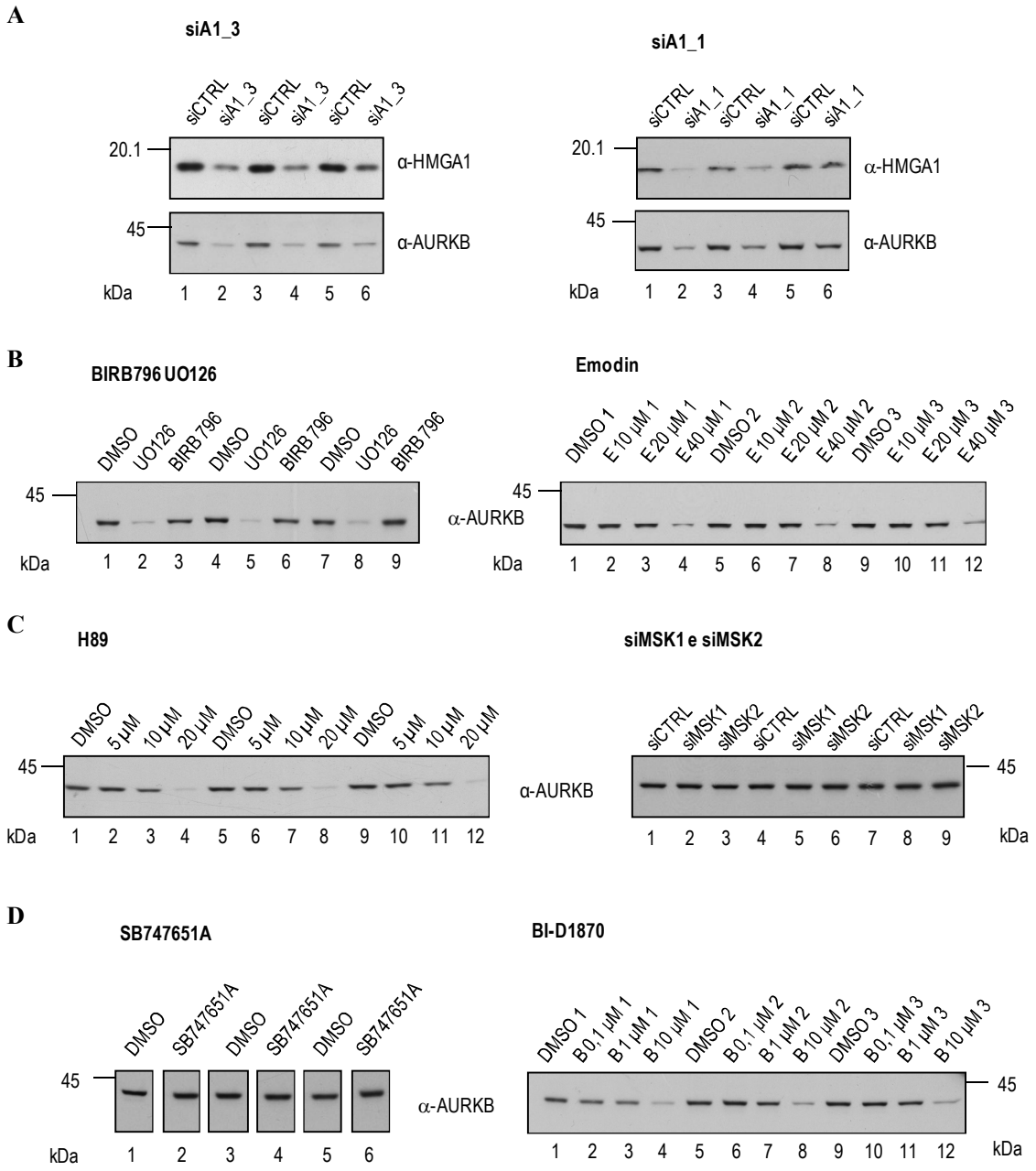

Figure 4.19: Aurora B protein is down-regulated by H3S10/H3S28ph decrement. (A), (B), (C), and (D) Western blot analyses performed using α-AURKB antibody. (A) MDA-MB-231 cells transfected with control (siCTRL – lanes 1, 3, and 5) and HMGA1 (siA1_3 – lanes 2, 4, and 6) siRNAs and harvested after 72 h. (B) MDA-MB-231 cells treated with UO126 10 µM (lanes 2, 5, and 8), BIRB796 10 µM (lanes 3, 6, and 9) and DMSO as negative control (lanes 1, 4, and 7) and MDA-MB-453 cells treated with Emodin 10 µM (lanes 2, 6, and 10), 20 µM (lanes 3, 7, and 11) and 40 µM (lanes 4, 8, and 12), and DMSO as negative control (lanes 1, 5, and 9) and harvested after 48 h. (C) MDA-MB-231 cells treated with H89 5 µM (lanes 2, 6, and 10), 10 µM (lanes, 3, 7, and 11), and 20 µM (lanes 4, 8, and 12) and DMSO as negative control (lanes 1, 5, and 9) and harvested after 24 h and MDA-MB-231 cells transfected with control (lanes 1, 4, and 7), MSK1 (lanes 2, 5, and 8) and MSK2 (lanes 3, 6, and 9) siRNAs and harvested after 24 h. (D) MDA-MB-231 cells treated with SB747651A (lanes 2, 4, and 6) and DMSO as negative control (lanes 1, 3, and 5) and with BI-D1870 0,1 µM (lanes 2, 6, and 10), 1 µM (lanes, 3, 7, and 11), and 10 µM (lanes 4, 8, and 12) and DMSO as negative control (lanes 1, 5, and 9). All the experiments were run and are shown in triplicate. A representative red ponceau stained membrane is shown as loading control. Molecular weight markers (kDa) are indicated on the left.

4.14 RSK2 inhibition decreases H3S10 phosphorylation at the level of AURKB gene

As previously described, H3 phosphorylation at S10 and S28 is known to be associated with the activation of gene transcription and in particular, it has been found at the level of both promoters and enhancers (Drobic et al., 2010; Khan et al., 2013). Therefore, we asked whether the analysed genes could be down-regulated by H3 phosphorylation decrease at the level of their own regulatory sequences. To look into this possibility, we performed a Chromatin Immuno-Precipitation (ChIP) experiment (fig. 4.20) in MDA-MB-231 cells treated with 10 μM BI-D1870 and DMSO as negative control. Lysates were immunoprecipitated with α-H3S10ph antibody and non-specific control IgG as negative control and immunoprecipitated DNA was analysed by qPCR. For the same reasons described above, we choose for analysis AURKB as representative gene. Literature data achieved by luciferase activity assays reported that AURKB promoter contains a positive regulatory region between -74 and -104 bp upstream to one of two main transcription start sites (TSS +1; the second one localises at +12). Moreover, this promoter exhibits a CCAAT box at -45 bp and two regulatory regions between CCAAT box and TSS +1, called the cell cycle-dependent element (CDE) and cell cycle gene homology region (CHR). These regions regulate the cell cycle-dependent activity of AURKB promoter (Kimura et al., 2004). Another study reported that AURKB gene is activated by FoxM1 transcription factor (Forkhead Box M1) through the binding to the -749 bp promoter region (Wang et al., 2005).

Therefore, we choose for analysis a 5' distal region approximately at -800 bp (indicated as -800), a region including CCAAT box, CDE and CHR regions and the two transcription start sites (indicated as TSS) and an intragenic region (indicated as intrag), localising on the last exon. This region was arbitrarily chosen, in order to analyse a DNA fragment distant from the promoter as comparison.

Results show that H3S10ph was efficiently immunoprecipitated from all samples with respect to the negative control IgG, suggesting that this modification is present at the level of the examined sequences. Notably, H3S10ph seems to be differently distributed on the various DNA regions. In particular, the intragenic region is the most efficiently co-immunoprecipitated by H3S10ph, indicating that this modification is more abundant at this level with respect to the other regions taken into consideration.

Following BI-D1870 treatment, H3S10ph abundance did not vary in the TSS region while it substantially decreased in the intragenic region and albeit not significantly, also in the -800 region.

Taken together, these data indicate that H3S10ph is present at the level of AURKB gene, that its level in the intragenic region is inhibited by BI-D1870 treatment and that this decrement is associated with AURKB transcription down-regulation. However, we were not able to detect significant H3S10ph changes at the level of AURKB promoter, even though it is still unknown whether regulatory sequences, such as downstream enhancer, are present in the analysed intragenic region.

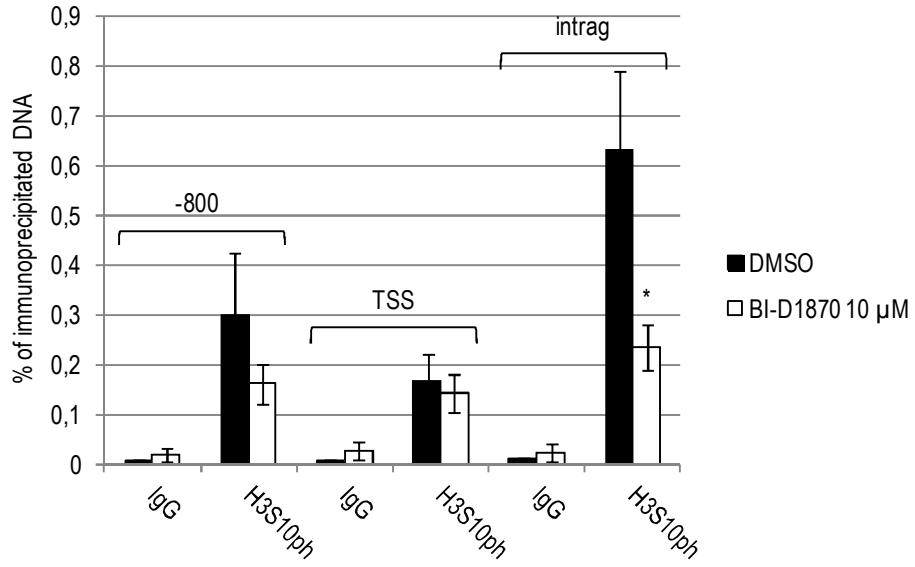

Figure 4.20: BI-D1870 inhibits H3S10 phosphorylation on AURKB gene. ChIP-qPCR experiments of MDA-MB-231 cells treated with 10 µM BI-D1870. Cell lysates were immunoprecipitated using α-H3S10ph antibody and non-specific IgG as negative control and immunoprecipitated DNA was amplified with primers targeting a 5' distal region (-800), a region including promoter and transcription start sites (TSS) and a 3' distal region (intrag). Enrichments for the individual antibodies used are plotted as percent of input DNA. Error bars represent standard deviations calculated from three independent biological experiments. The statistical significance of the individual bars is compared to their respective control bar: *p-values* *p<0,05.

5. DISCUSSION

We previously demonstrated that the depletion of the architectural transcription factor HMGA1 induces the loss of malignant properties of breast cancer cells, leading to the mesenchymal to epithelial transition (Pegoraro et al., 2013). Here we show that the silencing of this protein is associated also with the down-regulation of the levels of H3S10ph and H3S28ph (fig. 4.4), providing evidence of a link between HMGA1 expression and the epigenetic status of cancer cells. Consistently, these modifications have been demonstrated to be indispensable for neoplastic transformation (Choi et al., 2005; Kim et al., 2008).

H3S10/H3S28ph has been mainly associated with mitosis and the transcriptional activation of IEGs during nucleosomal response (Goto et al., 1999; Thomson et al., 1999). However, recent evidence has highlighted the role of these modifications also in regulating genes not belonging to IEGs class (Lau and Cheung, 2011; Cha et al., 2013). Notably, H3S28ph has been demonstrated to activate the expression of tRNAs (Zhang et al., 2011), whose levels have been related to neoplastic transformation as well (Pavon-Eternod et al., 2009). These data provide further evidence of the role of these modifications in general transcriptional regulation.

The main kinases known to be responsible for H3 phosphorylation are MSK1/2 and RSK2 as regards transcription activation (Deak et al., 1998; Sassone-Corsi et al., 1999) and Aurora B kinase during mitosis (Petsalaki et al., 2011). We previously demonstrated that HMGA1 silencing causes the down-regulation of AURKB gene (Pegoraro et al., 2013) leading to the hypothesis that H3 phosphorylation decrease could be linked to Aurora B decrement. However, data previously obtained in our laboratory demonstrated that a very low percentage of MDA-MB-231 cells are mitotic. On the contrary, we showed by immunofluorescence that all cells were positive for H3S10/H3S28ph staining (fig. 4.5), indicating that these modifications are mainly linked to interphasic events in our model. Consistently, previous experiments showed that HMGA1 depletion does not alter the distribution of these cells among the cell cycle phases, demonstrating that the H3 phosphorylation we are looking at is not linked to mitosis but rather to transcription regulation. This is supported by the fact that by using different inhibitors targeting H3S10/H3S28ph we always observed the down-regulation of a specific set of HMGA1-regulated genes.

By using the inhibitor UO126 (targeting MEK1/2), we demonstrated that the RAS/RAF/MEKK/ERK pathway is responsible for the interphasic H3 phosphorylation in our model. This result could be somehow expected, since MDA-MB-231 cells exhibit the K-RAS

mutation (G13D) (Kozma et al., 1987), which leads to high levels of activated ERK, with respect to other cell lines expressing the wild-type form (Eckert et al., 2004).

We previously demonstrated that HMGA1 silencing is associated with the loss of malignant properties in breast cancer cells (Pegoraro et al., 2013). On the other hand, here we showed that HMGA1 depletion causes the decrease of H3S10/H3S28ph, suggesting that these modifications are strictly related to the tumour phenotype. Experiments performed by treating MDA-MB-453 cells with Emodin confirmed this hypothesis. Indeed, the tumour phenotype reversion induced by this molecule was associated with a dramatic down-regulation of H3 phosphorylation (fig. 4.9). Interestingly, very recently others demonstrated that Emodin treatment down-regulated H3S10ph at the level of promoters of cancer-related genes and inhibited the cell growth of four bladder cancer cell lines (Cha et al., 2013), further supporting our findings.

It is noteworthy that Emodin inhibits the Her2/neu receptor, which can activate different transduction pathways, among which the RAS/RAF/MEKK/ERK one (Long et al., 2010). Therefore, it is likely that the malignant phenotype reverted by Emodin depends also on the activity of this pathway. These data, along with the finding that HMGA1 silencing induces the mesenchymal to epithelial transition (Pegoraro et al., 2013), suggest that H3S10/H3S28ph decrease could have a role in the phenotype reversion observed in our models according to the causative role in neoplastic transformation described for these modifications (Choi et al., 2005; Kim et al., 2008).

Literature data reported that HMGA1 up-regulates the expression of proteins involved in sustaining the RAS/RAF/MEKK/ERK pathway located upstream to ERK (Treff et al., 2004). However, we demonstrated that the levels of activated ERK were unaffected by HMGA1 silencing (fig. 4.10), thus excluding this regulation mechanism in our model and suggesting that HMGA1 acts downstream to ERK activation. We demonstrated that HMGA1 does not regulate the expression of MSK1 and RSK2 (fig. 4.11), prompting us to hypothesise that HMGA1 could regulate H3 phosphorylation independently from its transcriptional activity. Our protein-protein interaction data showing that HMGA1 binds to histone H3 (figs. 4.1-3) led us to speculate about a novel mechanism of action for HMGA1 at the chromatin level, i.e. the modulation of H3 phosphorylation by participating in the recruitment of histone modifiers onto nucleosomes. Indeed, HMGA1 is a key factor for the binding of Brg1 protein (the ATPase subunit of SWI/SNF chromatin remodelling complex) to promoter regions (Duncan and Zhao, 2007). Notably, MSK1/2 is known to associate with this complex and

H3S10/H3S28ph carried out by this kinase is involved in the docking of SWI/SNF onto chromatin (Drobic et al., 2010). However, our data do not allow us to exclude that HMGA1 regulates the expression of phosphatases responsible for H3S10/H3S28ph removal.

To provide valuable insight into the epigenetic regulatory mechanism that HMGA1 participate in, we performed several experiments to determine which kinase was responsible for interphasic H3S10/H3S28ph in our model. Data obtained by the MSK1/2 inhibitor H89 (fig. 4.12) perfectly overlapped with those arising from HMGA1 silencing. Indeed, H3S10/H3S28ph was substantially down-regulated and this event was associated with cell morphological changes and with the loss of migratory properties. Since this kinase is well-known to activate IEGs expression by phosphorylating H3S10/H3S28ph and that the steady-state levels of these genes correlate with cancer progression (Healy et al., 2013), we hypothesised that the phenotype reversion mediated by HMGA1 silencing could be associated with the down-regulation of IEGs. However, the expression analyses of some of them suggested that HMGA1 did not regulate IEGs in our model (fig. 4.13).

Conversely, we demonstrated that H89-mediated H3S10/H3S28ph decrease was associated with the down-regulation of genes known to be activated by HMGA1 (fig. 4.15) and whose expression is related to malignant properties of MDA-MB-231 cells. Indeed, the depletion of AURKB, KIF23, KIF4A, and CENPF genes caused the loss of migratory properties in this cell line (Pegoraro et al., 2013).

These data led us to hypothesise that HMGA1 activated these genes by modulating H3 phosphorylation mediated by MSK1/2. However, validation experiments performed with a more specific MSK1/2 inhibitor (SB747651A) and siRNAs against these kinases did not confirm the role of MSK1/2 in this regulation mechanism (figs.4.16-17). H89 inhibitor is largely used to study MSK1/2 activity, even though it does not exhibit high specificity (Davies et al., 2000). In fact, it inhibits several other kinases, among which RSK2 that is responsible for H3 phosphorylation as well. Results obtained with a RSK2 inhibitor (BI-D1870 – fig. 4.18) overlapped with those achieved by HMGA1 silencing, as occurred for H89 treatment. Indeed, H3S10/H3S28ph was efficiently inhibited and this event was associated with the down-regulation of the genes listed above and the loss of migratory properties, suggesting that HMGA1 modulates H3 phosphorylation mediated by RSK2. However, these data need to be validated by specific siRNAs against this kinase.

Interestingly, H89 inhibitor is also able to block PKA (cAMP-dependent protein kinase). This kinase has an inhibitory activity towards the RAS/RAF-1/MEKK/ERK pathway, but in cells

expressing the B-RAF protein, such as MDA-MB-231 cells, it has a stimulatory activity towards to ERK activation (Stork and Schmitt, 2002). Therefore, results obtained with H89 could also be explained by the PKA inhibition of the RAS/RAF/MEKK/ERK pathway.

This pathway is fundamental for the maintenance of the aggressive features of MDA-MB-231 cells. Indeed, by targeting the activity of this axis at different levels we achieved overlapping results, i.e. the loss of migratory abilities. Phosphorylation of histone H3 is one of the most downstream events of this cascade, which has a role in transcriptional regulation (Deak et al., 1998). Our data suggest that HMGA1 is a master regulator of this pathway, acting downstream to ERK and possibly at chromatin level. We choose AURKB as a representative gene whose both gene and protein expression was dependent on HMGA1 presence and on the RAS/RAF/MEKK/ERK pathway (fig. 4.14, 4.15, 4.18, and 4.19; Bonet et al., 2012) to evaluate the site-specific H3S10/H3S28ph modulation. The available ChIP data regarding H3S10/H3S28ph localisation available nowadays were obtained by mitogenic or stress stimulation of serum starved cells and highlighted an induction of this modification at regulatory regions (Drobic et al., 2010; Lau and Cheung, 2011). However, it is noteworthy that we evaluated the basal H3S10ph level of an actively transcribed gene with respect to its inhibition. This situation is opposite to those analysed in literature. Moreover, ChIP-seq data regarding H3S10ph in mammalian cells are not available, at least to our knowledge. Therefore, we do not know where basal H3S10ph occurs at genome-wide level.

Our ChIP-qPCR results highlighted the presence of H3S10ph on AURKB gene and we found a relevant change in this modification levels upon RSK2 inhibition solely in an intragenic region. These data are inconsistent with the above mentioned literature information. However, even though these data must be considered as preliminary, they suggest a still unknown H3 phosphorylation-dependent regulatory mechanism for the control of AURKB gene expression.

Another aspect that has been well evidenced in this work but not fully investigated is the down-regulation of histone H3 (fig. 4.4, 4.7, 4.9, 4.12, 4.14, 4.15, and 4.18). This phenomenon has been observed in RSK2-/- MEFs by the group of Dong but it has not been discussed (Cho et al., 2007). These data support our finding that HMGA1 could regulate RSK2-mediated H3S10/H3S28ph. The down-regulation of histone H3 was intriguingly observed also in HMGB-/- MEFs affecting both genome-wide nucleosomal occupancy and transcriptional output (Celona et al., 2011). The regulation of histone abundance by HMGA1 could represent a yet unexplored mechanism of genome-wide transcriptional control exerted by this architectural transcription factor.

Since from their discovery, HMGA architectural transcription factors have been related to cancer development and progression. They act in these processes mainly by regulating gene expression through several well-characterised mechanisms, including DNA structure modulation and the interaction with other transcription factors. In conclusion, here we provide evidence that HMGA1 protein could promote the aggressiveness of cancer cells even by regulating their epigenetic status.

SUPPLEMENTARY FIGURES

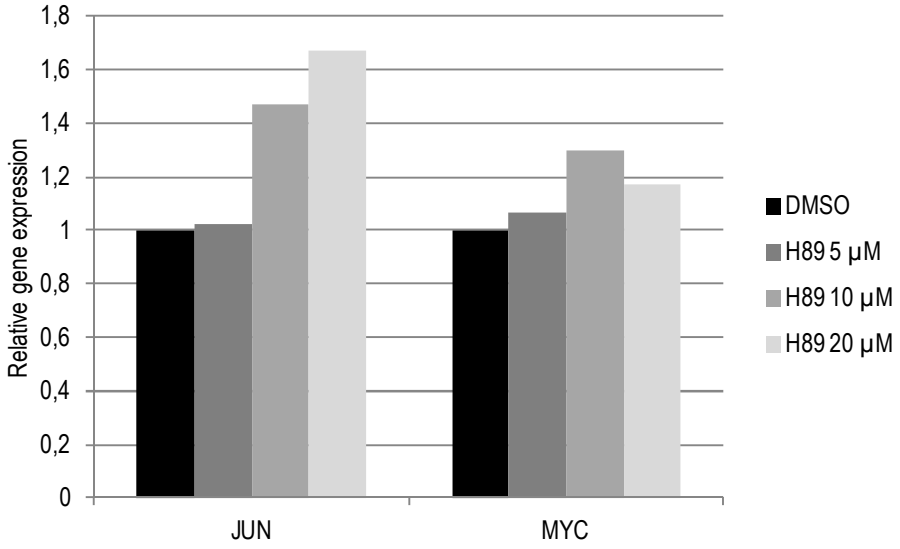

Figure S1: Steady-state levels of IEGs are not down-regulated by H89. RT-qPCR analysis of MDA-MB-231 cells treated with H89 5, 10, and 20 µM and harvested after 72 h. mRNA expression of JUN and MYC genes was analysed using GAPDH as internal control. The data are represented relative to control. The experiment was preliminarily run in single replicate; therefore standard deviations and statistical significance (*t test*) are not reported.

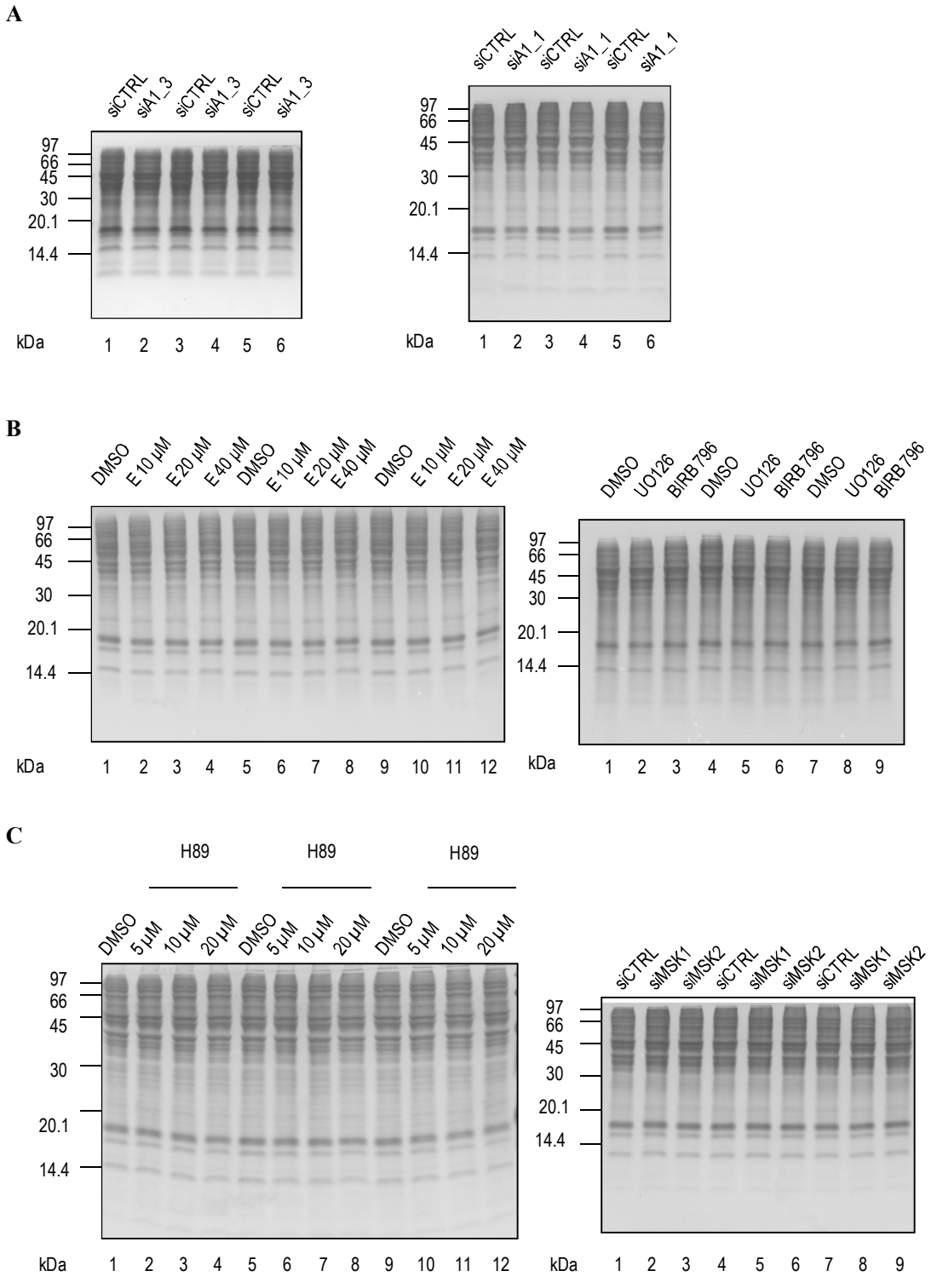
A
siCTRL
siA1_3
siCTRL
siA1_3
siCTRL
siA1_3
97
66
45
30
20.1
14.4
kDa
1 2 3 4 5 6
siCTRL
siA1_1
siCTRL
siA1_1
siCTRL
siA1_1
97
66
45
30
20.1
14.4
kDa
1 2 3 4 5 6
B
DMSO
E 10 µM
E 20 µM
E 40 µM
DMSO
E 10 µM
E 20 µM
E 40 µM
DMSO
E 10 µM
E 20 µM
E 40 µM
97
66
45
30
20.1
14.4
kDa
1 2 3 4 5 6 7 8 9 10 11 12
DMSO
UO126
BIRB796
DMSO
UO126
BIRB796
DMSO
UO126
BIRB796
97
66
45
30
20.1
14.4
kDa
1 2 3 4 5 6 7 8 9
C
H89
H89
H89
DMSO
5 µM
10 µM
20 µM
DMSO
5 µM
10 µM
20 µM
DMSO
5 µM
10 µM
20 µM
97
66
45
30
20.1
14.4
kDa
1 2 3 4 5 6 7 8 9 10 11 12
siCTRL
siMSK1
siMSK2
siCTRL
siMSK1
siMSK2
siCTRL
siMSK1
siMSK2
97
66
45
30
20.1
14.4
kDa
1 2 3 4 5 6 7 8 9

D

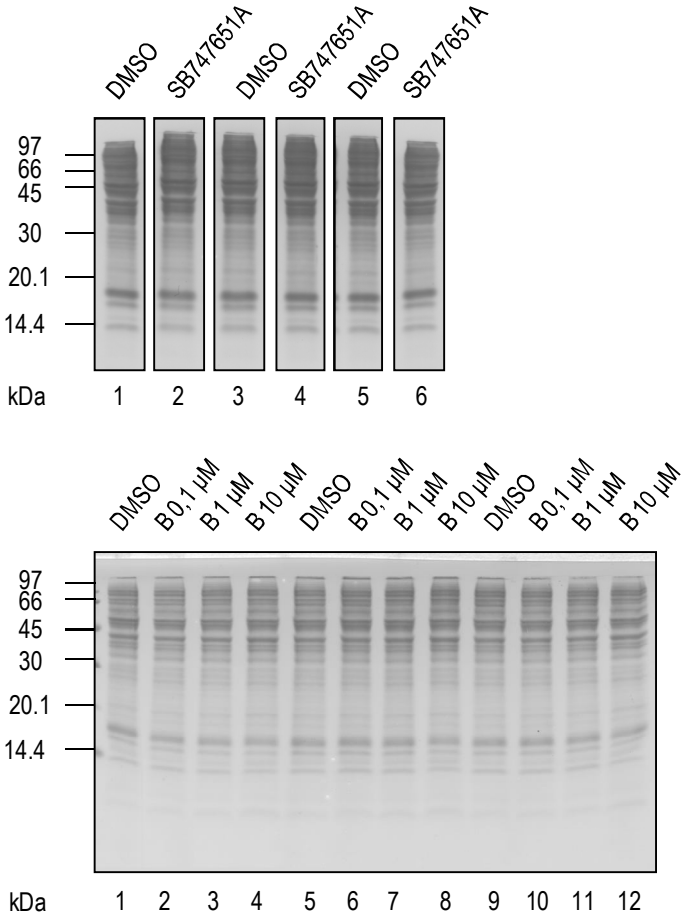

Figure S2: Red ponceau stained membranes reported as loading and quantification control relative to western blot analyses described in figure 4.19.

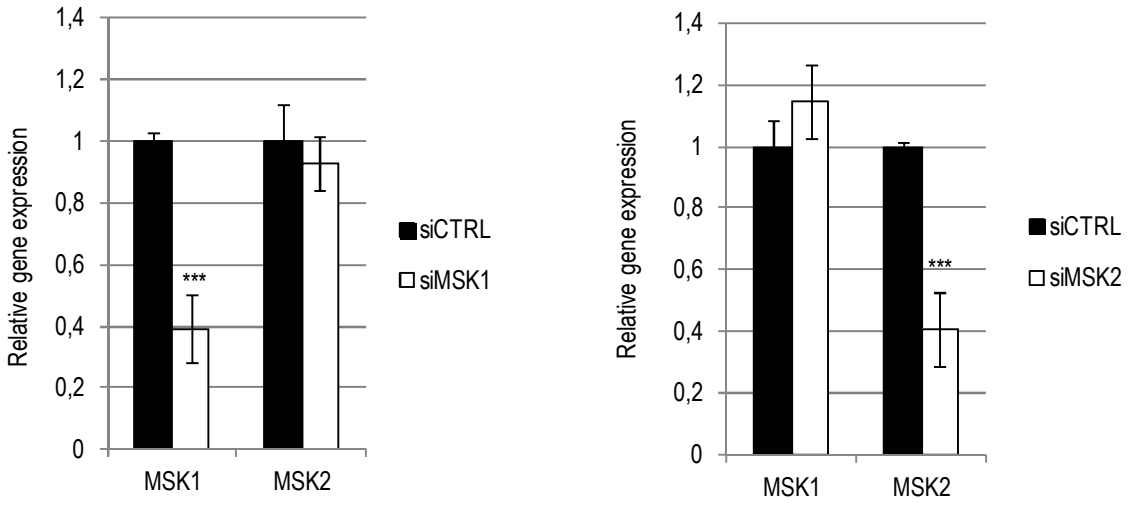

Figure S3: MSK1 and MSK2 silencing by siRNAs. RT-qPCR analysis of MDA-MB-231 cells transfected with control, MSK1, or MSK2 siRNAs and harvested after 72 h. mRNA expression of MSK1 and MSK2 genes was analysed using CYC33 as internal control. The experiment was run in triplicate. The data are represented as the means relative to siCTRL samples. Standard deviations and statistical significance (*t test*) are indicated (*p-values* ***p<0,001).

REFERENCES

Akaboshi, S., Watanabe, S., Hino, Y., Sekita, Y., Xi, I., Araki, K., Yamamura, K., Oshima, M., Ito, T., Baba, H. e*t al.* (2009). HMGA1 is induced by Wnt/beta-catenin pathway and maintains cell proliferation in gastric cells. The American journal of pathology *175*, 1675-1685.

Banks, G., Li, Y., and Reeves, R. (2000). Differential in vivo modifications of HMGI(Y) nonhistone chromatin proteins modulate nucleosome and DNA interactions. Biochemistry *39*, 8333-8346.

Bannister, A.J., and Kouzarides, T. (2011). Regulation of chromatin by histone modifications. Cell Res *21*, 381-395.

Berlingieri, M.T., Pierantoni, G.M., Giancotti, V., Santoro, M., and Fusco A. (2002). Thyroid cell transformation requires the expression of the HMGA1 proteins. Oncogene *21*, 2971-80.

Bernstein, B.E., Meissner, A., and Lander, E.S. (2007). The mammalian epigenome. Cell *128*, 669-681.

Bonet, C., Giuliano, S., Ohanna, M., Bille, K., Allegra, M., Lacour, J.P., Bahadoran, P., Rocchi, S., Ballotti, R., and Bertolotto, C. (2012). Aurora B is regulated by the mitogen-activated protein kinase/extracellular signal-regulated kinase (MAPK/ERK) signaling pathway and is a valuable potential target in melanoma cells. The Journal of biological chemistry *287*, 29887-29898.

Bos, J.L. (1988). The ras gene family and human carcinogenesis. Mutat Res *195*, 255-271.

Bourachot, B., Yaniv, M., and Muchardt, C. (1999). The activity of mammalian brm/SNFalpha is dependent on a high-mobility-group protein I/Y like DNA binding domain. Molecular and cellular biology *19*, 3931-3939.

Bustin, M. (2001). Chromatin unfolding and activation by HMGN chromosomal proteins. Trends Biochem. Sci. *26*, 431-437.

Bustin, M., and Reeves R. (1996). High mobility group chromosomal proteins: architectural components that facilitate chromatin function. Prog. Nucleic Acids Res. Mol. Biol. *54*, 35-100.

Bustin, M., Catez, F., and Lim, J.H. (2005). The dynamics of histone H1 function in chromatin. Molecular cell *17*, 617-620.

Bustin, M., Lehn, D.A., and Landsman, D. (1990). Structural features of the HMG chromosomal proteins and their genes. Biochimica et biophysica acta *1049*, 231-243.

Carriere, A., Ray, H., Blenix, J., and Roux, P.P. (2008). The RSK factors of activating the Ras/MAPK signaling cascade. Frontiers in bioscience *13*, 4258-4275.

Casalino, L., Bakiri, L., Talotta, F., Weitzman, J.B., Fusco, A., Yaniv, M., and Verde, P. (2007). Fra-1 promotes growth and survival in RAS-transformed thyroid cells by controlling cyclin A transcription. EMBO Journal *26*, 1878-1890.

Caterino,T.L., and Hayes, J.J. (2011). Structure of the H1 C-terminal domain and function in chromatin condensation. Biochemistry and cell biology *89*, 35-44.

Celona, B., Weiner, A., Di Felice, F., Mancuso, F.M., Cesarini, E., Rossi, R.L., Gregory, L., Baban, D., Rossetti, G., Grianti, P., Pagani, M., Bonaldi, T., Ragoussis, J., Friedman, N., Camilloni, G., Bianchi, M.E., and Agresti, A. (2011). Substantial histone reduction modulates genomewide nucleosomal occupancy and global transcriptional output. Plos biology *9*:e1001086.

Cha, T.L., Chuang, M.J., Tang, S.H., Wu, S.T., Sun, K.H., Chen, T.T., Sun, G.H., Chang, S.Y., Yu, C.P., Ho, J.Y., Liu, S.Y., Huang, S.M., and Yu, D.S. (2013). Emodin modulates epigenetic modifications and suppresses bladder carcinoma cell growth. Molecular carcinogenesis, Epub ahead of print.

Chau, K.Y., Patel, U.A., Lee, K.L., Lam, H.Y., and Crane-Robinson, C. (1995). The gene for the human architectural transcription factor HMGI-C consists of five exons each coding for a distinct functional element. Nucleic Acids Res. *23*, 4262-4266.

Cheung, P., Tanner, K.G., Cheung, W.L., Sassone-Corsi, P., Denu, J.M., and Allis, C.D. (2000). Synergistic coupling of histone H3 phosphorylation and acetylation in response to epidermal growth factor stimulation. Molecular cell *5*, 905-915.

Chi, P., Allis, C.D., and Wang, G.G. (2010). Covalent histone modifications – miswritten, misinterpreted and mis-erased in human cancers. Nature Reviews Cancer *10*, 457-469.

Chiappetta, G., Avantaggiato, V., Visconti, R., Fedele, M., Battista, S., Trapasso, F., Merciai, B.M., Fidanza, V., Giancotti, V., Santoro, M., Simeone, A., and Fusco, A. (1996). High level expression of the HMGI-C gene during embryonic development. Oncogene *13*, 2439-2446.

Chiefari, E., Iiritano, S., Paonessa, F., Le Pera, I., Arcidiacono, B., Filocamo, M., Foti, D., Liebhaber, S.A., and Brunetti, A. (2010). Pseudogene-mediated posttranscriptional silencing of HMGA1 can result in insulin resistance and type 2 diabetes. Nat. Commun. 1:40.

Cho, Y.Y., Yao, K., Kim, H.G., Kang, B.S., Zheng, D., Bode, A.M., and Dong, Z. (2007). Ribosomal S6 kinase 2 is a key regulator in tumor promoter induced cell transformation. Cancer Res. *67*, 8104,8112.

Choi, H.S., Choi, B.Y., Cho, Y.Y., Mizuno, H., Kang, B.S., Bode, A.M., and Dong, Z. (2005). Phosphorylation of histone H3 at serine 10 is indispensable for neoplastic cell transformation. Cancer research *65*, 5818-5827.

Cleynen, I., Huysmans, C., Sasazuki, T., Shirasawa, S., Van de Ven, W., and Peeters, K. (2007). Transcriptional control of the human high mobility group A1 gene: basal and oncogenic Ras-regulated expression, Cancer Res. *67*, 4620-4629.

Davies, S.P., Reddy, H., Caivano, M., and Cohen, P. (2000). Specificity and mechanism of action of some commonly used protein kinase inhibitors. The Biochemical journal *351*, 95-105.

Deak, M., Clifton, A.D., Lucocq, L.M., and Alessi, D.R. (1998). Mitogen- and stress-activated protein kinase-1 (MSK1) is directly activated by MAPK and SAPK2/p38, and may mediate activation of CREB. The EMBO journal *17*, 4426-4441.

Drobic, B., Perez-Cadahia, B., Yu, J., Kung, S.K., and Davie, J.R. (2010). Promoter chromatin remodeling of immediate-early genes is mediated through H3 phosphorylation at either serine 28 or 10 by the MSK1 multi-protein complex. Nucleic acids research *38*, 3196-3208.

Duncan, B., and Zhao, K. (2007). HMGA1 mediates the activation of the CRYAB promoter by BRG1. DNA and cell biology *26*, 745-752.

Dunn, K.L., Espino, P.S., Drobic, B., He, S., and Davie, J.R. (2005). The Ras-MAPK signal transduction pathway, cancer and chromatin remodeling. Biochem Cell Biol *83*, 1-14.

Eckert, L.B., Repasky, G.A., Ulkü, A.S., McFall, A., Zhou, H., Sartor, C.I., and Der, C.J. (2004). Involvement of Ras activation in human breast cancer cell signaling, invasion, and anoikis. Cancer research *64*, 4585-4592.

Edberg, D., Bruce, J., William, F., Siems, F., and Reeves, R. (2004). In vivo posttranslational modifications of high mobility group A1a protein in breast cancer of differing metastatic potential. Biochemistry *43*, 11500-11515.

Elsheikh, S.E., Green, A.R., Rakha, E.A., Powe, D.G., Ahmed, R.A., Collins, H.M., Soria, D., Garibaldi, J.M., Paish, C.E., Ammar, A.A., Grainge, M.J., Ball, G.R., Abdelghany, M.K., Martinez-Pomares, L., Heery, D.M., and Ellis, I.O. (2009). Global histone modifications in breast cancer correlate with tumor phenotypes, prognostic factors, and patient outcome. Cancer Res. *69*, 3802-3809.

Evans, J.N., Zajicek, J., Nissen, M.S., Munske, G., Smith, V., and Reeves, R. (1995). 1H and 13C NMR assignments and molecular modeling of a minor groove DNA-binding peptide from the HMG-I protein. Int. J. Pept. Protein Res. *45*, 554-560.

Fedele, M., Battista, S., Kenyon, L., Baldassarre, G., Fidanza, V., Klein-Szanto, A.J., Parlow, A.F., Visone, R., Pierantoni, G.M., Outwater, E., Santoro, M., Croce, C.M., and Fusco, A. (2002). Overexpression of the HMGA2 gene in transgenic mice leads to the onset of pituitary adenomas. Oncogene *21*, 3190-3198.

Fedele, M., Fidanza, V., Battista, S., Pentimalli, F., Klein-Szanto, A.J., Visone, R., De Martino, I., Curcio, A., Morisco, C., Del Vecchio, L., Baldassarre, G., Arra, C., Viglietto, G., Indolfi, C., Croce, C,M,, and Fusco, A. (2006). Haploinsufficiency of the Hmga1 gene causes cardiac hypertrophy and myelo-lymphoproliferative disorders in mice. Cancer Res. *66*, 2536-2543.

Fedele, M., Pentimalli, F., Baldassarre, G., Battista, S., Klein-Szanto, A.J., Kenyon, L., Visone, R., De Martino, I., Ciarmiello, A., Arra, C., Viglietto, G., Croce, C.M., and Fusco, A. (2005). Transgenic mice overexpressing the wild-type form of the HMGA1 gene develop mixed growth hormone/prolactin cell pituitary adenomas and natural killer cell lymphomas. Oncogene *24*, 3427-3435.

Fedele, M., Visone, R., De Martino, I., Troncone, G., Palmieri, D., Battista, S., Ciarmiello, A., *et al.* (2006). HMGA2 induces pituitary tumorigenesis by enhancing E2F1 activity, Cancer Cell *9*, 459-471.

Foti, D., Iuliano, R., Chiefari, E., and Brunetti, A. (2003). A nucleoprotein complex containing Sp1, C/EBP beta, and HMGI-Y controls human insulin receptor gene transcription. Molecular and cellular biology *23*, 2720-2732.

Frangini, A., Sjöberg, M., Roman-Trufero, M., Dharmalingam, G., Haberle, V., Bartke, T., Lenhard, B., Malumbres, M., Vidal, M., and Dillon, N. (2013). The aurora B kinase and the polycomb protein ring1B combine to regulate active promoters in quiescent lymphocytes. Mol Cell *51*, 647-661.

Frasca, F., Rustighi, A., Malaguarnera, R., Altamura, S., Vigneri, P., Del Sal, G., Giancotti, V., *et al.* (2006). HMGA1 inhibits the function of p53 family members in thyroid cancer cells. Cancer Res. *66*, 2980-2989.

Friedmann, M., Holth, L.T., Zoghbi, H.Y., and Revees, R. (1993) Organization, inducible-expression and chromosome localization of the human HMG-I(Y) nonhistone protein gene. Nucleic Acids Res. *21*, 4259-4267.

Fusco, A. and Fedele, M. (2007). Roles of HMGA proteins in cancer. Nature *7*, 899-910.

Gehani, S.S., Agrawal-Singh, S., Dietrich, N., Christophersen, N.S., Helin, K., and Hansen, K. (2010). Polycomb group protein displacement and gene activation through MSK-dependent H3K27me3S28 phosphorylation. Molecular cell *39*, 886-900.

Goodwin, G.H., Sanders, C., and Johns, E.W. (1973). A new group of chromatin-associated proteins with a high content of acidic and basic amino acids. Eur. J. Biochem. *38*, 14-19.

Goto, H., Tomono, Y., Ajiro, K., Kosako, H., Fujita, M., Sakurai, M., Okawa, K., Iwamatsu, A., Okigaki, T., Takahashi, T., and Inagaki, M. (1999). Identification of a novel phosphorylation site on histone H3 coupled with mitotic chromosome condensation. The journal of biological chemistry *274*, 25543-25549.

Goto, H., Yasui, Y., Nigg, E.A., and Inagaki, M. (2002). Aurora-B phosphorylates Histone H3 at serine28 with regard to the mitotic chromosome condensation. Genes Cells *7*, 11-17.

Healy, S., Khan, P., and Davie, J.R. (2013). Immediate early response genes and cell transformation. Pharmacology and therapeutics *137*, 64-77.

Helin, K., and Dhanak, D. (2013). Chromatin proteins and modifications as drug targets. Nature *502*, 480-488.

Hendzel, M.J., Wei, Y., Mancini, M.A., Van Hooser, A., Ranalli, T., Brinkley, B.R., Bazett-Jones, D.P., and Allis, C.D. (1997). Mitosis-specific phosphorylation of histone H3 initiates primarily within pericentromeric

heterochromatin during G2 and spreads in an ordered fashion coincident with mitotic chromosome condensation. Chromosoma *106*, 348-360.

Hess, J.L. (1998). Chromosomal translocations in benign tumors: the HMGI proteins. American journal of clinical pathology *109*, 251-261.

Hill, C.S., and Treisman, R. (1995). Transcriptional regulation by extracellular signals: mechanisms and specificity. Cell *80*, 199-211.

Hill, D.A., and Reeves, R. (1997). Competition between HMGI-(Y), HMG-1 and histone H1 on four-way junction DNA. Nucleis Acids Res. *25*, 3523-3531.

Hirota, T., Lipp, J.J., Toh, B.H., and Peters, J.M. (2005). Histone H3 serine 10 phosphorylation by Aurora B causes HP1 dissociation from heterochromatin. Nature *438*, 1176-1180.

Hock, R., Furusawa, T., Ueda, T., Bustin, M. (2007). HMG chromosomal proteins in development and disease. Trend Cell Biol. *17*, 72-79.

Hsu, Y.L., Hou, M.F., Kuo, P.L., Huang, Y.F., and Tsai, E.M. (2013). Breast tumor-associated osteoblast-derived CXCL5 increases cancer progression by ERK/MSK1/Elk-1/snail signaling pathway. Oncogene *32*, 4436-4447.

Huang, K.T., Chen, Y.H., and Walker, A.M. (2004). Inaccuracies in MTS assays: major distorting effects of medium, serum albumin, and fatty acids. BioTechniques *37*, 406,408, 410-412.

Huth, J.R., Bewley, C.A., Nissen, M.S., Evans, J.N., Reeves, R., Gronenborn, A.M., and Clore, G.M. (1997). The solution structure of an HMG-I(Y)-DNA complex defines a new architectural minor groove binding motif. Nat. Struct. Biol. *4*, 657-665.

Iyer, V.R. (2012). Nucleosome positioning: bringing order to the eukaryotic genome. Trends in cell biology *22*, 250-256.

John, S., Reeves, R.B., Lin, J.X., Child, R., Leiden, J.M., Thomson, C.B., and Leonard, W.J. (1995).Regulation of cell-type-specific interleukin-2 receptor alpha-chain gene expression: potential role of physical interactions between Elf-1, HMG-I(Y), and NF-kappa B family proteins. Molecular and cellular biology *15*, 1786-1796.

Karin, M. (1992). Signal transduction from cell surface to nucleus in development and disease. FASEB journal: official publication of the Federation of American Societies for Experimental Biology *6*, 2581-2590.

Khan, P., Drobic, B., Pérez-Cadahía, B., Healy, S., He, S., and Davie, J.R. (2013). Mitogen- and stress-activated protein kinases 1 and 2 are required for maximal trefoil factor 1 induction. Plos one *8*, e63189.

Kim, H.G., Lee, K.W., Cho, Y.Y., Kang, N.J., Oh, S.M., Bode, A.M., and Dong, Z. (2008). Mitogen- and stress-activated kinase 1-mediated histone H3 phosphorylation is crucial for cell transformation. Cancer Res. *68*, 2538-2547.

Kimura, M., Uchida, C., Takano, Y., Kitagawa, M., and Okano, Y. (2004). Cell-cycle dependent regulation of the human aurora B promoter. Biochemical and biophysical research communications *316*, 930-936.

Kozma, S.C., Bogaard, M.E., Buser, K., Saurer, S.M., Bos, J.L., Groner, B., and Hynes, N.E. (1987). The human c-Kirsten ras gene is activated by a novel mutation in codon 13 in the breast carcinoma cell line MDA-MB231. Nucleic acids research *15*, 5963-5971.

Kumar, M.S., Armenteros-Monterroso, E., East, P., Chakravorty, P., Matthews, N., Winslow, M.M., and Downward, J. (2014). HMGA2 functions as a competing endogenous RNA to promote lung cancer progression. Nature *505*, 212-217.

Laemmli, U.K., Kas, E., Polijak, L., and Adachi, Y. (1992). Scaffold-associated regions: cis acting determinants of chromatin structural loops and functional domains. Curr. Opin. Genet. Dev. *2*, 75-85.

Lai, J.S., and Herr, W (1992). Ethidium bromide provides a simple tool for identifying genuine DNA-independent protein associations. Proceedings of the National Academy of Sciences of the United States of America *89*, 6958-6962.

Lau, P.N., and Cheung, P. (2011). Histone code pathway involving H3 S28 phosphorylation and K27 acetylation activates transcription and antagonizes polycomb silencing. Proceedings of the National Academy of Sciences of the United States of America *108*, 2801-2806.

Lee, Y.S., and Dutta, A. (2007). The tumor suppressor microRNA let-7 represses the HMGA2 oncogene. Genes & development *21*, 1025-1030.

Lewis, R.T., Andreucci, A., and Nikolajczyk, B.S., (2001). PU.1 mediated transcription is enhanced by HMGI(Y)-dependent structural mechanism. The Journal of biological chemistry *276*, 9550-9557.

Lin, Y., Chen, H., Hu, Z., Mao, Y., Xu, X., Zhu, Y., Xu, X., Wu, J., Li, S., Mao, Q., et al. (2013). miR-26a inhibits proliferation and motility in bladder cancer by targeting HMGA1. FEBS Letters *587*, 2467-2473.

Long, J.S., Fujiwara, Y., Edwards, J., Tannahill, C.L., Tigyi, G., Pyne, S., and Pyne, N.J. (2010). Sphingosine 1-phosphate receptor 4 uses HER2 (ERBB2) to regulate extracellular signal regulated kinase-1/2 in MDA-MB-453 breast cancer cells. The Journal of biological chemistry *285*, 35957-35966.

Luger, K., Mader, A.W., Richmond, R.K., Sargent, D.F., and Richmond, T.J. (1997). Crystal structure of the nucleosome core particle at 2.8 A resolution. Nature *389*, 251-260.

Macdonald, N., Welburn, J.P., Noble, M.E., Nguyen, A., Yaffe, M.B., Clynes, D., Moggs, J.G., Orphanides, G., Thomson, S., Edmunds, J.W., Clayton, A.L., Endicott, J.A., and Mahadevan, L.C. (2005). Molecular basis for the recognition of phosphorylated and phosphoacetylated histone h3 by 14-3-3. Molecular cell *20*, 199-211.

Margueron, R., and Reinberg, D. (2011). The polycomb complex PRC2 and its mark in life. Nature *469*, 343-349.

Maurizio, E., Cravello, L., Brady, L., Spolaore, B., Arnoldo, L., Giancotti, V., Manfioletti, G., and Sgarra, R. (2011). Conformational role for the C-terminal tail of the intrinsically disordered High Mobility Group A (HMGA) chromatin factors. Journal of proteome research *10*, 3283-3291.

McKay, M.M., and Morrison, D.K. (2007). Integrating signals from RTKs to ERK/MAPK. Oncogene *26*, 3113-3121.

Merienne, K., Pannetier, S., Harel-Bellan, A., and Sassone-Corsi, P. (2001).Mitogen-regulated RSK2-CBP interaction controls their kinase and acetylase activity. Molecular and cellular biology *21*, 7089-7096.

Mishra, S., Saleh, A., Espino, P.S., Davie, J.R., and Murphy, L.J. (2006). Phosphorylation of histones by tissue transglutaminase. The journal of biological chemistry *281*, 5532-5538.

Munshi, N., Merika, M., Yie, J., Senger, K., Chen, G., and Thanos, D. (1998). Acetylation of HMGI(Y) by CBP turns off IFN beta expression by disrupting the enhanceosome *2*, 457-467.

Naqvi, S., Macdonald, A., McCoy, C.E., Darragh, J., Reith, A.D., and Arthur, J.S.C. (2012). Characterization of the cellular action of the MSK inhibitor SB-747651A. The Biochemical journal *441*, 347-357.

Nissen, M.S., and Reeves, R. (1995). Changes in superhelicity are introduced into closed circular DNA by binding of high mobility group proteinI/Y. The Journal of biological chemistry. *270*, 4355-4360.

Nissen, M.S., Langan, T.A., Reeves, R. (1991). Phosphorylation by cdc2 kinase modulates DNA binding activity of high mobility group protein I nonhistone chromatin protein. The journal of biological chemistry *266*, 19945-19952.

Nowak, S.J., and Corces, V.G. (2004). Phosphorylation of histone H3: a balancing act between chromosome condensation and transcriptional activation. Trends in genetics: TIG *20*, 214-220.

Park, J.H., Lin, M.L., Nishidate, T., Nakamura, Y., and Katagiri, T. (2006). PDZ-binding kinase/T-LAK cell-originated protein kinase, a putative cancer/testis antigen with an oncogenic activity in breast cancer. Cancer research *66*, 9186-9195.

Pavon-Eternod, M., Gomez, S., Geslain, R., Dai, Q., Rosner, M.R., and Pan, T. (2009). tRNA over-expression in breast cancer and functional consequences. Oncogene *37*, 7268-7280.

Pegoraro, S., Ros, G., Piazza, S., Sommaggio, R., Ciani, Y., Rosato, A., Sgarra, R., Del Sal, G., and Manfioletti, G. (2013). HMGA1 promotes metastatic processes in basal-like breast cancer regulating EMT and stemness. Oncotarget *4*, 1293-1308.

Pérez-Cadahía, B., Drobic, B., Espino, P.S., He, S., Mandal, S., Healy, S., and Davie, J.R. (2011). Role of MSK1 in the malignant phenotype of Ras-transformed mouse fibroblasts. The journal of biological chemistry *286*, 42-49.

Petsalaki, E., Akoumianaki, T., Black, E.J., Gillespie, D.A., and Zachos, G. (2011). Phosphorylation at serine 331 is required for Aurora B activation. The journal of cell biology *195*, 449-466.

Pierantoni, G.M., Esposito, F., Giraud, S., Bienvenut, W.V., Diaz, J.J., and Fusco, A. (2007). Identification of new high mobility group A1 associated proteins. Proteomics *7*, 3735-3742.

Rahman, M.A., Kohno, H., and Nagasue, N. (2002). COX-2 – a target for preventing hepatic carcinoma? Expert opinion on therapeutic target *6*, 483-490.

Reeves, R., and Adair, J. (2005) Role of high mobility group (HMG) chromatin proteins in DNA repair. DNA repair *4*, 926-938.

Reeves, R., and Beckerbauer, L. (2001). HMGI/Y proteins: flexible regulators of transcription and chromatin structure. Biochimica et biophysica acta *1519*, 13-29.

Reeves, R., and Nissen, M.S, (1993). Interaction of high mobility group-I(Y) nonhistone proteins with nucleosome core particles. The Journal of biological chemistry *268*, 21137-21146.

Reeves, R., and Wolffe, A.P. (1996). Substrate structure influences binding of the non-histone protein HMG-I(Y) to free nucleosomal DNA. Biochemistry *35*, 5063-5074.

Reeves, R., Edberg, D.D., and Li, Y. (2001). Architectural transcription factor HMGI(Y) promotes tumor progression and mesenchymal transition of human epithelial cells. Molecular and cellular biology *21*, 575-594.

Reeves, R., Leonard, W.J., and Nissen, M.S. (2000). Binding of HMG-I(Y) imparts architectural specificity to a positioned nucleosome on the promoter of the human interleukin-2 receptor alpha gene. Molecular and cellular biology *20*, 4666-4679.

Rossetto, D., Avvakumov, N., and Côté, J. (2012). Histone phosphorylation: a chromatin modification involved in diverse nuclear events. Epigenetics *7*, 1098-1108.

Roux, P.P., and Blenis, J. (2004). ERK and p38 MAPK-activated protein kinases: a family of protein kinases with diverse biological functions. Microbiology and molecular biology review *68*, 320-344.

Sassone-Corsi, P., Mizzen, C.A., Cheung, P., Crosio, C., Monaco, L., Jacquot, S., Hanauer, A., and Allis, C.D. (1999). Requirement of Rsk-2 for epidermal growth factor-activated phosphorylation of histone H3. Science *285*, 886-891.

Sawicka, A., and Seiser, C. (2012). Histone H3 phosphorylation – a versatile chromatin modification for different occasions. Biochimie *94*, 2193-2201.

Seligson, D.B., Horvath, S., Shi, T., Yu, H., Tze, S., Grunstein, M., and Kurdistani, S.K. (2005). Global histone modification patterns predict risk of prostate cancer recurrence. Nature *435*, 1262-1266.

Sgarra, R., Diana, F., Bellarosa, C., Dekleva, V., Rustighi, A., Toller, M., Manfioletti, G., and Giancottti, V. (2003). During apoptosis ot tumor cells HMGA1a protein undergoes methylation: identification of the modification site by mass spectrometry. Biochemistry *42*, 3575-3585.

Sgarra, R., Furlan, C., Zammitti, S., Lo Sardo, A., Maurizio, E., Di Bernardo, J., Giancotti, V., and Manfioletti, G. (2008). Interaction proteomics of the HMGA chromatin architectural factors. Proteomics *8*, 4721-4732.

Sgarra, R., Maurizio, E., Zammitti, S., Lo Sardo, A., Giancotti, V., and Manfioletti, G. (2009). Macroscopic differences in HMGA oncoproteins post-translational modifications: C-terminal phosphorylationof HMGA2 affects its DNA-binding properties. Journal of proteome research *8*, 2978-2989.

Sgarra, R., Rustighi, A., Tessari, M.A., Di Bernardo, J., Altamura, S., Fusco, A., Manfioletti, G., and Giancotti, V. (2004). Nuclear phosphoproteins HMGA and their relationship with chromatin structure and cancer. FEBS Letters *574*, 1-8.

Sgarra, R., Tessari, M.A., Di Bernardo, J., Rustighi, A., Zago, P., Liberatori, S., Armini, A., Bini, L., Ginacotti, V., and Manfioletti, G. (2005). Discovering high mobility group A molecular partners in tumour cells. Proteomics *5*, 1494-1506.

Sgarra, R., Zammitti, S., Lo Sardo, A., Maurizio, E., Arnoldo, L., Pegoraro, S., Giancotti, V., and Manfioletti, G. (2010). HMGA molecular network: From transcriptional regulation to chromatin remodeling. Biochimica et biophysica acta *1799*, 37-47.

Shah, S.N., Cope, L., Poh, W., Belton, A., Roy, S., Talbot, C.C. Jr, Sukumar, S., Huso, D.L., and Resar, L.M. (2013). HMGA1: a master regulator of tumor progression in triple-negative breast cancer cells. Plos One *8*, e63419.

Shen, W., Xu, C., Huang, W., Zhang, J., Carlson, J.E., Tu, X., Wu, J., and Shi, Y. (2007). Solution structure of human Brg1 bromodomain and its specific binding to acetylated histone tails. Biochemistry *46*, 2100-2110.

Shogren-Knaak, M., Ishii, H., Sun, J.M., Pazin, M.J., Davie, J.R., and Peterson, C.L. (2006). Histone H4-K16 acetylation controls chromatin structure and protein interactions. Science *311*, 844-847.

Stork, P.J.S., and Schmitt, J.M. (2002). Crosstalk between cAMP and MAP kinase signaling in the regulation of cell proliferation. Trends in cell biology *12*, 258-266.

Tesfaye, A., Di Cello, F., Hillion, J., Ronnett, B.M., Elbahloul, O., Ashfaq, R., Dhara, S., Prochownik, E., Tworkoski, K., Reeves, R., Roden, R., Ellenson, L.H., Huso, D.L., and Resar, L.M. (2007). The high-mobility group A1 gene up-regulates cyclooxygenase 2 expression in uterine tumorigenesis. Cancer research *67*, 3898-4004.

Tessari, M.A., Gostissa, M., Altamura, S., Sgarra, R., Rustighi, A., Salvagno, C., Caretti, G., Imbriano, C., Mantovani, R., Del Sal, G. *et al.* (2003). Transcriptional activation of the cyclin A gene by the architectural transcription factor HMGA2. Molecular and cellular biology *23*, 9104-9116.

Thanos, D., and Maniatis, T. (1995). Virus induction of human IFN beta gene expression requires the assembly of an enhanceosome. Cell *83*, 1091-1100.

Thomson, S., Clayton, A.L., Hazzalin, C.A., Rose, S., Barratt, M.J., and Mahadevan, L.C. (1999). The nucleosomal response associated with immediate-early gene induction is mediated via alternative MAP kinase cascades: MSK1 as a potential histone H3/HMG-14 kinase. The EMBO journal *18*, 4779-4793.

Thuault, S., Valcourt, U., Petersen, M., Manfioletti, G., Heldin, C.H., and Moustakas, A. (2006). Transforming growth factor-beta employs HMGA2 to elicit epithelial-mesenchymal transition. The Journal of cell biology *174*, 175-183.

Treff, N.R., Pouchnik, D., Dement, G.A., Britt, R.L., and Reeves, R. (2004). High-mobility group A1a protein regulates Ras/ERK signaling in MCF-7 human breast cancer cells. Oncogene *23*, 777-785.

Ueda, Y., Watanabe, S., Tei, S., Saitoh, N., Kuratsu, J., and Nakao, M. (2007). High mobility group protein HMGA1 inhibits retinoblastoma protein-mediated cellular G0 arrest. Cancer Sci. *98*, 1893-1901.

Vader, G., and Lens, S.M. (2008). The Aurora kinase family in cell division and cancer. Biochimica et biophysica acta *1786*, 60-72.

Vallone, D., Battista, S., Pierantoni, G.M., Fedele, M., Casalino, L., Santoro, M., Viglietto, G., Fusco, A., and Verde, P. (1997). Neoplastic transformation of rat thyroid cells requires the junB and fra-1 gene induction which is dependent on the HMGI-C gene product. EMBO Journal *16*, 5310-5321.

Vo, N., and Goodman, R.H. (2001). CREB-binding protein and p300 in transcriptional regulation. The Journal of biological chemistry *276*, 13505-13508.

Waldmann, T., and Schneider, R. (2013). Targeting histone modifications - epigenetics in cancer. Current opinion in cell biology *25*, 184-189.

Wang, F., and Higgins, J.M. (2013). Histone modifications and mitosis: countermarks, landmarks, and bookmarks. Trends Cell Biol *23*, 175-184.

Wang, I., Chen, Y., Hughes, D., Petrovic, V., Major, M. L., Park, H.J., Tan, Y., Ackerson, T., and Costa, R.H. (2005). Forkhead Box M1 regulates the transcriptional network of genes essential for mitotic progression and genes encoding the SCF (Skp2-Cks1) ubiquitin ligase. Molecular and cellular biology *25*, 10875-10894.

Wang, Z., Zang, C., Rosenfeld, C.A., Schones, D.E., Barski, A., Cuddapah, S., Cui, K., Roh, T.Y., Peng, W., Zhang, M.Q., and Zhao, K. (2008) Combinatorial patterns of histone acetylations and methylations in the human genome. Nature genetics *40*, 897-903.

Wei, Y., Mizzen, C.A., Cook, R.G., Gorovsky, M.A., and Allis, C.D. (1998). Phosphorylation of histone H3 at serine 10 is correlated with chromosome condensation during mitosis and meiosis in Tetrahymena. Proceedings of the National Academy of Sciences of the United States of America *95*, 7480-7484.

Wilkins, B.J., Rall, N.A., Ostwal, Y., Kruitwagen, T., Hiragami-Hamada, K., Winkler, M., Barral, Y., Fischle, W., and Neumann, H. (2014). A cascade of histone modifications induces chromatin condensation in mitosis. Science *343*, 77-80.

Wilkinson, A.W., and Gozani, O. (2014) Histone-binding domains: Strategies for discovery and characterization. Biochimica et biophysica acta, Epub ahead of print.

Yamamoto, Y., Verma, U.N., Prajapati, S., Kwak, Y.T., and Gaynor, R.B. (2003). Histone H3 phosphorylation by IKK-alpha is critical for cytokine-induced gene expression. Nature *423*, 655-659.

Yie, J., Merika, M., Munshi, N., Chen, G., and Thanos, D. (1999). The role of HMG I(Y) in the assembly and function of the IFN-beta enhanceosome. EMBO Journal *18*, 3074-3089.

Zhang, L., Chang, C.J., Bacus, S.S., and Hung, M.C. (1995). Suppressed transformation and induced differentiation of HER-2/neu-overexpressing breast cancer cells by emodin. Cancer research *55*, 3890-3896.

Zhang, Q., Zhong, Q., Evans, A.G., Levy, D., and Zhong, S. (2011). Phosphorylation of histone H3 serine 28 modulates RNA polymerase III-dependent transcription. Oncogene *30*, 3943-3952.

Zhao, K., Kas, E., Gonzales, E., and Laemmli, U.K. (1993). SAR-dependent mobilization of histone H1 by HMG-I/Y in vitro: HMG-I/Y is enriched in H1-depleted chromatin. The EMBO journal *12*, 3237-3247.

Zhou, B.R., Feng, H., Kato, H., Dai, L., Yang, Y., Zhou, Y., and Bai, Y. (2013). Structural insights into the histone H1-nucleosome complex. Proceedings of the National Academy of Sciences of the United States of America *110*, 19390-19395.

Zippo, A., De Robertis, A., Serafini, R., and Oliviero, S. (2007). PIM1-dependent phosphorylation of histone H3 at serine 10 is requie for MYC-dependent transcriptional activation and oncogenic transformation. Nature cell biology *9*, 932-944.

Zou, Y., Webb, K., Perna, A.D., Zhang, Q., Clarke, S., and Wang, Y. (2007). A mass spectrometric study on the in vitro methylation of HMGA1a and HMGA1b proteins by PRMTs: methylation specificity, the effect of binding to AT-rich duplex DNA, and the effect of C-terminal phosphorylation. Biochemistry *46*, 7896-7906.